

INFORMATION TO USERS

This manuscript has been reproduced from the microfilm master. UMI films the text directly from the original or copy submitted. Thus, some thesis and dissertation copies are in typewriter face, while others may be from any type of computer printer.

The quality of this reproduction is dependent upon the quality of the copy submitted. Broken or indistinct print, colored or poor quality illustrations and photographs, print bleedthrough, substandard margins, and improper alignment can adversely affect reproduction.

In the unlikely event that the author did not send UMI a complete manuscript and there are missing pages, these will be noted. Also, if unauthorized copyright material had to be removed, a note will indicate the deletion.

Oversize materials (e.g., maps, drawings, charts) are reproduced by sectioning the original, beginning at the upper left-hand corner and continuing from left to right in equal sections with small overlaps. Each original is also photographed in one exposure and is included in reduced form at the back of the book.

Photographs included in the original manuscript have been reproduced xerographically in this copy. Higher quality 6" x 9" black and white photographic prints are available for any photographs or illustrations appearing in this copy for an additional charge. Contact UMI directly to order.

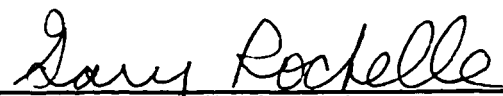
UMI

A Bell & Howell Information Company
300 North Zeeb Road, Ann Arbor MI 48106-1346 USA
313/761-4700 800/521-0600

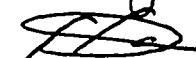
Copyright
by
Chen H. Shen
1997

**NITROGEN DIOXIDE ABSORPTION
IN AQUEOUS SODIUM SULFITE**


**Approved by
Dissertation Committee:**



Gary T. Rochelle, Supervisor




George Georgiou



David M. Himmelblau



Desmond F. Lawler



Isaac Trachtenberg

**NITROGEN DIOXIDE ABSORPTION
IN AQUEOUS SODIUM SULFITE**

by

CHEN HUA SHEN, B.S., M.S.

DISSERTATION

Presented to the Faculty of the Graduate School of

The University of Texas at Austin

in Partial Fulfillment

of the Requirements

for the Degree of

DOCTOR OF PHILOSOPHY

THE UNIVERSITY OF TEXAS AT AUSTIN

May, 1997

UMI Number: 9803020

**Copyright 1997 by
Shen, Chen Hua**

All rights reserved.

**UMI Microform 9803020
Copyright 1997, by UMI Company. All rights reserved.**

**This microform edition is protected against unauthorized
copying under Title 17, United States Code.**

UMI
**300 North Zeeb Road
Ann Arbor, MI 48103**

Acknowledgments

I am most grateful to Professor Gary Rochelle for his guidance and support in completing my dissertation work. His knowledge and experience in this area are so vast that after a short consultation with him, I no longer had the need to turn to any other text books or technical journals. I would also like to thank the other faculty members on my committee for their continuous interest and support.

I wish to acknowledge the Environmental Solutions Program at the University of Texas for its financial support of this project.

My parents have been a source of continuing inspiration for me throughout my education. With a Ph.D. or equivalent each, they have repeatedly warned me of the unpleasantness of leaving the university with anything less.

Finally, I would like to thank my wife, Sabine, for her encouragement, patience, and understanding. She has kept me going for the past five years by constantly reminding me about how much money I would be making once I earned my degree. I hope she is right.

NITROGEN DIOXIDE ABSORPTION IN AQUEOUS SODIUM SULFITE

Publication No. _____

Chen Hua Shen, Ph.D.

The University of Texas at Austin, 1997

Supervisor: Gary T. Rochelle

The Clean Air Act of 1990 requires additional reduction of acid gases, sulfur dioxide, and nitrogen oxides released into the atmosphere from coal-fired electric power plants. In the case of older existing power plants, a possible retrofit strategy is to oxidize nitric oxide (NO, the major constituent of NO_x in flue gas) to nitrogen dioxide (NO_2) by the addition of methanol or other hydrocarbons into the duct at an optimum temperature regime. NO_2 can then be removed by either modifying existing SO_2 control equipment or by adding a limestone (CaCO_3) slurry scrubbing process. Limestone reacts with SO_2 to form CaSO_3 , and the free sulfite (SO_3^{2-}) in the solution is reactive toward NO_2 . The focus of this research is to study the reaction between NO_2 and aqueous sulfite at elevated temperature and in the presence of gas phase O_2 .

The removal of NO_2 by limestone slurry scrubbing involves the reaction between NO_2 and SO_3^{2-} , bisulfite (HSO_3^-) and water. The reactions between NO_2 and $\text{SO}_3^{2-}/\text{HSO}_3^-$ are first order in both reactants, while the NO_2 -water reaction is second order in NO_2 concentration. The rate constants of the above reactions and the NO_2 -thiosulfate ($\text{S}_2\text{O}_3^{2-}$) reaction were determined at 55 °C. SO_3^{2-} was found to be the most reactive toward NO_2 , while the contribution of chemical reaction still dominated in the absorption of NO_2 into water. The effect of gas phase SO_2 and O_2 , and liquid phase additives such as $\text{S}_2\text{O}_3^{2-}$, Ca^{++} , Mg^{++} , and Cl^- on NO_2 absorption was also investigated.

The absorption of NO_2 catalyzes free radical reactions that lead to sulfite oxidation. A semi-empirical model was proposed to relate the rate of sulfite oxidation to the rate of NO_2 absorption. Thiosulfate inhibits sulfite oxidation by providing an alternative route for the termination of the free radical reactions, and a fundamental model was derived to quantify the effect of $\text{S}_2\text{O}_3^{2-}$ on sulfite oxidation.

The absorption of NO_2 into aqueous bisulfide (HS^-) was studied in an attempt to discover alternative scrubbing technologies. The reaction between NO_2 and HS^- is twice as fast as the NO_2 - SO_3^{2-} reaction at 55 °C. A semi-empirical model was proposed to relate NO_2 absorption to HS^- oxidation.

This study has shown that acceptable level of NO_2 removal by a conventional limestone slurry scrubber is not probable. However, aqueous scrubbing of NO_2 by Na_2SO_3 and Na_2S solutions are viable options. Furthermore, significant reduction in hold tank liquid depth and/or oxidizing air stoichiometry is possible by NO_2 injection.

Table of Contents

List of Tables	xi
List of Figures	xiii
Chapter 1 Introduction.....	1
Chapter 2 Chemistry and Theory	8
2.1 Oxidation of NO by Methanol Injection.....	8
2.2 Chemistry of NO ₂ -S(IV) Reaction	11
2.2.1 NO ₂ -S(IV) Reaction with N ₂ as Diluent	11
2.2.2 NO ₂ -S(IV) Reaction with Air as Diluent.....	13
2.2.3 Product of NO ₂ -S(IV) Reaction	15
2.2.4 Simultaneous SO ₂ and NO ₂ Absorption into S(IV) Solutions	17
2.3 NO ₂ Hydrolysis	17
2.4 Chemistry of NO ₂ -Sulfide Reaction	18
2.4.1 NO ₂ -S(-II) Reaction.....	18
2.4.2 S(-II) Oxidation with Air and NO ₂	19
2.4.3 Reaction Product.....	20
2.5 Theory of Simultaneous Mass Transfer with Chemical Reaction	20
2.5.1 Film Theory	21
2.5.2 Penetration Theory.....	21
2.5.3 Surface Renewal Theory.....	21
2.5.4 The Effect of Chemical Reactions	22
2.5.5 Application of Theory to NO ₂ -S(IV) System.....	25
Chapter 3 Experimental and Analytical Methods	29
3.1 Experimental Methods	29
3.1.1 Stirred Cell Contactor and Supporting Equipment.....	29
3.1.2 Mode of Operation.....	34
3.2 Gas and Solids Phase Analyses	36

3.2.1	Gas Phase Analysis	37
3.2.2	Liquid Phase Analysis	38
Chapter 4	Results of Batch Experiments	42
4.1	NO ₂ Absorption into 0.1 M Solutions	42
4.2	Reaction Rate Constants	46
4.2.1	Agreement of NO ₂ -S(IV) Rate Constants	47
4.2.2	Discrepancy Between NO ₂ -water Rate Constant	48
4.3	Effect of Air Dilution on Rate of NO ₂ Absorption	50
4.4	Effect of Thiosulfate in Inhibiting Oxidation	52
4.5	Effect of Temperature on NO ₂ Absorption	53
4.6	Chapter Summary	56
Chapter 5	NO ₂ Absorption in Continuous Stirred Cell Contactor	57
5.1	Results of Continuous NO ₂ Absorption Experiments	57
5.2	Regression of Reaction Rate Constants	58
5.3	Effect of Gas Phase Variables on NO ₂ Absorption	62
5.3.1	Nitrogen Dilution	62
5.3.2	Presence of SO ₂	62
5.4	Effect of Liquid Phase Variables on NO ₂ Absorption	64
5.4.1	Presence of Thiosulfate	64
5.4.2	Other Additives	65
5.4.3	Product Accumulation	68
5.4.4	Liquid Phase Agitation Speed	70
5.5	Chapter Summary	71
Chapter 6	Sulfite Oxidation in the Presence of NO ₂	78
6.1	Significance of Sulfite Oxidation	78
6.2	Sulfite Oxidation Measurement	79
6.3	Model of Sulfite Oxidation	80
6.4	Effect of Gas Phase Variables on Sulfite Oxidation	86
6.4.1	Oxygen Partial Pressure	88
6.4.2	Presence of SO ₂	87

6.5	Effect of Liquid Phase Variables on Sulfite Oxidation	89
6.5.1	Presence of Thiosulfate.....	89
6.5.2	Other Additives.....	98
6.5.3	Liquid Phase Agitation Speed	103
6.6	Chapter Summary	104
Chapter 7	NO ₂ Absorption in Aqueous Na ₂ S	106
7.1	Literature Review	106
7.2	NO ₂ -S(-II) Reaction.....	108
7.3	S(-II) Oxidation in the Presence of NO ₂	113
7.4	NO ₂ Reaction with Polysulfide	117
7.5	Chapter Summary	121
Chapter 8	Industrial Implications	124
8.1	NO ₂ Removal by Conventional Limestone Slurry Scrubbing.....	124
8.2	NO ₂ removal by Aqueous Scrubbing	127
8.2.1	Scrubbing with Na ₂ SO ₃ Solution	127
8.2.2	Scrubbing with Na ₂ S Solution.....	129
8.3	Hold Tank Depth Reduction by NO ₂ Injection	130
Chapter 9	Conclusions and Recommendations	135
9.1	Conclusions.....	135
9.1.1	NO ₂ Absorption into S(IV) Solutions.....	135
9.1.2	S(IV) Oxidation in the Presence of NO ₂	136
9.1.3	NO ₂ Absorption into S(-II) Solutions.....	136
9.1.4	Industrial Implications	137
9.2	Recommendations.....	137
Appendix A	Review of Post Combustion Methods for NO _x Emissions Control	139
Appendix B	Rate Constants of Sulfur-Nitrogen Reactions.....	141
Appendix C	Sample Calculation of Iodometric Titration	142

Appendix D	Sample Calculation for Batch Experiments.....	144
Appendix E	Sample Calculation of Rate of S(IV) Oxidation.....	148
Appendix F	FORTTRAN Program for Equilibrium Speciation Calculation.....	150
Appendix G	Rate Constant Estimation by BETAV3	162
Appendix H	Model of Sulfite Oxidation with Thiosulfate.....	167
Appendix I	Sample Calculation of NO ₂ Removal in Typical Scrubber.....	170
Appendix J	Sample Calculation of Hold Tank Depth Reduction	172
Glossary	177
References	180
Vita	185

List of Tables

Table 2.1	Henry's Constants and Diffusion Coefficient of NO ₂	26
Table 3.1	Calibration of Gas and Liquid Phase Mass Transfer Coefficients ...	32
Table 3.2	Range and Calibration Equations for Brooks Mass Flow Meters	35
Table 3.3	Operating Ranges of Synthesized Flue Gas	35
Table 4.1	NO ₂ Absorption into 0.1 M Solutions	43
Table 4.2	Comparison of Second Order Rate Constants at 25 °C	47
Table 5.1	Results of Continuous Experiments, no Additive.....	73
Table 5.2	Results of Continuous Experiments with SO ₂	75
Table 5.3	Results of Continuous Experiments with Thiosulfate	76
Table 5.4	Results of Continuous Experiments with Liquid Phase Additives ...	77
Table 7.1	Summary of Experiments with S(-II)	123
Table 7.2	NO ₂ Absorption into Aqueous Na ₂ S ₄	119
Table B.1	Rate Constants of Sulfur-Nitrogen Reactions.....	141

List of Figures

Figure 1.1	NO _x Removal by Methanol Injection Followed by Limestone Slurry Scrubbing	4
Figure 2.1	Methanol Performance at Bench and Pilot Scale	10
Figure 2.2	NO ₂ Absorption into Aqueous Na ₂ SO ₃ Solution	12
Figure 2.3	Overall Sulfur-Nitrogen Reaction Scheme	16
Figure 3.1	Stirred Cell Contactor	30
Figure 3.2	Dimensions of the Gas-Liquid Contactor	31
Figure 3.3	Agitator Propeller Design and Dimensions	32
Figure 3.4	Top View of Top Cover Plate	34
Figure 4.1	Batch Results of NO ₂ Absorption	44
Figure 4.2	Absorption Rates of NO ₂ into 0.1 M Solutions	45
Figure 4.3	NO ₂ Absorption into Water and 0.1 M NaOH at 25 °C	50
Figure 4.4	Effect of Air Dilution on NO ₂ Absorption at 25 °C	51
Figure 4.5	Effect of 0.1 M Na ₂ S ₂ O ₃ on NO ₂ Absorption	53
Figure 4.6	Effect of Temperature on NO ₂ Absorption	54
Figure 4.7	Second Order Rate Constant as a Function of Reaction Temperature	55
Figure 5.1	Fit of NO ₂ Absorption Rate by Equation 2.40	60
Figure 5.2	Predicted and Measured Rates of NO ₂ Absorption in Sulfite Solution	61
Figure 5.3	Calculated Effect of SO ₂ Absorption on NO ₂ Absorption	64

Figure 5.4	Effect of Additives on NO ₂ Absorption	66
Figure 5.5	Effect of Product Accumulation on NO ₂ Absorption.....	69
Figure 5.6	Effect of Liquid Phase Agitation on NO ₂ Absorption.....	71
Figure 6.1	Effect of NO ₂ Absorption on Sulfite Oxidation	81
Figure 6.2	Model Prediction of Rates of Sulfite Oxidation	83
Figure 6.3	Model Prediction of Sulfite Oxidation	85
Figure 6.4	Effect of O ₂ on Sulfite Oxidation	87
Figure 6.5	Calculated effect of SO ₂ Absorption on Sulfite Oxidation	89
Figure 6.6	Model Fit of Rate of Sulfite Oxidation with Thiosulfate	93
Figure 6.7	Model Prediction of Rates of Sulfite Oxidation with Thiosulfate	94
Figure 6.8	Calculated Effect of NO ₂ Concentration on the Ratio of Sulfite Oxidation to NO ₂ Absorption.....	96
Figure 6.9	Calculated Contribution of NO ₂ Reaction and S ₂ O ₃ ⁼ Oxidation to Overall Rate of S(IV) Depletion.....	98
Figure 6.10	Effect of Fe ⁺⁺ on Sulfite Oxidation	100
Figure 6.11	Effect of Additives on Rate of Sulfite Oxidation	102
Figure 6.12	Effect of Liquid Phase Agitation on Sulfite Oxidation	104
Figure 7.1	Model Fit of Rate of NO ₂ Absorption	111
Figure 7.2	Effect of Y _{NO₂,i} on Rate of NO ₂ Absorption	112
Figure 7.3	Model Fit of Rate of S(-II) Oxidation.....	115
Figure 7.4	Model Prediction of S(-II) Oxidation	116
Figure 7.5	Equilibrium Composition of HS ⁻ and Polysulfides	118
Figure 7.6	Effect of pH on Second Order Rate Constant.....	120
Figure 8.1	NO ₂ Removal in a Typical Limestone Slurry Scrubber	126

Figure 8.2	NO ₂ Removal in an Aqueous Na ₂ SO ₃ Scrubber	128
Figure 8.3	NO ₂ Removal in an Aqueous Na ₂ S Scrubber	130
Figure 8.4	Hold Tank Liquid Depth Reduction by NO ₂ Injection	132
Figure 8.5	Sulfite Oxidation Catalyzed by NO ₂ Absorption in Hold Tank	133

Chapter 1

Introduction

The Acid Rain Program (Title IV) of the Clean Air Act Amendments (CAAA), signed into law in 1990, requires the electric power industry to significantly reduce sulfur dioxide (SO₂) and nitrogen oxide (NO_x) emissions from fossil-fueled boilers. Implemented by the US. Environmental Protection Agency (EPA), Title IV calls for reductions in SO₂ and NO_x emissions by ten million tons and two million tons, respectively, from 1980 levels (Duval, 1991).

To achieve its SO₂ reduction goals, CAAA deviates from previous air pollution legislation by promoting a market-based approach that relies on economic incentives to determine a utility's choice of compliance. To meet its SO₂ emission requirements, a power plant may implement one or more of the following options: (1) switch to a lower sulfur coal, (2) purchase allowances, (3) retrofit with conventional technology such as limestone slurry scrubbing or lime spray drying, and (4) retrofit with newer, lower capital cost technology such as in-duct injection processes.

Limestone slurry scrubbing accounts for more than 90% of the SO₂ control equipment installed at utility plants (Kuehn, 1993). Because of their considerable level of commercial operating experience and potential for high SO₂ removal (> 95%), both slurry scrubbing and lime spray drying are expected to remain the preferred choices for meeting SO₂ emission standard.

The regulation of NO_x emissions by Title IV is fundamentally different from that of the SO₂ control policy (Smith, 1993). The rules specify a more traditional command and control approach. The limits set for NO_x emissions are based upon levels believed to be achievable by the application of low-NO_x burner technology. Depending upon boiler type, limits are set at 0.45 and 0.50 lb/MMBtu. Low-NO_x burner technology, by a variety of methods and designs, essentially creates a staged combustion effect within the boiler. Staged combustion and the creation of fuel-rich and fuel-lean zones in the boiler reduce peak flame temperature and oxygen availability which in turn lower NO_x production. Combustion modifications of this sort typically reduce existing NO_x emissions by 40-70% (Wood, 1994).

In the coming years, NO_x regulations are expected to tighten as new low-NO_x technology develops. Any additional removal of NO_x beyond the current level of reductions set forth in Title IV will require a post-combustion process. These processes usually fall into one of two major categories, commonly known as "dry" and "wet" methods. The common dry methods fall into one of four groups: 1) catalytic decomposition of NO_x; 2) sorption by solids; 3) selective catalytic reduction with NH₃ to form N₂ or nonselective catalytic reduction with reducing gases; and 4) homogeneous reduction to N₂ with NH₃. The wet methods, on the other hand, usually involve the absorption of NO_x by liquids followed by either a liquid phase reduction to form NH₄⁺, or a liquid phase oxidation to form NO₂⁻/NO₃⁻. Other wet methods involve gas phase oxidation of NO to NO₂ followed by absorption by liquids. NO₂, once absorbed, can either

be reduced to N_2 or oxidized to NO_2^-/NO_3^- . A full review of all major post combustion technology for NO_x emissions control is given in Appendix A.

Among the various wet technologies, NO_x removal by methanol injection followed by limestone slurry scrubbing emerges as an attractive candidate. It has several advantages over the other technologies for NO_x removal. First of all, it is economical. A spray scrubber or spray dryer can be retrofitted to an existing power plant to achieve additional NO_x control on top of the state-of-the-art technology already employed by the power plant for SO_2 emission control. Since many of the required equipment already exist, the capital cost associated with this process is significantly lower than other NO_x technologies such as selective catalytic reduction or absorption of NO_x by liquid with liquid phase oxidation or reduction. Furthermore, since limestone is a cheaper raw material than lime, the operating cost associated with such a process will also be lower.

Another advantage of the limestone slurry scrubbing process is the possibility of simultaneous SO_2 and NO_x removal. When SO_2 is absorbed into limestone ($CaCO_3$) slurry, $CaSO_3$ is formed as product, and it can react with NO_2 to remove it from the gas phase. The final product is $CaSO_4$ and a relatively small amount of calcium nitrogen-sulfur compounds which can be landfilled.

A simplified diagram of the process is shown in Figure 1.1. A typical coal-fired power plant equipped with a low- NO_x burner will emit approximately 200-400 ppm of NO_x (NO and NO_2 combined) where nitric oxide (NO) accounts for 90% of NO_x . Since NO is relatively unreactive and insoluble in aqueous solutions, a possible retrofit strategy is to oxidize nitric oxide to nitrogen dioxide (NO_2) by the addition of methanol or other hydrocarbons into the duct at an

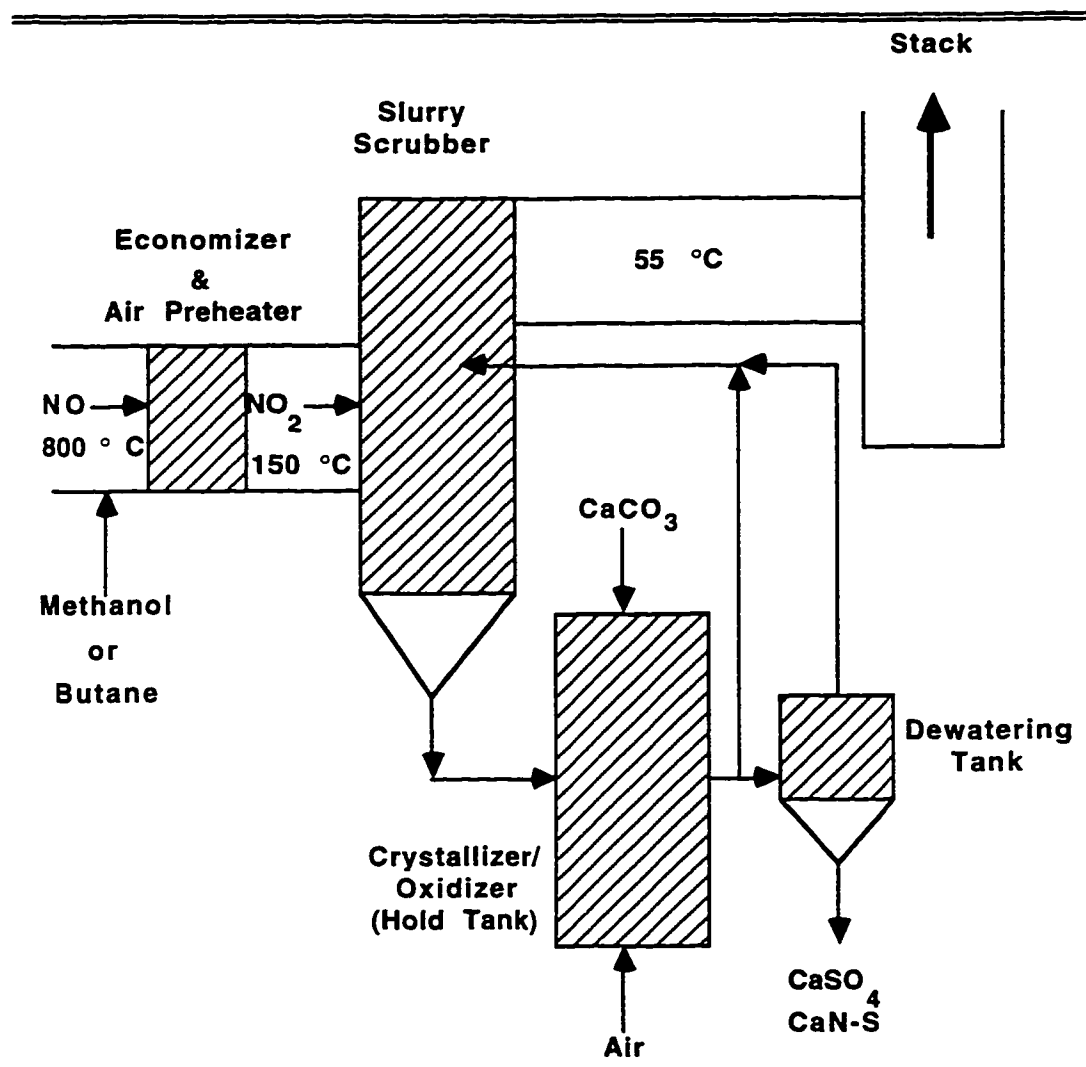


Figure 1.1 NO_x removal by methanol injection followed by limestone slurry scrubbing.

optimum temperature regime (Hori et al., 1992; Lyon et al., 1990). NO_2 can then be removed by reacting with limestone slurry inside the scrubber. The spent

slurry leaving the scrubber is sent to a hold tank where the unused sulfite ($\text{SO}_3^{=}$) in the slurry is oxidized to sulfate via forced oxidation by sparging air into the tank. The reaction products, i.e., sulfate and calcium nitrogen-sulfur compounds, are partially removed by a waste bleed and can be sold as construction material or landfilled. The slurry is mixed with fresh feed and recycled back into the scrubber.

Two sets of chemical reactions are important in the above process. The first is the reaction between NO_2 and $\text{SO}_3^{=}$, the latter formed by the reaction between limestone and gas phase SO_2 . In a system where the absorption of NO_2 is greatly enhanced by chemical reaction, the reaction between NO_2 and sulfite is the determining factor in the removal of NO_x . The other important reaction is the oxidation of sulfite to sulfate by air. This reaction depletes the amount of sulfite in the solution so that there is less sulfite available to react with NO_2 ; therefore it should be minimized in the scrubber where NO_2 absorption takes place. On the other hand, this oxidation reaction is desirable in the hold tank, where the objective is the quantitative oxidation of calcium sulfite to calcium sulfate.

A fair amount of work has been done by other researchers on the subject of NO_2 reaction with sulfite. Takeuchi et al. (1977) measured NO_2 absorption into aqueous sodium sulfite and bisulfite solutions, both in a gas liquid contactor and a spray column, and they reported the reaction rate constant for the above reaction at 25 °C. They studied the effect of sulfite concentration, gas phase NO_2 partial pressure, and agitation speed on the rate of NO_2 absorption, and they investigated the effect of temperature between 10 and 25 °C. In another study, Takeuchi et al. (1978) performed simultaneous absorption of SO_2 and NO_2 in

aqueous solutions of NaOH and Na₂SO₃. Pigford et al. (1977) studied the absorption of NO₂ into water, sulfuric acid, NaOH and alkaline Na₂SO₃ solutions in a wetted sphere absorber. Their results show that the dimer form of NO₂, N₂O₄, was the species actually being absorbed, and they have proposed a reaction mechanism to account for this observation.

Relatively little work has been done on the subject of sulfite oxidation in the presence of gas phase NO₂. Takeuchi et al. (1977) studied the absorption of NO₂ in Na₂SO₃ solution from air as a diluent, and they reported that the rate of NO₂ absorption was lowered by 40% when air, instead of N₂, was used as a diluent. They did not provide an explanation or a mechanism to account for this observation. They did, however, look at the effect of certain additives in the liquid phase, among them EDTA-2Na, Glycine, Acetic acid, and MEA.

This work has several objectives. First of all, it reproduces the kinetic rate constants at 25 °C and provides new kinetic information at 55 °C, the typical temperature inside a scrubber. Second, it studies the effect of solution pH, gas and liquid phase mass transfer coefficients, and liquid phase additives such as Fe⁺⁺, Mg⁺⁺ and thiosulfate (S₂O₃⁼) on the rate of NO₂ absorption. Third, it proposes a model to account for sulfite oxidation in the presence of NO₂, supported by actual measurements of oxidation rates. And the final objective is to determine the feasibility of limestone slurry scrubbing and/or aqueous sulfite scrubbing in achieving an acceptable level of NO₂ removal. Furthermore, this work also investigates the chemistry and mechanism of NO₂ reaction with sodium sulfide (Na₂S).

The reaction chemistry, experimental methods, and results derived from this work are presented in the forthcoming chapters. Chapter 2 reviews the relevant chemistry and literature associated with NO_2 -S(IV) reactions. Chapter 3 details the experimental methods and analytical techniques used to investigate SO_2 and NO_2 rates of removal, rate of sulfite and sulfide oxidation, solution speciation, and reaction products. Chapters 4-6 present empirical and modeling results on NO_2 -S(IV) reactions and sulfite oxidation in the presence of NO_2 and oxygen. Chapter 7 deals with the study of NO_2 absorption into solutions of sulfide (S^{2-}). Chapter 8 discusses the implications of the results of this study on commercial processes, and finally chapter 9 lists the major conclusions from this study and gives recommendations in future work.

Chapter 2

Chemistry and Theory

Two important steps are involved in the removal of NO_x by solutions of S(IV). The first step is the oxidation of NO to NO_2 by injecting an oxidant such as methanol at elevated temperatures. The second step is the actual absorption of the NO_2 into the solution, enhanced by the reaction between NO_2 and various S(IV) species in the liquid phase. Since our study is mainly concerned with the absorption of NO_2 , the oxidation of NO to NO_2 will be discussed briefly in the following section. The chemistry and theory involved in the absorption of NO_2 into S(IV) solution will be discussed in greater detail, followed by a brief review of the chemistry involved in the reaction between NO_2 and sulfide, or S(-II).

2.1 OXIDATION OF NO BY METHANOL INJECTION

Several oxidants, including ozone (O_3), urea (NH_2CONH_2), and hydrogen peroxide (H_2O_2), have been used in the homogeneous gas phase oxidation of NO to NO_2 . Borders et al. (1982) studied the reaction:



They reported an absolute rate constant k_1 of 1.90×10^{-14} $\text{cm}^3/\text{molecule-s}$ at 298 K. Rosenberg et al. (1984) studied the oxidation of NO to NO_2 by the addition of ozone and ClO_2 . Their results showed that ozone was the best oxidizing agent but it was too expensive. The cost of ClO_2 was 30-40% less than that of ozone, but the use of ClO_2 introduced a considerable amount of chloride into the scrubbing liquor, thus causing waste disposal problems.

The oxidation of NO to NO₂ by methanol was first reported by Yano and Ito (1983) in their study of reactions that occur in the exhaust of methanol-fueled automobiles. They noted limited conversion of NO to NO₂ and suggested HO₂ free radicals formed during combustion reacted with NO to produce NO₂. Lyon et al. (1990), in bench scale experiments, achieved high NO-to-NO₂ conversions by methanol under a variety of temperature and residence time conditions. Based on their data and previous kinetic studies, they proposed the following reaction mechanism:

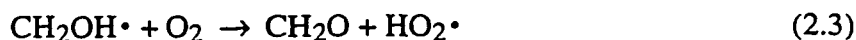
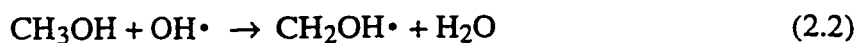


Figure 2.1 shows both bench and pilot scale results of a later study by the same research group (Pont et al., 1993). Zamanksy et al. (1995) were able to demonstrate 98% conversion of NO to NO₂ at pilot scale with a 50/50 mixture of hydrogen peroxide (H₂O₂) and methanol at a molar feed ratio of 1.5:1. Though more expensive, the addition of H₂O₂ reduced carbon monoxide (CO) production by more than half. Otherwise, methanol will produce one molecule of CO for every molecule of NO converted to NO₂.

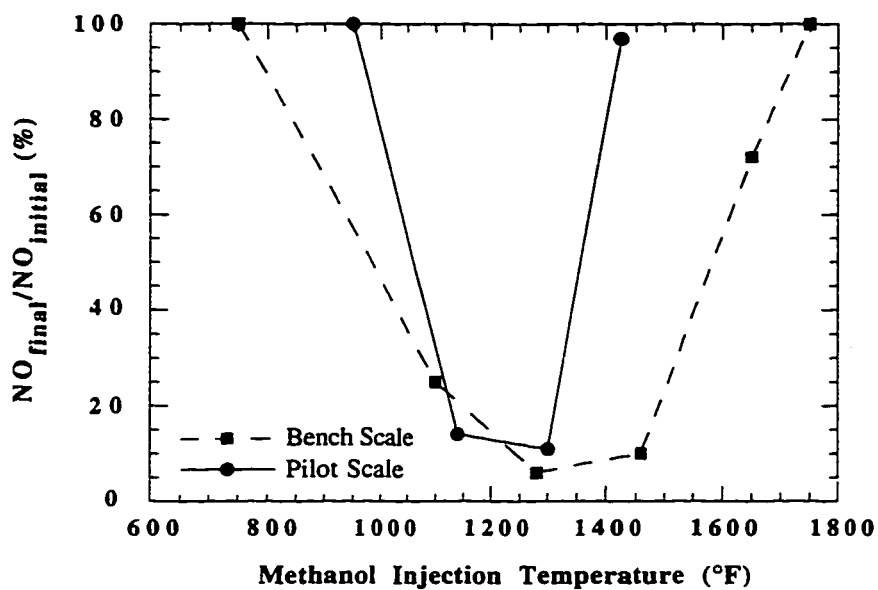


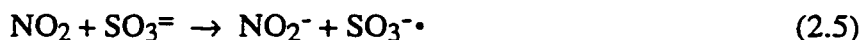
Figure 2.1 Methanol performance at bench and pilot scale. Methanol molar feed rate relative to NO was 2 to 1. Residence time was 0.6 seconds (Pont et al., 1993).

In related work, Hori et al. (1992) have shown hydrocarbon fuels to be similarly effective in oxidizing NO to NO₂ by means of the same HO₂ mechanism. However, the effectiveness in producing HO₂ radicals was found to be strongly dependent on fuel type.

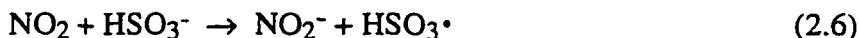
2.2 CHEMISTRY OF NO₂-S(IV) REACTION

2.2.1 NO₂-S(IV) Reaction with N₂ as Diluent

The reactions between NO₂ and S(IV) compounds take place via a free radical mechanism (Nash, 1979). The following step represents the initial reaction between NO₂ and sulfite:



A parallel mechanism can be written for the reaction between NO₂ and bisulfite (HSO₃⁻):



Takeuchi et al. (1977) studied the absorption of NO₂ from N₂ into solutions of sodium sulfite and bisulfite in an agitated vessel at 25 °C. They found that both reactions were first order with respect to NO₂ and S(IV) concentrations, and the respective rate expressions were:

$$r_{\text{SO}_3^{2-}} = k_2[\text{NO}_2][\text{Na}_2\text{SO}_3] \quad (2.7)$$

$$r_{\text{HSO}_3^-} = k_2[\text{NO}_2][\text{NaHSO}_3] \quad (2.8)$$

Figure 2.2 is a summary of their results of NO₂-sulfite reactions. Based upon their experimental data, they reported the following rate constants at 25 °C:

$$\text{NO}_2\text{-SO}_3^{2-}: \quad k_2 = 6.6 \times 10^5 \text{ L/mol-s}$$

$$\text{NO}_2\text{-HSO}_3^-: \quad k_2 = 1.5 \times 10^4 \text{ L/mol-s}$$

Takeuchi et al. (1977) also studied the effect of temperature between 10 and 25 °C on the rate of NO₂ absorption into SO₃²⁻ solution. They discovered that a rise in temperature in the above range lowered the rate of NO₂ absorption in aqueous solutions of low sulfite concentration. They attributed such an effect to

the decreased solubility of NO_2 in the liquid at higher temperature, and the reduced equilibrium concentration at higher temperature of the NO_2 dimer, N_2O_4 , which was highly soluble. However, they found that the higher the sulfite concentration, the smaller the effect of temperature on the absorption rate. They believed that this was due to the increase in reaction rate at the higher temperature, which more than offsets the decreased solubility.

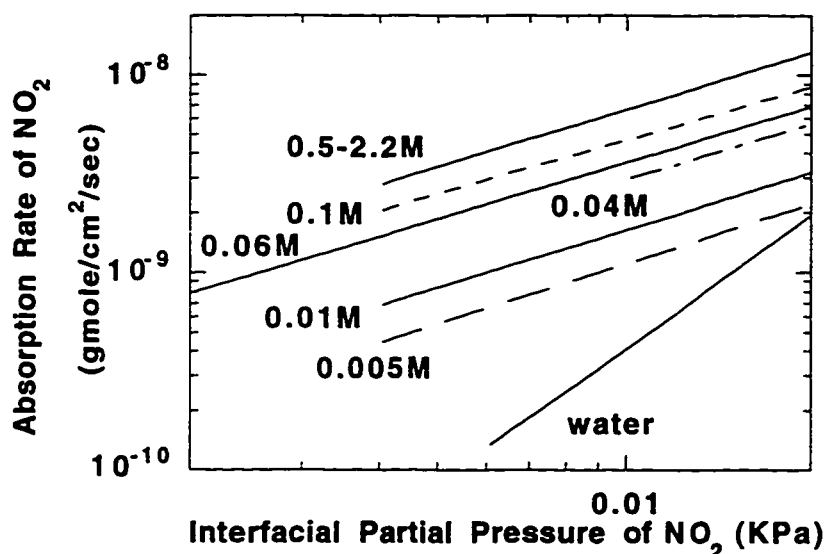


Figure 2.2 NO_2 absorption into aqueous Na_2SO_3 solution. (Takeuchi et al., 1977)

2.2.2 NO₂-S(IV) Reaction with Air as Diluent

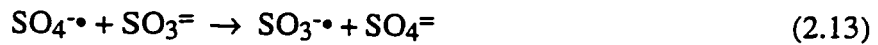
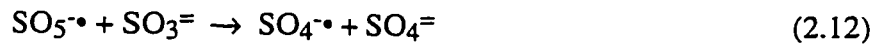
When air instead of N₂ is used as diluent, the presence of O₂ in the gas phase leads to additional reaction that causes sulfite oxidation. The stoichiometry of this reaction can be written as:



The net effect of this reaction is the depletion of sulfite, especially in the liquid boundary layer where the NO₂-sulfite reaction takes place, and the overall rate of NO₂ absorption is reduced.

Takeuchi et al. (1978) studied the absorption of NO₂ in Na₂SO₃ solution from air as a diluent in an agitated vessel at 25 °C. Their results showed that when air was used instead of N₂, the rate of NO₂ absorption into the same sulfite solution was reduced by 40%, and they believed that this was due to the oxidation of sulfite to sulfate by the O₂ in air.

We accept the following mechanism for NO₂-sulfite reaction when O₂ is present in the gas phase:

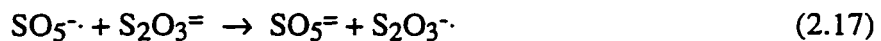


Equation 2.10 was first outlined by Nash (1979), and equations 2.11-2.14 were proposed by Huie and Neta (1984). These reactions are expected to occur in the mass transfer boundary layer. One direct consequence of this mechanism is

the depletion of sulfite in the liquid boundary. For every mole of NO₂ absorbed, several moles of SO₃⁼ can be consumed if oxygen is present. Therefore, when oxygen is present, the rate of NO₂ absorption is expected to be lower.

This mechanism also suggests that the absorption of NO₂ can catalyze sulfite oxidation by initializing the free radical formation. Rosenberg et al. (1980) studied the influence of NO_x on sulfite oxidation in lime/limestone flue gas desulfurization systems, and they discovered that NO inhibited CaSO₃ oxidation while NO₂ promoted it. An NO/NO₂ mole ratio of 12 to 1 was required to offset the promoting action of NO₂ and returned the rate of oxidation to the level where it should have been with no NO_x present. Nash (1979) also observed the catalytic effect of NO₂ on sulfite oxidation in a similar study.

If the mechanism proposed above is true, then it follows that the addition of an oxidation inhibitor to the liquid phase should serve to reduce the rate of sulfite oxidation. Sodium thiosulfate (Na₂S₂O₃) is an effective oxidation inhibitor because it acts as a free radical scavenger. It competes favorably with SO₃⁼ in reacting with SO₅[·] and thus is able to provide an alternative route for the termination of the sulfite oxidation mechanism. In the system where NO₂ is absorbed into sulfite solution, thiosulfate could reduce the rate of sulfite oxidation via the following mechanism:



Equations 2.17-2.19 in the above mechanism were outlined by Owens (1984). Takeuchi et al. (1977) studied the effect of several other antioxidants on the rate of sulfite oxidation when NO_2 was absorbed into the solution. The compounds they studied include hydroquinone (HQ), phenol, ethanolamines (MEA and DEA), ethylene glycol monoethyl ether (ethyle cellosolve), glycine, ethylenediaminetetraacetic acid (EDTA), and acetic acid. In all cases the addition of these antioxidants caused a slower rate of sulfite oxidation.

2.2.3 Product of NO_2 -S(IV) Reaction

The reaction between NO_2 and S(IV) species leads to a variety of products in the solution. In addition to nitrite (NO_2^-), nitrate (NO_3^-), SO_4^- , and dithionate (S_2O_6^-), other products include a family of nitrogen sulfur compounds. Chang et al. (1981) studied the reactions between NO_2 and sulfite, and they found that the products of this reaction were a series of nitrososulfonic acid and sulfonates, including $\text{HON}(\text{SO}_3)_2^-$ (Hydroxylamine disulfonic acid, or HADS), HONHSO_3^- (Hydroxylamine monosulfonic acid, or HAMS), $\text{HN}(\text{SO}_3)_2^-$ (Amine disulfonic acid, or ADS), and $\text{N}(\text{SO}_3)_2^-$ (Amine trisulfonic acid, or ATS). Figure 2.3 shows the reaction steps by which these products are formed:

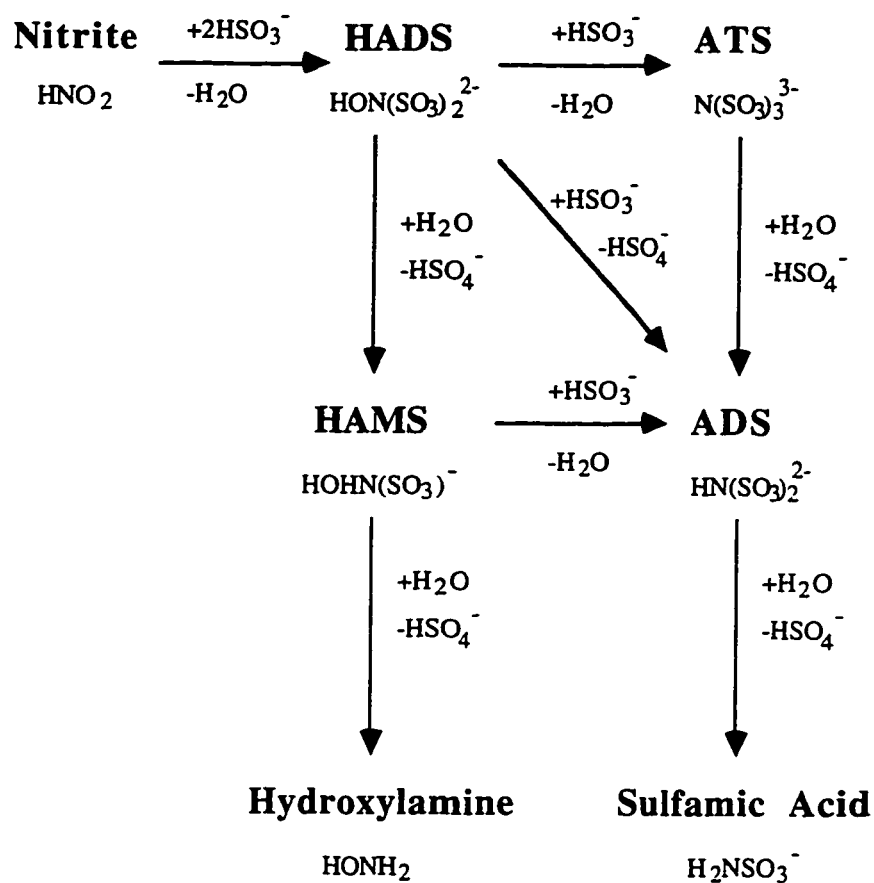


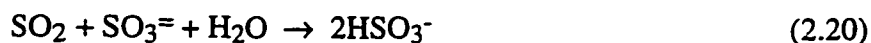
Figure 2.3 Overall sulfur-nitrogen reaction scheme. (Chang et al., 1981)

The reaction rate constants for the above reactions are given in Appendix B. This reaction scheme is consistent with the experimental results of Jarvis et al. (1985) who reported significant concentrations of the above N-S compounds as

well as SO_4^{2-} and $\text{S}_2\text{O}_6^{2-}$ in the scrubbing solution under normal flue gas conditions.

2.2.4 Simultaneous SO_2 and NO_2 Absorption into S(IV) Solutions

When an appreciable concentration of SO_2 is added to the gas phase, the following reaction of SO_2 dissolved in aqueous solution of Na_2SO_3 takes place:



The absorption of SO_2 occurs by mass transfer with instantaneous reaction. Since this reaction leads to the formation of bisulfite, which is much less reactive toward NO_2 than sulfite, the rate of NO_2 absorption will consequently drop. Takeuchi et al. (1978) studied the simultaneous absorption of SO_2 and NO_2 in aqueous Na_2SO_3 , and their results showed that the rate of NO_2 absorption into Na_2SO_3 solution was reduced than in the absence of SO_2 , while the rate of SO_2 absorption remained essentially the same regardless of the presence of NO_2 .

2.3 NO_2 HYDROLYSIS

In a NO_2 -S(IV) system, when the sulfite concentration is low but the NO_2 partial pressure is high, the NO_2 -water reaction becomes more important. Pigford et al. (1977) studied the absorption of NO_2 into water, and they proposed that N_2O_4 was the species actually being absorbed. The overall reaction can be written as:



Nitrous acid (HNO_2) may decompose via the following step:



However, this reaction does not take place rapidly if nitrous acid concentration is low. They also indicated that the rate-determining step was reaction (2.22), the slow hydrolysis of nitrogen tetroxide.

Takeuchi et al. (1977) also studied the hydrolysis of NO_2 , and they found that the reaction was second order with respect to NO_2 concentration, and the rate expression was:

$$r_{\text{H}_2\text{O}} = k_2[\text{NO}_2]^2 \quad (2.24)$$

They reported a rate constant of $7.4 \times 10^7 \text{ L/mol-s}$ for the hydrolysis reaction at 25°C .

2.4 CHEMISTRY OF NO_2 -SULFIDE REACTION

Although not directly related to NO_2 removal by limestone slurry scrubbing, the reaction between NO_2 and S(-II) species, i.e., sulfide ($\text{S}^{=}$) and bisulfide (HS^-) is relevant to this study because aqueous scrubbing of NO_2 by Na_2S solution has been used on an industrial scale and has been proven efficient in NO_2 removal. Shen (1990) documented the removal of NO_2 in a whirlwind plate tower by solutions of 5% Na_2S and 3% NaOH , and he reported over 90% removal of NO_2 at a gas rate of $4000 \text{ m}^3/\text{hr}$ and NO_2 partial pressure as high as 14000 ppm.

2.4.1 NO_2 -S(-II) Reaction

The actual mechanism of the reaction between NO_2 and S(-II) (mostly bisulfide, the dominant species in the solution under most conditions) has never been documented. Kuropka et al. (1981) studied the removal of NO_2 in a gas

liquid contactor by solutions of Na₂SO₃ and Na₂S at various concentrations, and they discovered that the NO₂ removal efficiency was higher for Na₂S than that of Na₂SO₃. Shen (1990) also observed that Na₂S was more reactive toward NO₂ than Na₂SO₃.

We believe that the reaction between NO₂ and HS⁻ is likely to involve charge transfer that leads to a free radical mechanism. The following reaction may occur in the boundary layer and enhance NO₂ absorption:



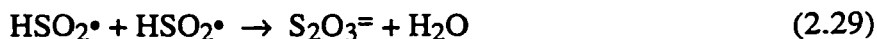
The rate expression is:

$$r_{\text{HS}^-} = k_2[\text{HS}^-][\text{NO}_2] \quad (2.26)$$

This rate expression is consistent with the findings of Kurokpa et al. (1980), who concluded that the rate of NO₂-sulfide reaction was first order with respect to both NO₂ and sulfide concentration.

2.4.2 S(-II) Oxidation with Air and NO₂

When oxygen is present in the gas phase, the free radicals produced by NO₂ reaction with HS⁻ will catalyze sulfide oxidation by reactions such as:



This mechanism is consistent with the findings of Kuhn et al. (1983), who reviewed the air oxidation of aqueous sulfide solutions. They observed that the rate of sulfide oxidation was first order with respect to both sulfide concentration

and O_2 partial pressure, and $S_2O_3^{2-}$ was determined to be one of the oxidation products.

Because NO_2 absorption can catalyze S(-II) oxidation by a mechanism similar to that of S(IV) oxidation, i.e., by initializing the formation of free radicals, it is expected that a free radical scavenger such as thiosulfate can reduce the rate of S(-II) oxidation when it is added to the solution.

2.4.3 Reaction Product

Seel and Wagner (1988) have studied the reactions of NaHS, Na_2S_2 , and Na_2S_4 with NO by UV-visible and NMR spectroscopy. The formation of N-nitrosohydroxylamine monosulfonate, $ONNOSO_3^-$ was confirmed, via the reaction



They also observed that unstable orange-yellow perthionitrite, $ONSS^-$, formed temporarily.

2.5 THEORY OF SIMULTANEOUS MASS TRANSFER WITH CHEMICAL REACTION

The study of NO_2 absorption into S(IV) solutions is fundamentally a study in the field of simultaneous mass transfer with chemical reaction. The physical absorption of NO_2 is slow, but the rate of absorption is greatly enhanced by the chemical reaction between NO_2 and various S(IV) species in the solution. Several theories have been developed to deal with such problems in mass transfer, among which are the film theory, the penetration theory, and the surface renewal theory. A brief description will be given to each of these theories, and the final form of our model will be justified.

2.5.1 Film Theory

The earliest and simplest model to describe mass transfer at a fluid boundary is the film theory proposed by Whitman (1923). This model is based on the assumption that for a fluid flowing turbulently over a solid, the entire resistance to mass transfer resides in a stagnant film in the fluid next to the surface. It pictures a stagnant film of thickness δ at the surface of the liquid next to the gas. While the rest of the liquid is kept uniform in composition by agitation, the concentration in the film falls from $\frac{P_i}{H}$ at its surface to C^* at its inner edge, where C^* is the average concentration of dissolved gas in the bulk liquid. There is no convection in the film, and dissolved gas crosses it by molecular diffusion alone. The mass transfer coefficient is equal to $\frac{D}{\delta}$, where δ is the thickness of the stagnant film.

2.5.2 Penetration Theory

Higbie (1935) suggested a penetration theory for transfer across a gas-liquid interface. This theory assumes that the liquid surface consists of small fluid elements that contact the gas phase for an average time, after which they penetrate into the bulk liquid. Each element is then replaced by another element from the bulk liquid phase. The penetration theory predicts the mass transfer coefficient to be $2\sqrt{\frac{D}{\pi t_s}}$, where t_s is the exposure time of the fluid element.

2.5.3 Surface Renewal Theory

On the basis of the penetration theory, Danckwerts (1970) suggested that the constant exposure time in penetration theory be replaced by an average

exposure time determined from an assumed time distribution. The chance of an element being replaced on the surface was independent of the time during which it had been exposed. For this model the mass transfer coefficient is equal to \sqrt{Ds} , where s is the rate of surface renewal and is equal to the reciprocal of the exposure time of the elements.

2.5.4 The Effect of Chemical Reactions

The above discussed models can be modified to predict the effect of a chemical reaction on the rate of absorption. Predictions based on the three models are quite similar, except in regard to the effect of the diffusivity of the solute gas and of dissolved reactants on the rate of absorption. For instance, the film model predicts that mass transfer coefficient is proportional to diffusivity while both penetration and surface renewal theory predict that it varies as \sqrt{D} . It is difficult to make an accurate test of this dependence, since the diffusivities of typical solute gases do not cover a wide range and are difficult to determine accurately. For the same reasons, the dependence of mass transfer coefficient on the diffusivity is usually of lesser importance. In most cases the film theory would lead to almost the same predictions as the penetration and surface renewal theory. Furthermore, the difference between predictions made on the basis of the three models discussed above will be less than the uncertainties associated with the different variables used in the calculation. Therefore, these three models can be regarded as interchangeable for many purposes, and it is then merely a question of convenience which of the three is used.

The governing equation, in the case of an irreversible first-order reaction, is given by the material balance:

$$D \frac{\partial^2 C}{\partial x^2} = \frac{\partial C}{\partial t} + k_1 C \quad (2.31)$$

with the following boundary conditions:

1. $C = 0$ at $x > 0$ and $t=0$
2. $C = \frac{P_i}{H}$ at $x = 0$ and $t > 0$
3. $C = 0$ at $x = \infty$ and $t > 0$

C is the concentration of the absorbed gas in the solution, P_i the interfacial partial pressure of the gas being absorbed, H its Henry's constant, and x the liquid depth.

According to the surface renewal theory, k_l° , the liquid phase mass transfer coefficient, is given as (Danchwerts, 1970):

$$k_l^\circ = \sqrt{Ds}$$

D is the diffusivity of the absorbed gas species in the solution, and s is the fraction of the area of the surface which is replaced with fresh liquid in unit time. The hydrodynamic properties of the system so far as they affect k_l° are accounted for by the parameter s which has the dimensions of reciprocal time.

In order to remove the term $\frac{\delta C}{\delta t}$ in equation 2.31 so as to simplify the integration, Danckwerts (1970) used an average concentration C_{ave} . C_{ave} is averaged over the various elements comprising the surface and therefore it is independent of time. The solution of C_{ave} is:

$$C_{ave} = \frac{P_i}{H} \exp\left(-\frac{x k_l^\circ}{D} \sqrt{1 + \frac{D k_1}{k_l^{\circ 2}}}\right) \quad (2.32)$$

The average rate of absorption per unit area of gas-liquid interface, or flux, is obtained from:

$$N = -D \left(\frac{dC_{ave}}{dx} \right)_{x=0} = k_l^\circ \left(\frac{P_i}{H} \right) \sqrt{1 + \frac{D k_1}{k_l^{\circ 2}}} \quad (2.33)$$

Similarly, for an irreversible reaction that is second-order in the absorbing gas, this theory predicts the average flux to be:

$$N = k_l^\circ \left(\frac{P_i}{H} \right) \sqrt{1 + \frac{2 D k_2 P_i}{3 k_l^{\circ 2}}} \quad (2.34)$$

If the reaction is fast enough (large k_1 and k_2), the fluxes can be simplified as :

$$N = \left(\frac{P_i}{H} \right) \sqrt{D k_1} \quad (2.35)$$

and

$$N = \left(\frac{P_i}{H} \right) \sqrt{\frac{2 D k_2 P_i}{3}} \quad (2.36)$$

In the above derivation, N is flux, k_1 and k_2 are first-order and second-order rate constants, D is the diffusion coefficient in liquid phase, k_l° is liquid film mass transfer coefficient, H is Henry's constant, P_i is interfacial partial pressure of the dissolving gas, C is the concentration of the gas in the liquid, x is the distance below the gas-liquid surface and t is time.

In equation 2.33, the quantity $\sqrt{1 + \frac{D k_1}{k_l^{\circ 2}}}$ is known as the enhancement factor E . E is defined as the ratio of flux accompanied by chemical reactions to the flux without reaction, i.e., physical absorption. For surface renewal theory, E can be defined as:

$$E = \sqrt{1 + Ha^2} \quad (2.37)$$

In the above equation, Ha is the Hatta number, defined as:

$$Ha = \sqrt{\frac{Dk_1}{k_1^{\circ 2}}} \quad (2.38)$$

If E is 1, it represents physical absorption with no reaction, in which case the dissolved gas diffuses from the surface to the bulk without reaction on the way. If $E \gg 1$, the dissolved gas all reacts in the film and none diffuses in the unreacted state into the bulk of the liquid. In this case the film thickness, or the value of k_1° , is irrelevant and does not appear in the expression for flux N.

2.5.5 Application of Theory to NO₂-S(IV) System

In the baseline case of NO₂ absorption into solutions of S(IV), three reactions contribute to the overall removal of NO₂. They are the reactions between NO₂ and sulfite, bisulfite, and water, whose respective rate expressions were given in equations (2.7), (2.8), and (2.24). In the case when thiosulfate is also present in the solution, S₂O₃⁼ can also react directly with NO₂ with the following rate expression:

$$r_{S_2O_3=} = k_2[NO_2][S_2O_3=] \quad (2.39)$$

After substituting the above rate expressions into equation (2.35), and by using the approximation for fast reactions as developed by Glasscock and Rochelle (1993), the absorption flux expression of NO₂ absorption into S(IV) solutions is obtained:

$$N_{NO_2} = \frac{P_{NO_2,i}}{H_{NO_2}} \sqrt{D_{NO_2} \left(k_{2,S_2O_3=} [SO_3^{=}]_i + k_{2,HSO_3-} [HSO_3^-]_i + \frac{2}{3} \frac{k_{2,H_2O} P_{NO_2,i}}{H_{NO_2}} + k_{2,S_2O_3=} [S_2O_3=]_i \right)} \quad (2.40)$$

In the above equation, H_{NO_2} and D_{NO_2} are the Henry's constant and the diffusivity of NO₂, respectively. $P_{NO_2,i}$, the interfacial partial pressure of NO₂, is

used instead of $P_{\text{NO}_2,b}$, the bulk gas phase NO_2 partial pressure, in order to correct for gas film control. $P_{\text{NO}_2,i}$ is calculated by the following equation:

$$P_{\text{NO}_2,i} = P_{\text{NO}_2,b} - \frac{N_{\text{NO}_2}}{k_g} \quad (2.41)$$

In the above equation, k_g is the gas film mass transfer coefficient. The value of H_{NO_2} was reported by Andrew and Hanson (1965), and the correlation for D_{NO_2} was given by Wilke and Chang (1955). Table 2.1 lists the values of H_{NO_2} and D_{NO_2} at different temperatures.

Table 2.1 Henry's constants and diffusion coefficient of NO_2 .

Temperature (°C)	H_{NO_2} ($10^4 \text{ cm}^3\text{-atm/mol}$)	D_{NO_2} ($10^{-5} \text{ cm}^2/\text{s}$)
10	1.54	1.68
15	1.82	1.86
25	2.44	2.16
55	4.76	3.28

Because the reaction between NO_2 and S(IV) species and the oxidation of sulfite to sulfate are all believed to occur in the liquid boundary, the interfacial concentrations of $\text{SO}_3^{=}$ and HSO_3^- can be significantly different from their bulk solution concentration. To correct for this difference, all concentrations in equation (2.40) are reported at their interfacial condition. These concentrations are calculated by using the Bechtel-Modified Radian Equilibrium Program (Epstein, 1975), an equilibrium program capable of calculating the concentrations of all major species in the $\text{SO}_3^{=}$ system, given the ionic strength, pH, total [S(IV)] and [S(VI)], total $[\text{Na}^+]$ and other metal ions present, and the concentration of buffer when it is present. To calculate $[\text{SO}_3^{=}]_i$ and $[\text{HSO}_3^-]_i$, the bulk solution $[\text{SO}_3^{=}]$ and $[\text{HSO}_3^-]$ were first calculated by the equilibrium program, then by

using the experimentally measured rate of sulfite oxidation, the $[S(IV)]$ at the interface was estimated from the following equation:

$$[S(IV)]_i = [S(IV)]_b - \frac{N_{ox}}{k_l^\circ S(IV)} \quad (2.42)$$

The equilibrium program was used again at interfacial condition to obtain the interfacial concentrations of sulfite and bisulfite. In equation 2.42, $k_l^\circ S(IV)$ is the liquid phase mass transfer coefficient of $S(IV)$ species, which is taken to be the same as $k_l^\circ SO_3=$.

Since our objective is to eventually regress the four reaction rate constants from equation (2.40), we can linearize the expression by using a normalized rate of absorption, R_g , defined as:

$$R_g = \frac{N_{NO_2}}{P_{NO_2} i} \quad (2.43)$$

In the absence of gas film resistance, R_g is identical to K_g , the overall gas phase mass transfer coefficient. By using R_g , equation (2.40) can be simplified to:

$$\frac{R_g^2 H_{NO_2}^2}{D_{NO_2}} = k_2 SO_3=[SO_3=]_i + k_2 HSO_3-[HSO_3^-]_i + \frac{2}{3} \frac{k_2 H_2O P_{NO_2} i}{H_{NO_2}} + k_2 S_2O_3=[S_2O_3=]_i \quad (2.44)$$

A parameter estimation program, BETAV3 (Daniel and Wood, 1980), is then used to regress the four rate constants for any given set of experiments.

The absorption flux expression of NO_2 absorption into $S(-II)$ solutions is much simpler. It is given as:

$$N_{NO_2} = \frac{P_{NO_2} i}{H_{NO_2}} \sqrt{D_{NO_2} (k_2 HS-[HS^-]_i + \frac{2}{3} \frac{k_2 H_2O P_{NO_2} i}{H_{NO_2}})} \quad (2.45)$$

Since HS^- is more reactive toward NO_2 than sulfite, in most cases the NO_2 - HS^- rate term is far greater than the NO_2 -water rate term, so the latter can be

neglected. It is only under conditions of low HS^- concentration and higher NO_2 partial pressure that the NO_2 -water reaction becomes important.

Chapter 3

Experimental and Analytical Methods

This chapter describes the stirred cell contactor in which NO₂ absorption was studied, and the analytical methods used for liquid and gas phase speciation. The experimental procedures and operating range of important variables are also presented.

3.1 EXPERIMENTAL METHODS

3.1.1 Stirred Cell Contactor and Supporting Equipment

All experiments were performed in a stirred-cell contactor, the schematic of which is given in Figure 3.1. This design was based upon similar gas-liquid contactor devices for which mass transfer properties had been determined by several previous investigators, including Chang and Rochelle (1981), Versteeg (1987), Sada (1981), Huasheng (1988) and Uchida (1978). This reactor was originally used by McGuire (1990) in studying the absorption of SO₂ in Ca(OH)₂ slurries, and certain modifications had been made for the purpose of this study. A similar contactor was used by Zhao (1997) in studying the aqueous absorption of mercury.

The dimension of the stirred cell is given in Figure 3.2. The cylindrical contactor had a 4-inch diameter cross section and 6 1/2-inch height. The total volume of the reactor was 1.275 liters, of which 1.10 liters was the typical liquid volume. The gas/liquid contact area was 81 cm². The reactor vessel was a thick

glass cylinder with 316 stainless steel metal plates sealed to the top and bottom by thick gasket clamps. Four 3/8" wide, equally spaced baffles of 316 stainless steel were welded to the base plate. The base plate also contained Swagelock fitted ports for liquid inlet and outlet. The top plate contained Swagelock fitted ports for the gas inlet and outlet and the thermocouple.

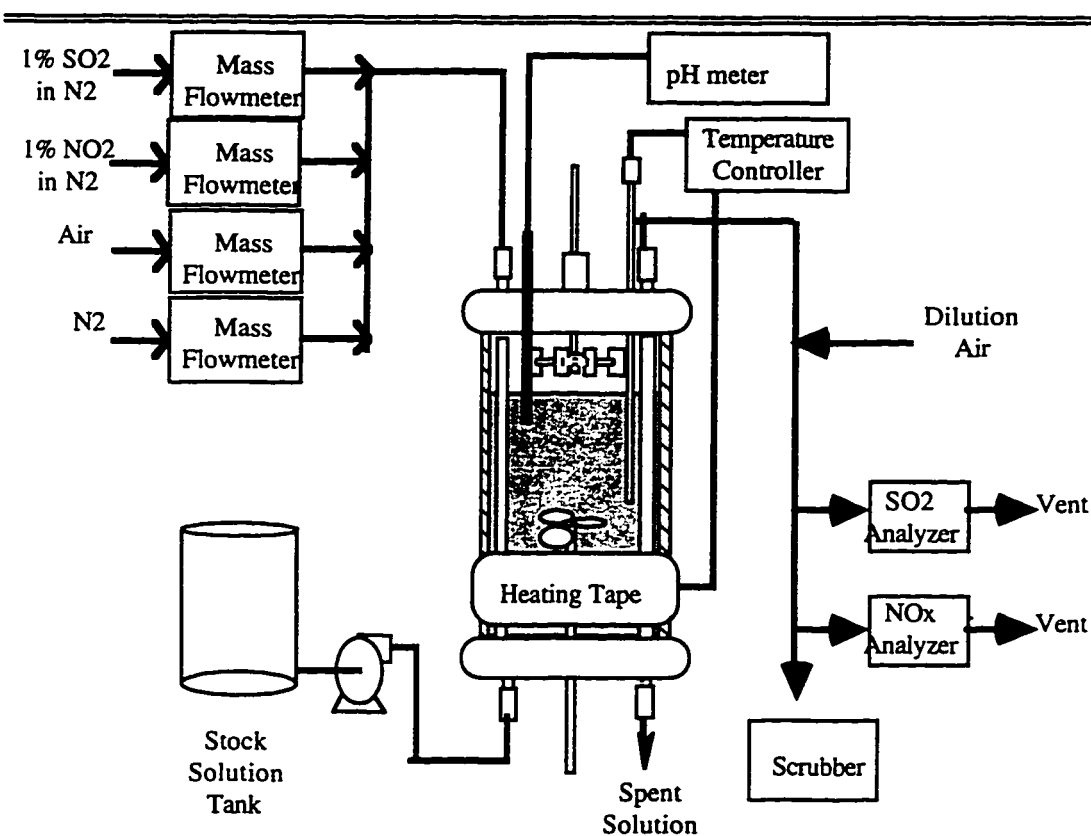


Figure 3.1 Stirred cell contactor.

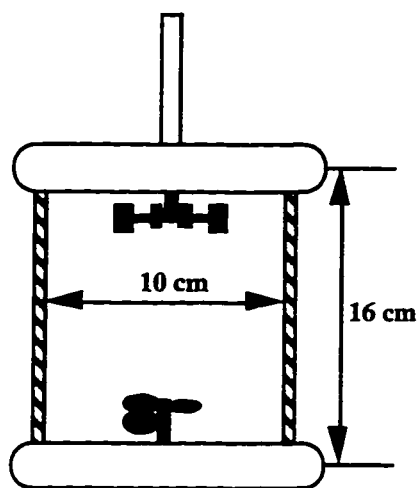


Figure 3.2 Dimensions of the gas-liquid contactor.

The reactor was equipped with separate gas phase and liquid phase agitators which are controlled independently. The dimensions of the agitator propellers are given in Figure 3.3. The gas phase propeller was a six-blade flat turbine with a diameter of 6.35 cm. The liquid phase was agitated by a three-blade marine type agitator with a diameter of 5.08 cm. FisherBrand StedFast Stirrers (Model SL 1200) were used to drive gas and liquid phase propellers. Agitator speeds were measured by a hand-held Ono Sokki HT-4100 digital tachometer, and for most of the experiments the agitation speed for the gas phase was kept at 550-650 rpm and the liquid phase at 650-800 rpm. The gas and liquid phase mass transfer coefficients were calibrated as functions of gas and liquid

agitation rates in this exact contactor by McGuire (1990), and the calibration results are tabulated in table 3.1.

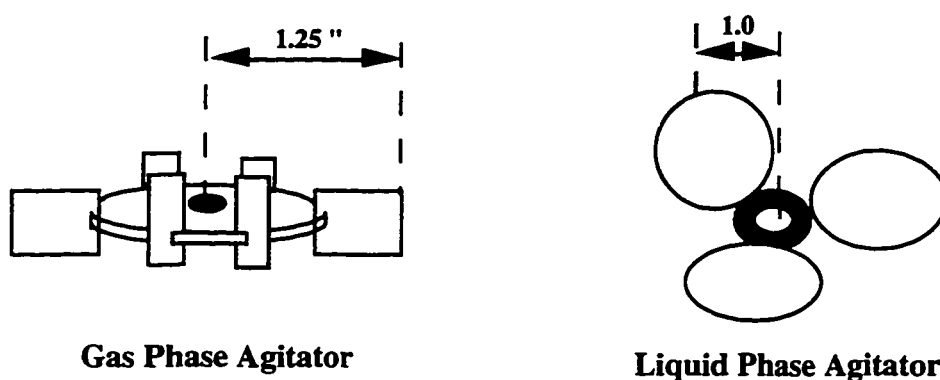


Figure 3.3 Agitator propeller design and dimensions.

Table 3.1 Calibration of gas and liquid phase mass transfer coefficients

Phase	Temp (°C)	Calibration Equation (A = 81 cm ²)
Gas	25 and 55	$k_g \cdot A \text{ (mol/s-bar)} = 4.95e-5 \cdot (\text{rpm})^{0.76}$
Liquid	25	$k_l \times 10^5 \text{ (m/s)} = 2.8e-2 \cdot (\text{rpm})^{0.74}$
	55	$k_l \times 10^5 \text{ (m/s)} = 8.84e-2 \cdot (\text{rpm})^{0.65}$

Since most of the experiments were performed at elevated temperature (55 °C), an Omegalux FGH101-060 heating tape was used to heat up the contents of the reactor. It was wrapped around the glass cylinder of the reactor, and the solution temperature was measured by an Omega K type Teflon coated thermal couple inserted into the reactor. The output of the heating tape was controlled by an Omega temperature controller connected to the thermal couple.

During our study we had made several modifications to the design of the contactor. We moved the gas inlet from the edge of the top plate to the near center, directly above the gas agitator blade, so as to avoid any problem caused by inadequate mixing of the inlet gas. Another change we made to the contactor was that we added an outlet on the top plate where a WIKA pressure gauge (range 0-60 psig) was connected. This allowed us to monitor any pressure change inside the contactor which might be caused by plugging of the line. A related modification was that we changed all tubing downstream of the air dilution point from 1/4" Teflon tubing to 3/8" Teflon tubing so that pressure drop in the lines was minimized. Finally, we added an inlet on the top plate where an Accumet SN 5115079 Pencil-Thin Epoxy Body Gel-Filled pH probe was inserted into the solution inside the contactor. The pH probe was connected to a Corning pH meter 125 so that the solution pH could be monitored continuously. A drawing of the final design of the top plate is given in Figure 3.4.

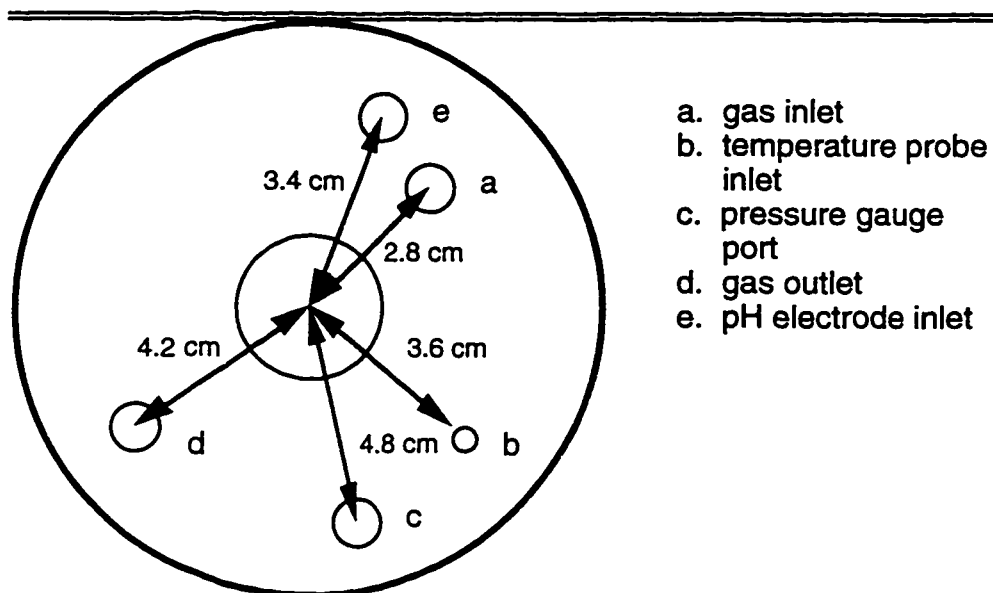


Figure 3.4 Top view of top cover plate.

3.1.2 Mode of Operation

Synthetic flue gas was prepared by quantitative blending of 1% NO_2 in nitrogen and 1.1% SO_2 in nitrogen with nitrogen or house air. The flow rate of all gas streams was measured by Brooks mass flow meters and controlled by Brooks mass flow controller model 5878. Table 3.2 gives the range and calibration equation of all flow meters used in this study. The synthetic flue gas entered the reactor through the gas inlet on the top plate, and NO_2 was absorbed across an unbroken interface into a well-mixed solution. Gas leaving the reactor was diluted by a factor of 20 or more with air, both to reduce the relative humidity of the gas so that condensation would not occur inside the analyzers, and to bring the

NO_x concentration to within the range detectable by the analyzer. The concentration of NO₂ in the outlet flow was monitored continuously, and a gas phase mass balance gave the rate of NO₂ absorption. A Thermo Electron chemiluminescent NO/NO_x analyzer (Model 10 AR) was used to measure the NO₂ concentration, and a Thermo Electron pulsed fluorescent SO₂ Analyzer (Series 45) was used to measure the SO₂ concentration when necessary. The range of inlet flue gas conditions are given in table 3.3.

Table 3.2 Range and calibration equations for Brooks mass flow meters

Serial number	Range	Calibration equation
8707HCO38406/2	0-100 cc/min	flow rate (cc/min) = -0.15 + 1.05x(% open)
8707HCO38404/2	0-250 cc/min	flow rate (cc/min) = -1.33 + 2.47x(% open)
8707HCO33415	0-1 SLPM	flow rate (cc/min) = 1.25 + 11.2x(% open)
8707HCO37101	0-2 SLPM	flow rate (cc/min) = 4.10 + 21.0x(% open)
9310HCO38402	0-5 SLPM	flow rate (L/min) = -0.31 + 0.13x(% open)
9310HCO37104	0-30 SLPM	flow rate (L/min) = -0.03 + 0.30x(% open)

Table 3.3 Operating Ranges of Synthesized Flue Gas

Process Variable	Range
NO ₂	0 - 1000 ppm
SO ₂	0 - 1000 ppm
O ₂	0 - 15 %
Temperature	25 & 55 °C
Flow Rate	0.5 - 2.0 slpm
Pressure	14.7-15.7 psia

The stirred-cell contactor was operated both in batch mode or continuously. When operating in batch mode, the solution was fed into the

reactor before each experiment and was withdrawn after each run. Nothing was added or withdrawn during the course of the experiment. While this mode of operation had the advantage of simplicity, the sulfite concentration in the solution as well as the solution pH underwent significant change during the course of a run, which was undesirable for parts of our study. Therefore, the majority of our experiments were performed in a continuous manner.

When operating in a continuous mode, a solution containing Na_2SO_3 , Na_2SO_4 and other additives such as succinic acid and sodium thiosulfate was freshly prepared and fed into the contactor. Between 100 to 300 mM of Na_2SO_4 was used to keep a constant ionic strength for all the runs. Once the run began, a mixture of $\text{Na}_2\text{SO}_3/\text{NaHSO}_3/\text{NaOH}$ of predetermined concentration was periodically fed into the contactor for the purpose of maintaining a constant solution pH and total S(IV) concentration, and the same volume of solution was withdrawn from the contactor at the same time for solution analysis. The addition and withdrawal of solutions were done using a Cole-Parmer Masterflex "Unified" Drive model 7521-25 with two QuickLoad Pump Heads model 7013-20. The maximum flow rate deliverable by the pump was 5 ml/min. Pressure inside the contactor was kept at 1.1 psig, and other important operating variables such as the temperature, the solution pH, and the liquid and gas agitation rates were monitored and controlled.

3.2 GAS AND LIQUID PHASE ANALYSIS

Both the gas and liquid phases were analyzed to determine their respective compositions. The concentrations of NO_2 and SO_2 in the gas phase were

analyzed by NO_x and SO_2 analyzers. In the liquid phase, the concentrations of SO_3^- and $\text{S}_2\text{O}_3^{2-}$ were determined by iodometric titration, the concentration of HS^- was determined by titrating with AgNO_3 , the concentration of metal ions such as Fe^{++} was determined by atomic absorption, and the concentration of the various nitrogen-sulfur compounds were determined by ion chromatography.

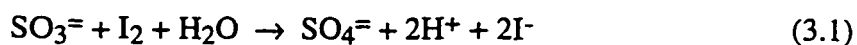
3.2.1 Gas Phase Analysis

The operating procedures of the NO_x and SO_2 analyzers are found in their respective manuals (Thermo Environmental Instruments Inc., 1975). Prior to each experiment, a five point calibration was performed on the NO_x analyzer by sending a constant flow of 500 ppm NO_2 gas diluted by different amounts of N_2 to the analyzer. This same procedure was repeated after each run to minimize the effect of base line drifting. During the course of an experiment, output signals from the NO_x analyzer were recorded on a Soltec strip chart recorder (Model 1242). The voltage output from the analyzer was monitored by a SOAR digital multimeter model 5030, and it was recorded by hand at 5 minute intervals. In most cases, the voltage output varied linearly with NO_2 concentration; therefore the instantaneous concentration of NO_2 could be determined directly. NO_2 concentrations taken from the multimeter or strip chart recorder were entered into a spreadsheet program and the rate of NO_2 absorption was calculated. The same procedure was used to determine the rate of SO_2 removal by using output from the SO_2 analyzer.

3.2.2 Liquid Phase Analysis

Iodometric titration of sulfite and thiosulfate

Sulfite and thiosulfate concentrations were determined analytically by an oxidation-reduction titration with iodine using a procedure implemented by Tseng (1984). The chemistry involved in iodometric titration can be described as follows:



When only sulfite or thiosulfate was present in the sample solution, the titration procedure used was of a single step. An excess amount of standard iodine solution was added to the sample, and the sample was then back-titrated with a standard thiosulfate solution until the end point was reached. Tseng (1984) used soluble starch as the end point indicator, while in this study we defined the end point as the disappearance of the reddish color of iodine from the sample solution. By titrating against a standard sulfite solution, we discovered that our method consistently yielded more accurate results, due to the fact that Tseng's method was dependent upon the time of starch addition. The difference between the amount of iodine solution and thiosulfate solution used gave the concentration of sulfite or thiosulfate in the sample. A sample calculation of this titration procedure is given in Appendix C1.

When both sulfite and thiosulfate were present in the sample, the concentration of individual SO_3^{2-} and $\text{S}_2\text{O}_3^{2-}$ was determined by a two-step titration method developed by Thorn (1981). First, the sample was titrated using

the standard method described above, and the result gave the total concentration of $\text{SO}_3^{=}$ plus half of $\text{S}_2\text{O}_3^{=}$. Then in a separate sample solution, several drops of phenolphthalein and enough NaOH solution were added until the sample turned pink. Then 2 ml of 35% formaldehyde was added to tie up all the sulfite in the solution via the following reaction:



The complex formed was unreactive to iodine. After 5 minutes an acetic acid solution was introduced into the sample until the solution returned to colorless, and then the sample was titrated with iodine. This step gave the thiosulfate concentration, and subtracting half of it from step one gave the total sulfite concentration. A sample calculation is given in Appendix C2.

AgNO₃ titration of bisulfide

In a sample containing S(-II), the concentration of bisulfide was determined by titrating with standard AgNO₃ solution (Stahl et al., 1987). The sample was diluted with distilled water 20 times and titrated with a standard AgNO₃ solution. A Fisher Scientific double junction specific ion electrode, model 90-02-00, was inserted into the sample and a prepared standard solution and it indicated the end point of the titration at 10 mV.

Nitrogen-sulfur compounds by ion chromatography

Ion chromatography (IC) was used to detect nitrite, nitrate, and various sulfur-nitrogen compounds formed as products of NO₂ absorption into sulfite solutions. The operating procedure of the IC was implemented by Nelli (1996). The sample solution was first diluted with distilled water then injected into the IC

column. In ion chromatography, the injected ion comes to equilibrium with the solid adsorbent and is held up until displaced by the eluent ion. Hold-up time is a function of the affinity of the injected ion for the adsorbent relative to that of the eluant ion. The conductivity of the solution exiting the column is measured as a function of time and is proportional to ion concentration.

The instrument used was a Dionex model 2000i/SP with a Hewlett-Packard 3390A reporting integrator. The guard and separator columns were Dionex AG4A and Dionex AS4A, respectively. The eluent was a 15 mM Na_2CO_3 solution. A pump setting of 6.0 regulated proper flow which resulted in an upstream pressure of 700 psi.

For typical IC analysis, a sample was diluted by a factor of 10, and injected into the IC. A sample loop within the IC controlled the sample size for each injection. Standard solutions of nitrite, nitrate, sulfate, hydroxylamine disulfonate (HADS), and amine disulfonate (ADS) were prepared for calibration purposes. Hydrogen peroxide (H_2O_2) was added to some of the sample solution to oxidize any S(IV) to S(VI). S(VI) species, such as sulfate, are easier to detect than S(IV) species. Analysis of the solution sample showed good closure of the gas phase material balances used to determine rates of removal of NO_2 and SO_2 . For example, $(96 \pm 10)\%$ of the nitrogen removed from the gas stream was recovered in the solution. Similarly, $(98 \pm 17)\%$ of the sulfur was recovered as well.

Fe⁺⁺ analysis by atomic absorption

In determining the effect of trace Fe⁺⁺ on the rate of sulfite oxidation, it became necessary to measure the background concentration of Fe⁺⁺ in solutions of Na₂SO₃. This was done by using a Varian Atomic Absorption (AA) Spectrophotometer Series AA-1475. To determine the concentration of total dissolved iron, an air-acetylene flame was used together with a SpectrAA iron (Fe) lamp, and the AA was calibrated by using an Aldrich Chemical standard iron solution. Within the concentration range indicated, the readout on AA varied linearly with iron concentration in the sample. Because the low concentration of Fe⁺⁺ in the sample, no dilution was performed on the samples. Each sample was run three times and an average readout was used to determine the Fe⁺⁺ concentration.

Chapter 4

Results of Batch Experiments

This chapter presents the results obtained by operating the stirred cell contactor in a batch mode. Rate constants of the reactions between NO_2 and sulfite, bisulfite, sulfide, thiosulfate, and water at 25 °C, with and without the presence of oxygen were measured by batch experiments and reported. The effects of bulk solution sulfite concentration, interfacial NO_2 partial pressure, the presence of oxygen, and temperature on the rate of NO_2 absorption were studied.

4.1 NO_2 ABSORPTION INTO 0.1 M SOLUTIONS

A series of batch experiments was performed in which NO_2 was absorbed into 0.1 M solutions of Na_2SO_3 , NaHSO_3 , $\text{Na}_2\text{S}_2\text{O}_3$, and Na_2S . Nitrogen was used as diluent in most of these experiments, but air was also used in some cases. The inlet concentration of NO_2 varied from 200 to 1000 ppm. The absorption was mostly performed at 25 °C, but several of the measurements were taken at 55 °C. The solutions were prepared by dissolving the required amount of chemicals in distilled water to give a nominal concentration of 0.1 M. No solution analysis was performed to determine the actual concentration of each species in the liquid phase, so a nominal concentration had to be assumed to take into account the effect of oxidation prior to and during the experiment. Furthermore, the concentration assumed was different for each case, depending upon the type and concentration of S(IV) compound used (see table 4.1), as the amount of oxidation occurred was directly related to the concentration of the S(IV) species. The gas

phase agitation rate was kept between 750-850 rpm, and the liquid phase agitation rate at 650-750 rpm. Nothing was added or withdrawn from the stirred cell contactor during the course of an experiment.

Table 4.1 summarizes the results of all batch experiments. A sample calculation of R_g and k_2 for batch experiments is given in Appendix D.

Table 4.1 NO_2 Absorption into 0.1 M Solutions. Batch Results. $Y_{\text{NO}_2} = 200\text{--}1000$ ppm.

Exp No.	Reagent (M)	pH	Y_{O_2} (%)	$R_g \times 10^6$ (mol/cm ² s-atm)	$k_2 \times 10^{-5}$ (M ⁻¹ s ⁻¹)	T (°C)
4.1.1	0.085* Na_2SO_3	9.6	0	39.5	6.3	25
4.1.2	0.085* Na_2SO_3	9.6	0	41.3	18.7	55
4.1.3	0.45* Na_2SO_3	10.1	0	57.7	0.94	10
4.1.4	0.45* Na_2SO_3	10.1	0	73.9	1.9	15
4.1.5	0.45* Na_2SO_3	10.1	0	49.5	2.0	25
4.1.6	0.085* Na_2SO_3	9.6	15	18.2	1.1	25
4.1.7	0.09* NaHSO_3	4.2	0	3.8	0.083	25
4.1.8	0.1 $\text{Na}_2\text{S}_2\text{O}_3$	8.7	0	4.7	0.079	25
4.1.9	0.1 Na_2SO_3 (+0.1 $\text{Na}_2\text{S}_2\text{O}_3$)	9.6	0	39.0	6.0	25
4.1.10	0.1 Na_2SO_3 (+0.5 $\text{Na}_2\text{S}_2\text{O}_3$)	9.2	0	35.6	5.1	25
4.1.11	pure H_2O	—	0	3.1	271	25
4.1.12	0.1 Na_2S (+0.1 NaOH)	12.3	0	34.6	4.7	25
4.1.13	0.1 Na_2S (+0.1 NaOH)	12.3	15	16.8	2.5	25
4.1.14	0.1 Na_2S (+0.5 $\text{Na}_2\text{S}_2\text{O}_3$ 0.1 NaOH)	12.7	15	32.8	9.4	25

*These concentrations were estimated empirically to account for the oxidation of $\text{SO}_3^{=}$ prior to each experiment. The correction was done by preparing solutions of 0.1 M nominal S(IV) concentration, and after the elapse of a similar period of time, the solution was analyzed and the actual concentration of S(IV) was measured experimentally. These concentrations were reported in the above table.

As mentioned previously, no solution analysis was performed to determine the actual concentrations of the various species in the solution, therefore a nominal concentration was assumed to account for oxidation of the S(IV) species both prior to and during the experiment. R_g is the rate of NO_2 absorption,

normalized by the interfacial partial pressure of NO_2 , and k_2 the second order rate constant. Figure 4.1 plots some representative batch results.

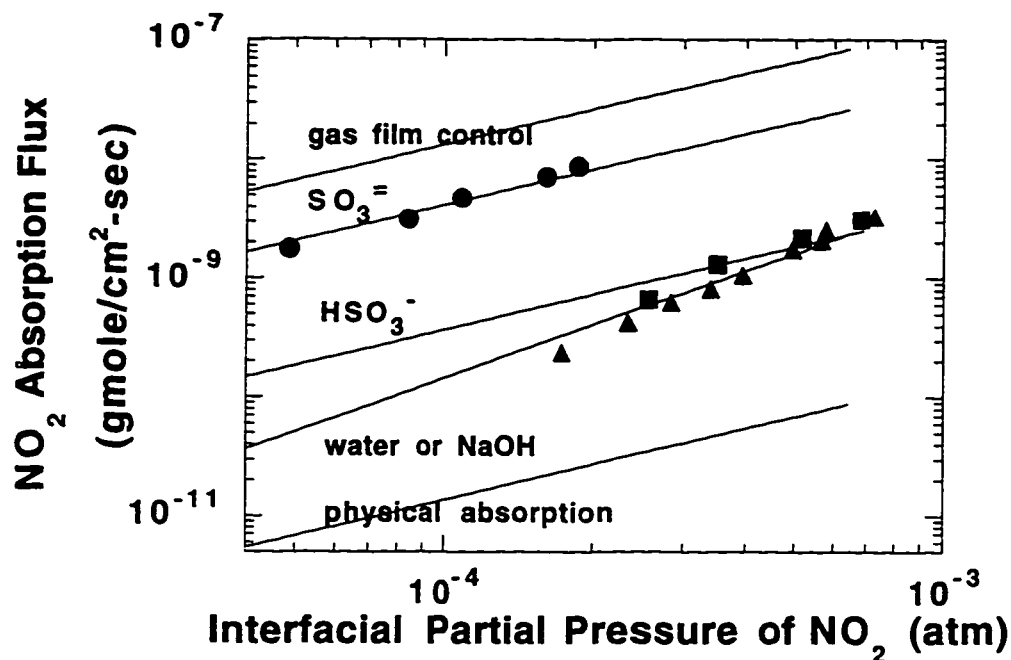


Figure 4.1 Batch results of NO_2 absorption. Runs 4.1.1, 4.1.7 and 4.1.11. 25 °C, with N_2 dilution.

The above plot indicates that the most effective reagent for reacting with NO_2 is sulfite. Bisulfite, on the other hand, is much less reactive. Therefore, the pH of a S(IV) solution is a very important factor in determining its efficiency in absorbing NO_2 , as the amount of S(IV) existing as sulfite decreases with pH. The absorption rate of NO_2 into water and NaOH solution is lower than that of bisulfite, but it is still an order of magnitude higher than that of pure physical

absorption of NO_2 , indicating that the chemical reaction between NO_2 and water is significant. Furthermore, figure 4.1 shows that the absorption of NO_2 into sulfite is still significantly below gas film control, indicating possibilities of improved NO_2 absorption by changing solution chemistry. When the absorption rate reaches gas film control, the rate of absorption is no longer affected by solution chemistry but rather limited by the transport of gas to the interface. Figure 4.2 gives the rate of NO_2 absorption into solutions containing 0.1 M of several other reagents.

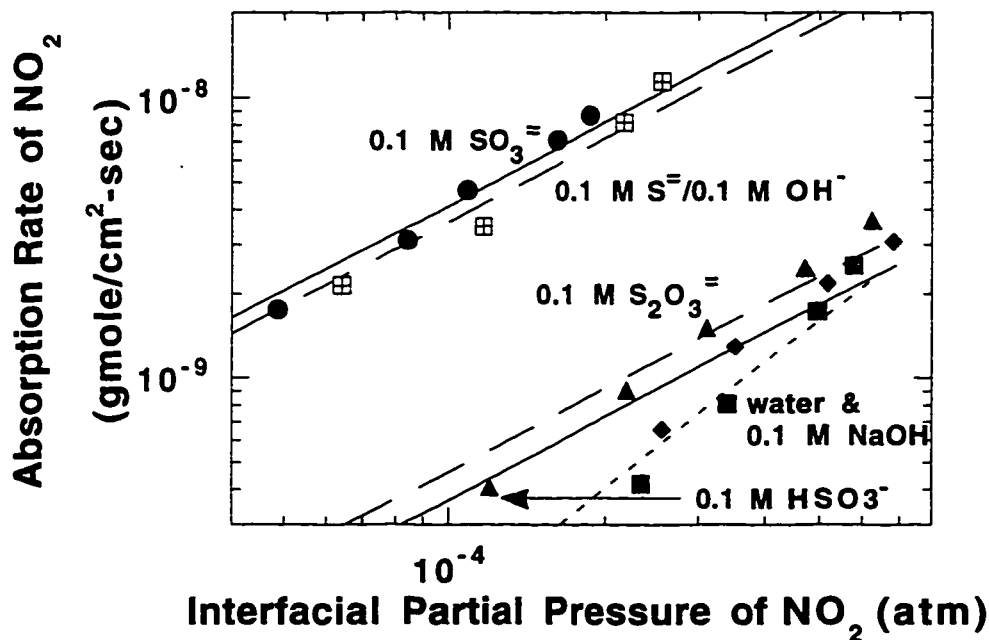


Figure 4.2 Absorption rates of NO_2 into 0.1 M Solutions. Runs 4.1.1, 4.1.7-4.1.8, 4.1.11-4.1.12. Batch results at 25 °C with N_2 dilution.

Figure 4.2 shows that sulfide was as effective in reacting with NO_2 as sulfite, as both reacted with NO_2 at similar rates with N_2 dilution at 25 °C. Thiosulfate was not very effective in reacting with NO_2 , as the rate of NO_2 absorption into 0.1 M thiosulfate was only slightly higher than that into 0.1 M bisulfite. The absorption rate of NO_2 into 0.1 M NaOH solution was essentially the same as that of water. This observation was consistent with the findings of Pigford et al. (1977), who concluded that hydrogen and hydroxyl ions had little effect on the absorption rate of NO_2 .

Figure 4.2 also shows the order of dependence of the reaction rate on the interfacial NO_2 partial pressure. The absorption curves of NO_2 into 0.1 M solutions of SO_3^{2-} , S^{2-} , HSO_3^- , and $\text{S}_2\text{O}_3^{2-}$ all have slope of 0.5, indicating a first order dependence of reaction rate on interfacial NO_2 concentration. The absorption curve of NO_2 into pure water, on the other hand, has a slope of 1.5, which suggests that the reaction rate is second order in NO_2 concentration. These observations are consistent with the reaction mechanism we have put forth in equations 2.10 and 2.22.

4.2 REACTION RATE CONSTANTS

By assuming a nominal concentration of the reactive species in the solution, it was possible for us to calculate the second order rate constant, k_2 , between NO_2 and various compounds, using equations 2.35 and 2.36. These rate constants are reported in table 4.1. To determine whether they are in agreement with results available from other researchers, a comparison of k_2 is given in table 4.2.

Table 4.2 Comparison of second order rate constants at 25 °C.

Reagent (M)	Diluent	k_2 , this study ($10^5 \text{ M}^{-1}\text{s}^{-1}$)	k_2 , Takeuchi et al. ($10^5 \text{ M}^{-1}\text{s}^{-1}$)
0.1 $\text{SO}_3^{=}$	N_2	6.3 ± 1.7	6.6
0.1 $\text{SO}_3^{=}$	Air	1.5 ± 0.18	2.5
0.1 HSO_3^-	N_2	0.083 ± 0.029	0.15
water	N_2	271 ± 130	740

4.2.1 Agreement of NO_2 -S(IV) Rate Constants

As mentioned earlier, although we did not attempt to assume an interfacial $\text{SO}_3^{=}$ concentration when calculating k_2 , we did make an empirical correction on $\text{SO}_3^{=}$ concentration that accounted for $\text{SO}_3^{=}$ oxidation prior to and during an experiment. Therefore, the sulfite concentration we used was actually fairly close to the interfacial $\text{SO}_3^{=}$ concentration. On the other hand, Takeuchi et al. (1977) used bulk sulfite concentrations when calculating the second order rate constants. As a result, it was not surprising that the best agreement of k_2 was at 25 °C with N_2 dilution, because when no oxygen was present, the oxidation of $\text{SO}_3^{=}$ was minimized, and the interfacial and bulk $\text{SO}_3^{=}$ concentration were very close to each other. Likewise, the discrepancy between k_2 with air dilution could be explained by the different $\text{SO}_3^{=}$ concentration used in our respective calculation. There is also a small difference between the NO_2 - HSO_3^- rate constants, and there may be two explanations for it. First, it could be due to the way we backcalculated the k_2 from Takeuchi's results. Takeuchi et al. (1977) did not report a k_2 for NO_2 - HSO_3^- . Instead they showed a family of absorption curves which represented the best fit of their experimental data. We took points off the 0.1 M HSO_3^- curve and backcalculated the k_2 . There could be error associated

with k_2 thus calculated. The second possible explanation was that we had not adequately account for bisulfite oxidation prior to the experiment. If the actual concentration of HSO_3^- in the solution was lower than our estimate of 0.09 M, it could result in a greater estimate of k_2 .

4.2.2 Discrepancy between NO_2 -Water Rate Constant

As can be seen from table 4.2, there is a large discrepancy between our NO_2 -water rate constant than that of Takeuchi's. This might be due to the different methods we used to derive our respective k_2 . The k_2 derived in this study was based upon absorption of NO_2 into pure water, while the k_2 reported by Takeuchi et al. (1977) was derived from NO_2 absorption into solution of Na_2SO_3 . Takeuchi et al. suggested that both the reaction between NO_2 and SO_3^{2-} and the hydrolysis of NO_2 contributed to the overall NO_2 absorption, and they proposed the following form of NO_2 absorption flux:

$$N_{\text{NO}_2} = [\text{NO}_2] \sqrt{\left(\frac{2}{3} k_{\text{hyd}} [\text{NO}_2] + k_2 \text{SO}_3 = [\text{SO}_3^{2-}] \right) D_{\text{NO}_2}} \quad (4.1)$$

They regressed the rate constants between NO_2 and sulfite and water from a linear form of the above equation. Therefore, any error in their estimation of the sulfite concentration and the NO_2 -sulfite rate constant would result in an error in their NO_2 -water rate constant. Furthermore, there seems to be disagreement among various researchers as to whether NO_2 or N_2O_4 was the species actually being absorbed. Peters et al. (1955) suggested that when the concentration of total nitrogen oxides in the gas phase was low, the species being absorbed into water was likely to be NO_2 . On the other hand, when the concentration of total nitrogen oxides was high, N_2O_4 was the species being absorbed. Since both Takeuchi

(1977) and us conducted our experiments with relatively low concentrations of NO₂ (<1000 ppm), we both assumed that NO₂ was the species being absorbed, and our rate equation assumes the form of:

$$r_{\text{H}_2\text{O}} = k_2[\text{NO}_2]^2 \quad (2.24)$$

On the other hand, Pigford et al. (1977) performed experiments with high concentrations of NO₂ (>1%), and they assumed that the species being absorbed was N₂O₄. Consequently, their rate expression has the form of:

$$r_{\text{H}_2\text{O}} = k_2[\text{H}_2\text{O}][\text{N}_2\text{O}_4] \quad (4.2)$$

This difference may account for the discrepancies in the normalized rate of nitrogen dioxide flux shown in figure 4.3.

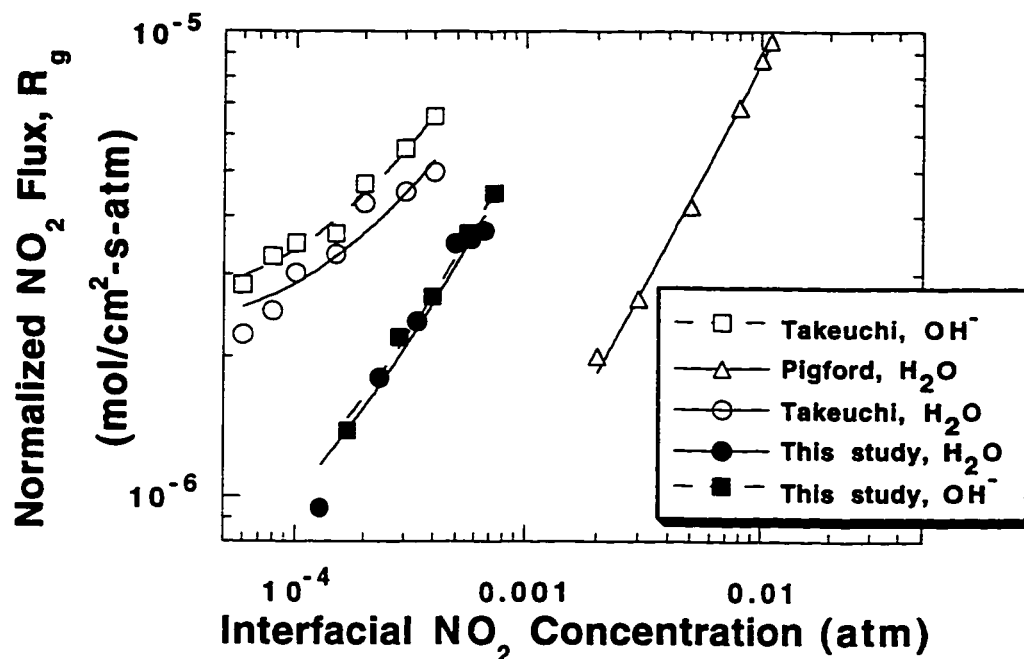


Figure 4.3 NO_2 absorption into water and 0.1 M NaOH at 25 °C. Our results contain both 0% and 15% O_2 . Other data contain only zero O_2 .

4.3 EFFECT OF AIR DILUTION ON RATE OF NO_2 ABSORPTION

Takeuchi et al. (1977) observed that when air instead of N_2 was used as diluent, the absorption rate of NO_2 into sulfite solutions decreased by 40%, and they believed that this was caused by the oxidation of SO_3^{2-} at the interface by O_2 in air. We measured the rate of NO_2 absorption into 0.1 M SO_3^{2-} , 0.1 M S^{2-} , and water, using first N_2 and then air as diluent, and the result is given in figure 4.4.

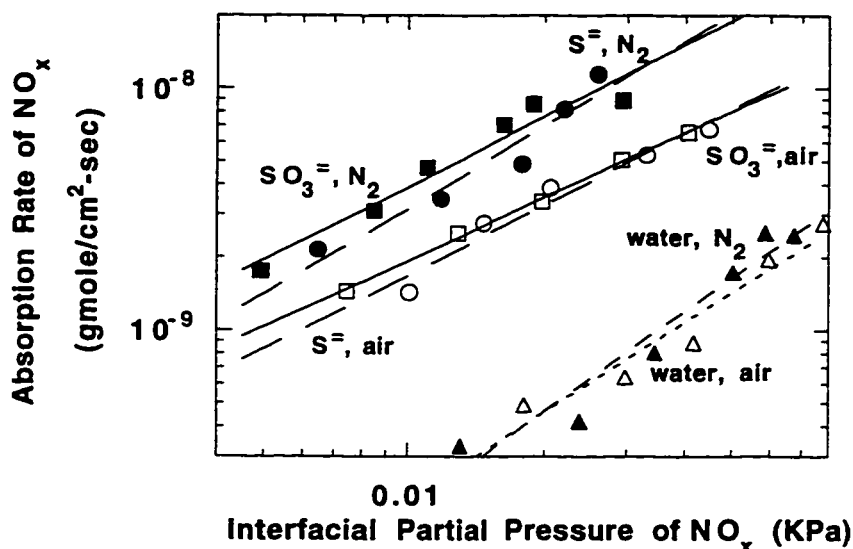


Figure 4.4 Effect of air dilution on NO_2 absorption at 25 °C. Runs 4.1.1, 4.1.6, 4.1.11-4.1.13. All concentrations except that of water were 0.1 M. Lines represent absorption rates predicted from average k_2 .

The absorption rates of NO_2 into sulfite and sulfide decreased by roughly 40% when air was used instead of N_2 , consistent with the observation by Takeuchi et al. (1977). The oxygen present in air reacted with SO_3^{2-} and S^{2-} at the liquid boundary and thus lowered their respective interfacial concentration, which in turn lowered the rate of NO_2 absorption. On the other hand, this oxidation mechanism does not apply to NO_2 absorption into pure water, therefore the presence of air should not affect the rate of NO_2 absorption into water, as reflected by the water absorption curves in figure 4.4.

4.4 EFFECT OF THIOSULFATE IN INHIBITING OXIDATION

When oxygen is present in the gas phase, it oxidizes sulfite at the liquid interface to sulfate, and thus reduces the rate of NO_2 absorption. If this hypothesis were true, then the presence of an oxidation inhibitor such as thiosulfate should be able to restore the rate of NO_2 absorption to where no O_2 is present. Sodium thiosulfate is an oxidation inhibitor because it acts as a free radical scavenger and is able to terminate the free radical mechanism by which sulfite is oxidized. We measured the rate of NO_2 absorption into 0.1 M Na_2SO_3 , using both air and N_2 as diluent, and compared the results to the rate of NO_2 absorption into 0.1/0.1 molar mixture of Na_2SO_3 and $\text{Na}_2\text{S}_2\text{O}_3$ (figure 4.5).

As we observed earlier, the use of air instead of N_2 as diluent caused a 40% decrease in the rate of NO_2 absorption into 0.1 M Na_2SO_3 solution. However, when 0.1 M $\text{Na}_2\text{S}_2\text{O}_3$ was added to the sulfite solution, the presence of oxygen no longer had any effect on the rate of NO_2 absorption, which is at the same level as NO_2 absorption into 0.1 M sulfite solution with N_2 as diluent. Since thiosulfate alone was not effective in removing NO_2 , this increase in NO_2 absorption rate with the addition of 0.1 M thiosulfate was too great to be explained by the additional removal caused by the direct reaction between NO_2 and thiosulfate, and therefore could only be contributed to the inhibiting effect of thiosulfate on sulfite oxidation.

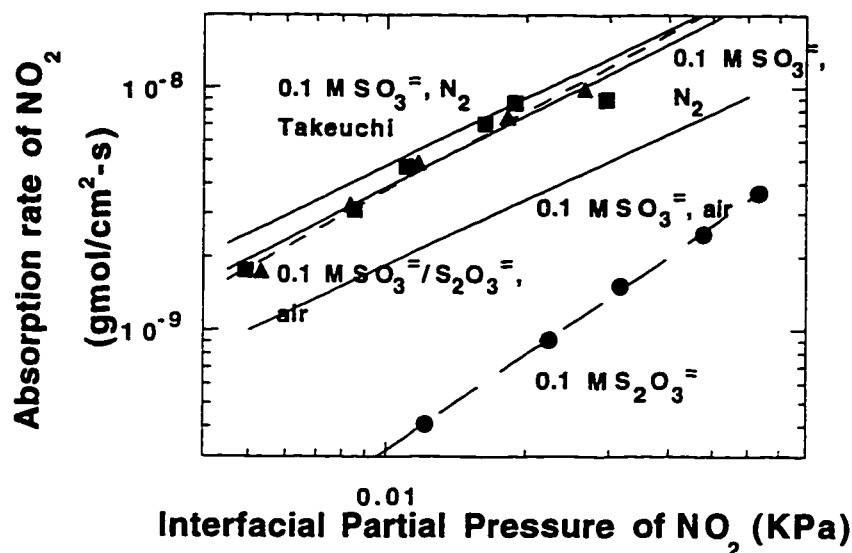


Figure 4.5 Effect of 0.1 M $\text{Na}_2\text{S}_2\text{O}_3$ on rate of NO_2 absorption into 0.1 M nominal Na_2SO_3 at 25 °C. Runs 4.1.1, 4.1.6, 4.1.8 and 4.1.14.

4.5 EFFECT OF TEMPERATURE ON NO_2 ABSORPTION

Takeuchi et al. (1977) studied the effect of temperature on NO_2 absorption. Their results showed that a temperature rise from 10 to 25 °C lowered the rate of NO_2 absorption in water and aqueous solutions of low SO_3^{2-} concentration. Wendel and Pigford (1958) have also reported such a decrease in the absorption of N_2O_4 into water. Takeuchi et al. (1977) attributed this effect to the decreased solubility of NO_2 in the liquid and the lower equilibrium concentration of N_2O_4 in the gas phase at higher temperature. However, they also

observed that the higher the sulfite concentration, the smaller the effect of temperature on the overall absorption rate, as the increase in reaction rate at higher temperature more than offset the decreased solubility.

We expanded the temperature range studied and measured the absorption of NO_2 into 0.1 M Na_2SO_3 solution and water at both 25 °C and 55 °C. The result is plotted in figure 4.6.

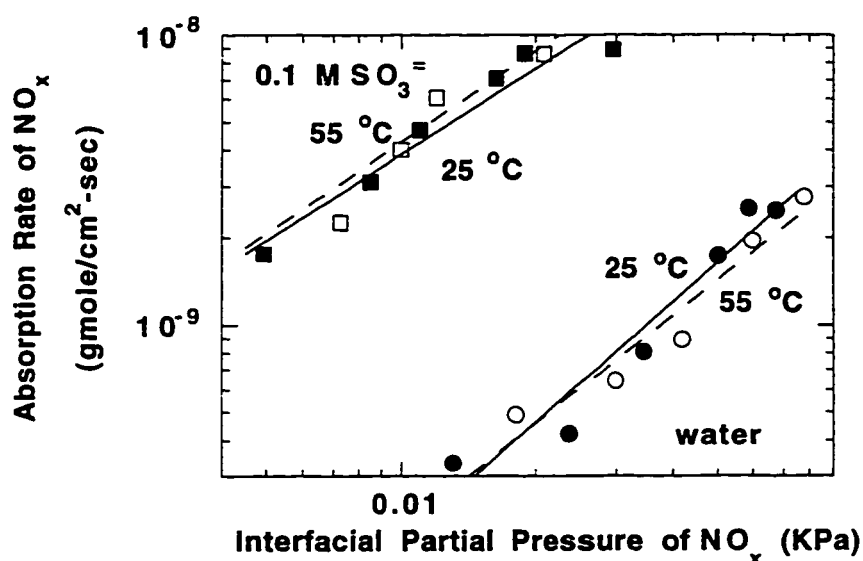


Figure 4.6 Effect of temperature on NO_2 absorption. Runs 4.1.1-4.1.2 and 4.1.11.

These results were consistent with the findings of Takeuchi et al. (1977). The absorption rate of NO_2 into water decreased slightly when temperature was raised from 25 °C to 55 °C due to the decrease in NO_2 solubility. On the other

hand, the rate of NO₂ absorption into 0.1 M Na₂SO₃ solution increased slightly with increasing temperature, caused by the increased reaction rate at higher temperature.

The second order reaction rate constant, k_2 , is related to the activation energy of the reaction via the following equation:

$$k_2 = k_2^\circ \exp\left(-\frac{E_{\text{act}}}{RT}\right) \quad (4.2)$$

Since we have obtained measurements of k_2 at 25 and 55 °C, by using the k_2 's measured by Takeuchi et al. (1977) at 10 and 15°C, we made an attempt to determine the energy of activation for the reaction between NO₂ and SO₃⁼. The result is plotted in figure 4.7.

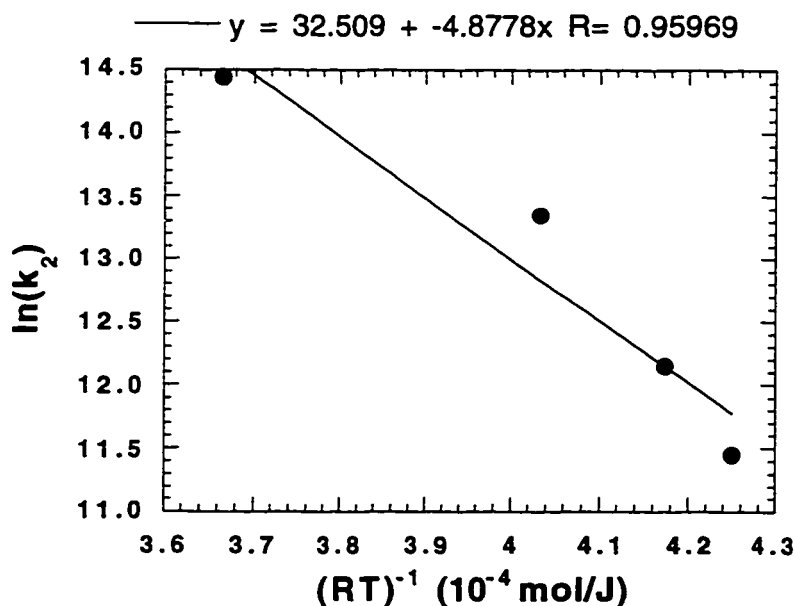


Figure 4.7 Second order rate constant k_2 for the reaction of NO₂ and Na₂SO₃ as a function of reaction temperature.

An activation energy of 48.8 kJ/mol was calculated from the above plot.

4.6 CHAPTER SUMMARY

In this chapter we presented experimental results of NO_2 absorption obtained by operating the stirred cell contactor in batch mode. We measured the second order rate constant between NO_2 and $\text{SO}_3^{=}$, HSO_3^- , $\text{S}_2\text{O}_3^{=}$, $\text{S}^{=}$, and water at 25 °C. Reasonably good agreement was obtained between our results and rate constants measured by other researchers.

By comparing various absorption curves, we concluded that $\text{SO}_3^{=}$ and $\text{S}^{=}$ were most effective in reacting with NO_2 . Neither HSO_3^- nor $\text{S}_2\text{O}_3^{=}$ reacted very fast with NO_2 , and the absorption rate of NO_2 into water or hydroxide solution was lower still. However, when comparing to pure physical absorption of NO_2 , the chemical reaction between NO_2 and water was found to be significant.

We have observed that the use of air instead of N_2 as diluent reduced the rate of NO_2 absorption into 0.1 M Na_2SO_3 and Na_2S solutions. This reduction is believed to be caused by the oxidation of $\text{SO}_3^{=}$ and $\text{S}^{=}$ at the liquid interface by oxygen in air. We have shown that the addition of an oxidation inhibitor such as $\text{Na}_2\text{S}_2\text{O}_3$ was able to minimize the effect of oxidation and restore the rate of NO_2 absorption.

We have shown that increasing temperature reduced the rate of NO_2 absorption into water but increased the rate of absorption into 0.1 M Na_2SO_3 . The activation energy for the reaction between NO_2 and water was determined to be 48.8 kJ/mol.

Chapter 5

NO₂ Absorption in Continuous Stirred Cell Contactor

This chapter summarizes the results of NO₂ absorption experiments obtained by operating the stirred cell contactor in a continuous or semi-continuous mode. Reaction rate constants between NO₂ and sulfite, bisulfite, thiosulfate and water at 55 °C are regressed from the full absorption model, and the predicted rates of NO₂ absorption are compared with the experimentally measured rates. The effect of additives such as Mg⁺⁺, Ca⁺⁺ and Cl⁻ on the rate of NO₂ absorption was investigated, and the effects of buffer, oxidation inhibitor, and gas phase SO₂ were also studied.

5.1 RESULTS OF CONTINUOUS NO₂ ABSORPTION EXPERIMENTS

When the stirred cell contactor was operated in a continuous or semi-continuous mode, the sulfite solution was prepared by dissolving the required amount of Na₂SO₃ in distilled water, and was fed into the contactor prior to the experiment. Normally, a high concentration of Na₂SO₄ (0.1-0.3 M) was introduced to maintain a stable background ionic strength. In some cases a buffer such as succinic anhydride was also used to maintain the solution pH at liquid boundary. The buffer was necessary to keep a relative stable concentration of interfacial sulfite so as to maintain a constant rate of NO₂ absorption.

A concentrated solution of Na₂SO₃/Na₂SO₄/buffer was prepared prior to the experiment. During the experiment, the solution pH was monitored continuously and the sulfite concentration in the solution was analyzed frequently.

Whenever the solution pH or the concentration of sulfite fell below the desired level, a pump was turned on to feed the concentrated solution into the contactor until the solution pH and $[\text{SO}_3^{2-}]$ were restored. This served to maintain a constant level of sulfite in the solution, which in turn kept the rate of NO_2 absorption relatively constant.

Tables 5.1 to 5.4 summarize the results of all continuous experiments. Table 5.1 lists all experiments of NO_2 absorption into sulfite solutions with no other additives. Tables 5.2, 5.3 and 5.4 consist of other experiments with gas phase SO_2 , thiosulfate, and various liquid phase additives. In all four tables, $[\text{S(IV)}]_b$ is the bulk solution S(IV) concentration measured experimentally by titration, pH the bulk solution pH, $Y_{\text{NO}_2,i}$ the interfacial concentration of NO_2 , and Y_{O_2} the bulk gas phase O_2 concentration. Na_2SO_4 and succinate were the nominal concentration of sodium sulfate and succinic acid. The rate of sulfite oxidation was measured experimentally, and it was used to estimate the interfacial concentration of S(IV) by following the procedures outlined in Appendix E. Appendix F gives the FORTRAN code used to perform the S(IV) speciation at the interface. $[\text{SO}_3^{2-}]_i$ was given as part of the output of the FORTRAN code.

5.2 REGRESSION OF REACTION RATE CONSTANTS

Results from experiments 5.1.1-5.1.11 and 5.3.11-5.3.18 were used to regress the reaction rate constants between NO_2 and SO_3^{2-} , HSO_3^- , $\text{S}_2\text{O}_3^{2-}$, and water, using equation 2.44 and BETAV3 (Appendix G).

$$\frac{R_g^2 \text{HNO}_2^2}{D_{\text{NO}_2}} = k_2 \text{SO}_3 = [\text{SO}_3^{2-}]_i + k_2 \text{HSO}_3^- [\text{HSO}_3^-]_i + \frac{2}{3} \frac{k_2 \text{H}_2\text{O} \text{PNO}_2 i}{\text{HNO}_2} + k_2 \text{S}_2\text{O}_3 = [\text{S}_2\text{O}_3^{2-}]_i \quad (2.44)$$

These experiments were performed with no additives other than buffer and thiosulfate, and with 15% O₂ in the gas phase. The regressed rate constants are as following:

$$k_{2,\text{SO}_3^{2-}} = (11.2 \pm 0.3) \times 10^5 \text{ M}^{-1}\text{s}^{-1}$$

$$k_{2,\text{HSO}_3^-} = (2.8 \pm 0.1) \times 10^4 \text{ M}^{-1}\text{s}^{-1}$$

$$k_{2,\text{H}_2\text{O}} = (1.6 \pm 1.1) \times 10^7 \text{ M}^{-1}\text{s}^{-1}$$

$$k_{2,\text{S}_2\text{O}_3^{2-}} = (5.4 \pm 0.6) \times 10^3 \text{ M}^{-1}\text{s}^{-1}$$

The relative magnitude of these rate constants were consistent with the results of our batch experiments, showing sulfite as being the most effective reagent in removing NO₂, while both HSO₃⁻ and S₂O₃⁼ react with NO₂ at a much slower rate. The relatively large confidence interval for $k_{2,\text{H}_2\text{O}}$ was due to the small number of pure water absorption experiments as well as the relatively minor contribution of water reaction to the overall rate of NO₂ absorption in most of the experiments. However, the use of the full model in equation 2.40 was justified, since in most of the experiments, the reaction between NO₂ and HSO₃⁻ and S₂O₃⁼ contributed significantly to the overall rate of NO₂ absorption.

To see how well these rate constants fit the other experiments not used in the regression, the rates of NO₂ absorption for the other runs in table 5.1-5.3 were calculated from equation 2.40 and compared to the experimentally measured rates. Figure 5.1 gives the ratio of the predicted rate of NO₂ absorption to the measured rate for each experiment as a function of the interfacial concentration of S(IV). The circles contain the experiments we used to regress the kinetic constants. Most of these points fall quite close to the perfect fit line, while the rest of the data display an even scatter around the line.

From figure 5.1, it can also be observed that our model is adequate in fitting data with SO₂, thiosulfate, and without O₂. All of these data points fall evenly above and below the perfect fit line with very small scattering, indicating a good fit by the model. The largest deviation from the model prediction was observed among data with no buffer and consequently near zero effective [SO₃⁼] at the interface. Under such extreme conditions, any small error in estimating the composition of S(IV) species at the interface could lead to significant error in predicting the rate of NO₂ absorption.

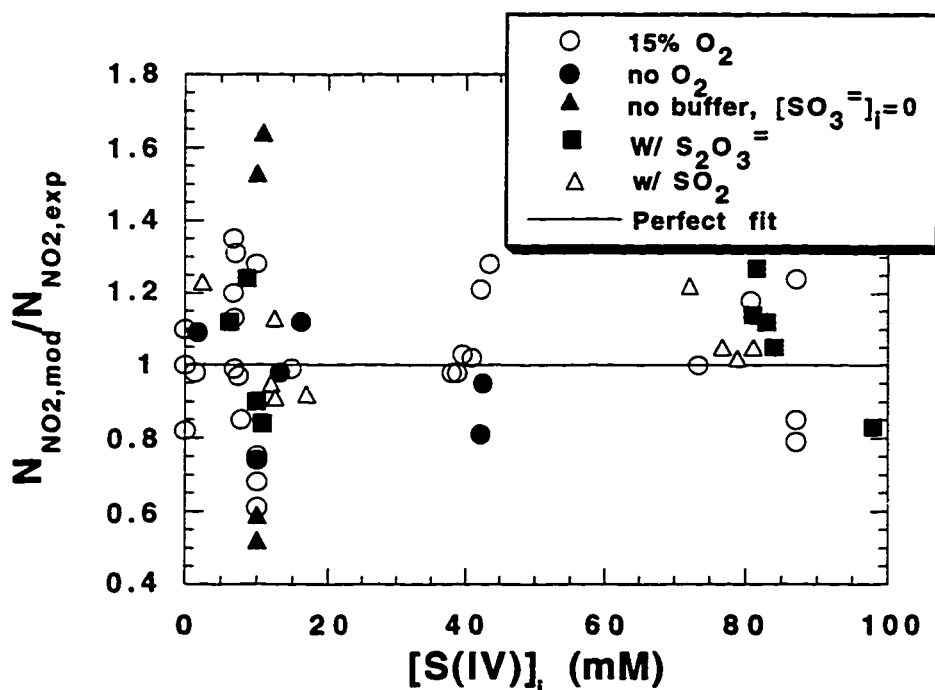


Figure 5.1 Fit of the rate of NO₂ absorption by equation 2.40. Runs 5.1.1-5.1.18, 5.2.1-5.2.10, and 5.3.11-5.3.18. 55 °C.

To further test how well the absorption model predicts NO_2 absorption over a wide range of conditions, we compared the calculated NO_2 absorption rate with the measured rate at various values of solution pH and dissolved S(IV) (figure 5.2). To eliminate the effect of NO_2 partial pressure on the predicted rates, the normalized rate of NO_2 absorption, R_g , was used.

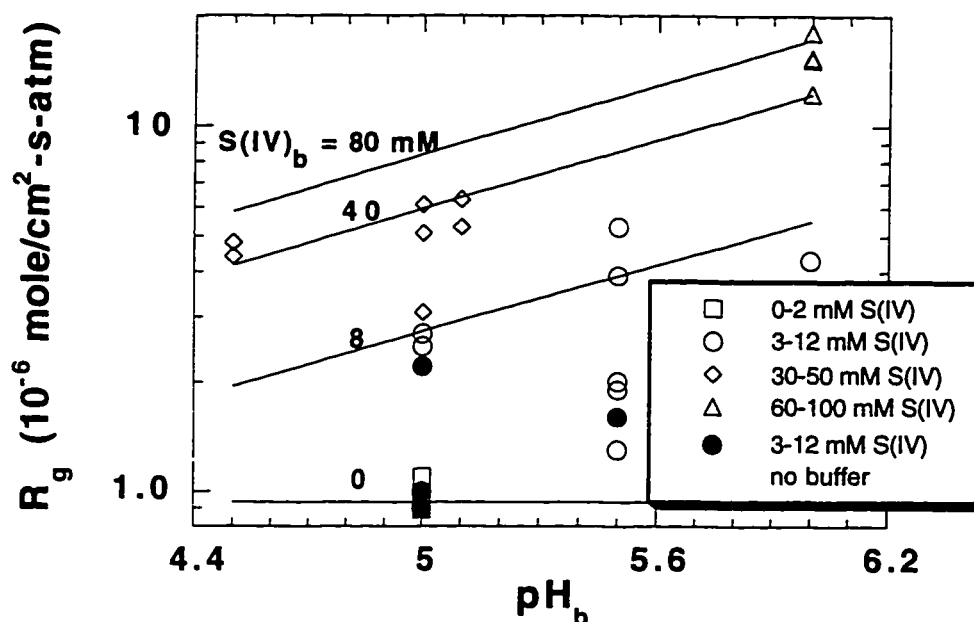


Figure 5.2 Predicted and measured rates of NO_2 absorption in sulfite solution. Runs 5.1.1-5.1.11, 5.1.29-5.1.35, and 5.1.39-5.1.45. All runs contain succinic buffer. 55°C , 15% O_2 . $Y_{\text{NO}_2,i}(\text{cal}) = 100$ ppm; measured = 15-290 ppm. Lines represent model prediction by equation 2.44.

As can be seen from figure 5.2, our model of NO_2 absorption is adequate in predicting rates of NO_2 absorption over a wide range of $[\text{S(IV)}]$ and pH. The

deviations between the measured and calculated rates were mainly caused by the variations in S(IV), as the model used a fixed value of [S(IV)] to generate each absorption curve, while the actual experiments had [S(IV)] varied over quite a wide range. Another observation is that the presence of a buffer was necessary for maintaining a high rate of NO₂ absorption by keeping a stable pH at the liquid boundary. In the absence of such a buffer, the experimental rate of NO₂ absorption fell significantly below its predicted value.

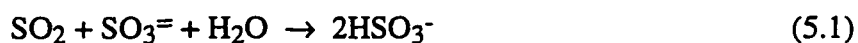
5.3 EFFECT OF GAS PHASE VARIABLES ON NO₂ ABSORPTION

5.3.1 Nitrogen Dilution

When nitrogen instead of air was used to dilute the NO₂ gas entering the stirred cell contactor, the rate of SO₃⁼ depletion was significantly reduced as oxidation of sulfite by oxygen no longer occurred. The net result was a higher concentration of sulfite at the interface. As our absorption model (equation 2.40) used interfacial concentration of S(IV) species instead of their bulk concentration, it automatically corrected for this increase in [SO₃⁼]_i when nitrogen was used as diluent. Therefore, this model is equally adequate in predicting rate of NO₂ absorption with nitrogen dilution, as indicated by figure 5.1. The six experiments with nitrogen dilution plotted in figure 5.1 had rates of NO₂ absorption very close to that predicted by equation 2.40, indicating a good fit by the model.

5.3.2 Presence of SO₂

When appreciable concentration of SO₂ is present in the gas phase inside the contactor, the following reaction takes place:



Therefore, for every mole of SO_2 absorbed, one mole of $\text{SO}_3^{=}$ is consumed, and two moles of HSO_3^- are formed. The net effect of SO_2 absorption is an increase in total S(IV) and a drop in pH at the interface. When a buffer such as succinate is present in the liquid phase, the change in pH is minimized, and the absorption of SO_2 leads to an increase in the rate of NO_2 absorption by adding to the total amount of S(IV). On the other hand, when no buffer is present, SO_2 absorption tends to inhibit the rate of NO_2 absorption by reducing the pH at the gas/liquid interface. In our study, sufficient concentration of buffer was used to maintain a relatively constant interfacial pH, and the bulk solution pH was controlled by periodically feeding into the contactor a concentrated stock solution. Therefore, the effect of SO_2 on solution pH was minimized, and the presence of gas phase SO_2 only had the effect of increasing interfacial [S(IV)]. As our model of NO_2 absorption takes into account this interfacial concentration effect, it is adequate in predicting NO_2 absorption in the presence of SO_2 (figure 5.1). Figure 5.3 shows the effect of SO_2 absorption on the rate of NO_2 absorption with or without the presence of a buffer.

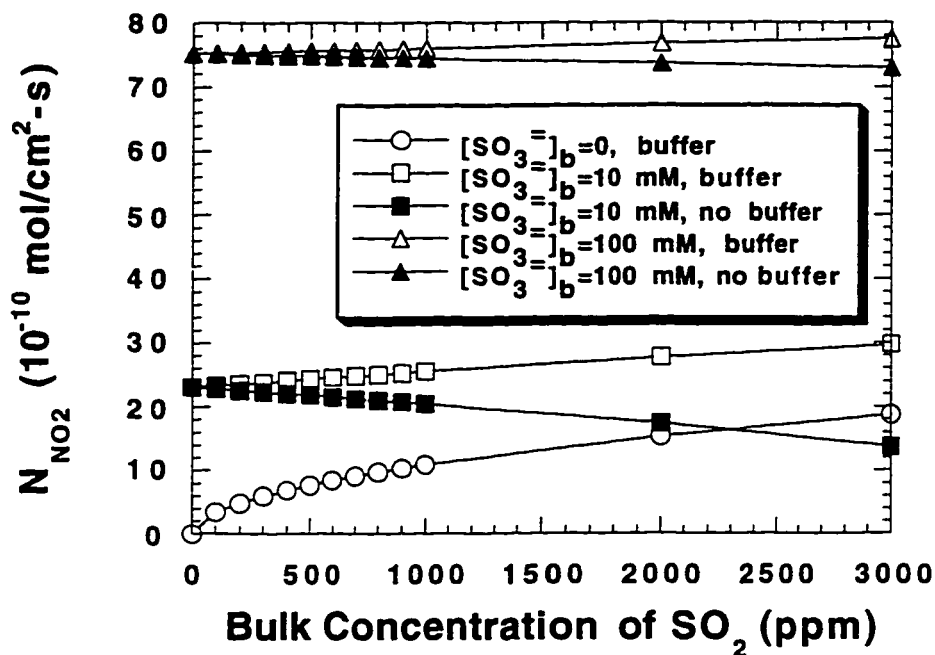


Figure 5.3 Calculated effect of SO₂ absorption on the rate of NO₂ absorption in the stirred-cell contactor. Bulk solution pH assumed to be constant. Values of k_g and k_l are typical for the stirred-cell contactor.

5.4 EFFECT OF LIQUID PHASE VARIABLES ON NO₂ ABSORPTION

5.4.1 Presence of Thiosulfate

As discussed in chapter 2, sodium thiosulfate functions as an oxidation inhibitor by scavenging the SO₃^{•-} and SO₅^{•-} radicals essential in the air oxidation of sulfite. Therefore, when Na₂S₂O₃ was added to the solution during the absorption of NO₂, the rate of sulfite oxidation was reduced dramatically, leading

to a higher concentration of SO_3^- at the interface. In addition, thiosulfate can react directly with NO_2 . However, as the reaction rate constant between NO_2 and $\text{S}_2\text{O}_3^{2-}$ is roughly 200 times lower than that between NO_2 and SO_3^- at 55 °C, the amount of NO_2 removed by directly reacting with $\text{S}_2\text{O}_3^{2-}$ was insignificant. Since our model of NO_2 absorption was based upon interfacial S(IV) concentrations, and also took into account the reaction between NO_2 and $\text{S}_2\text{O}_3^{2-}$, it did a good job in predicting the rate of NO_2 absorption in the presence of thiosulfate. All 9 runs containing thiosulfate exhibited small and even scatter around the perfect fit line in figure 5.1, indicating a good fit by the model.

5.4.2 Other Additives

Cl^- , Ca^{++} , and Mg^{++} have various degrees of effect on the rate of NO_2 absorption into sulfite solutions. Since our absorption model does not take into account the effect of these additives, it cannot accurately predict the rate of NO_2 absorption in the presence of these ions, as can be seen in figure 5.4. The effects of Cl^- , Ca^{++} and Mg^{++} on NO_2 absorption are discussed in greater detail in the following sections.

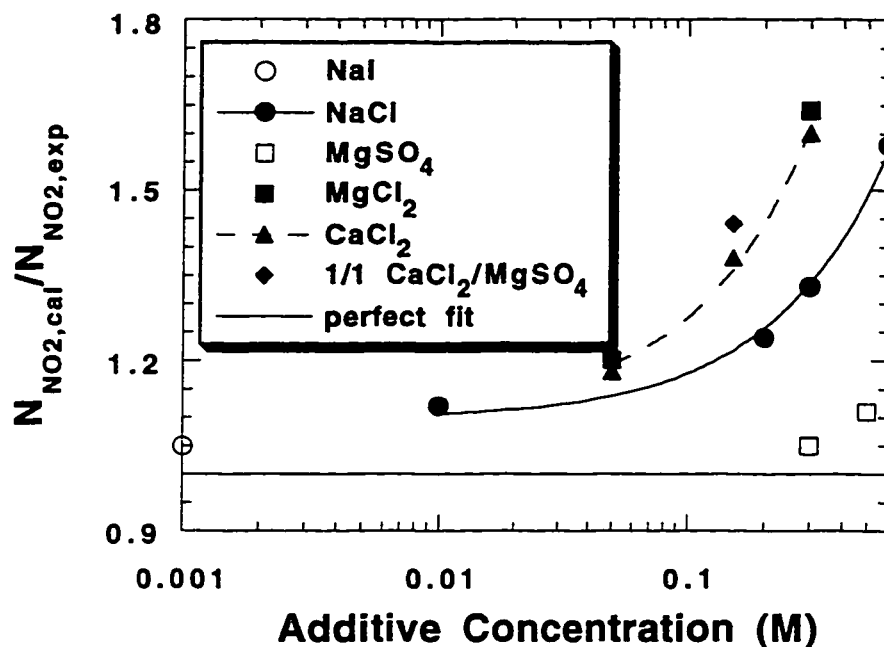


Figure 5.4 Effect of additives on rate of NO₂ absorption. Runs 5.4.1-5.4.15. All additive concentrations were nominal, not measured experimentally. 55 °C, 15% O₂.

Chloride ion (Cl⁻)

Cl⁻ significantly reduced the rate of NO₂ absorption into solutions of sulfite. There are two distinct reaction mechanisms to account for this strong effect of Cl⁻. First, as observed by Clarke and Radojevic (1982), the presence of Cl⁻ can lead to an additional free radical reaction such as:





The net result is an increasing rate of sulfite oxidation, leading to a lower concentration of $\text{SO}_3^=$, especially at the interface. A different mechanism suggests that the presence of Cl^- may lead to the regeneration of NO_2 via the following steps:



Therefore, in the presence of Cl^- , the rate of NO_2 absorption was reduced as a direct result of NO_2 formation.

As our model takes into account the decrease in sulfite concentration at the interface due to oxidation, it is able to account for the additional oxidation caused by the presence of Cl^- . However, since our model does not include the effect of NO_2 regeneration, it tends to overpredict the rate of NO_2 absorption when Cl^- is present, and the magnitude of overprediction increases with increasing Cl^- concentration. This overprediction is clearly seen in figure 5.4.

Calcium ion (Ca^{++}) and Magnesium ion (Mg^{++})

As observed by both Clarke and Radojevic (1982) and this study, the presence of Ca^{++} and Mg^{++} had little effect on the rate of sulfite oxidation. However, Ca^{++} and Mg^{++} can react with $\text{SO}_3^=$ to form complexes such as CaSO_3° and MgSO_3° , which to the best of our knowledge do not react directly with NO_2 . Therefore, when Ca^{++} or Mg^{++} is present, the amount of free sulfite in the solution is reduced, leading to a rate of NO_2 absorption lower than that predicted by equation 2.38. However, since the concentration of CaSO_3° and

MgSO₃[°] formed is quite low, the decrease in NO₂ absorption rate is not very significant. These trends can also be observed in figure 5.4.

The small overprediction by the model in cases of MgSO₄ can be contributed to the formation of MgSO₃[°]. The effect of Cl⁻ is pronounced in experiments with NaCl, MgCl₂, and CaCl₂. The slight difference in the amount of overprediction between NaCl and CaCl₂ can be explained again by the formation of CaSO₃[°], and the fact that the CaCl₂ and MgCl₂ data coincide with each other seems to suggest the similarity in the effects of Ca⁺⁺ and Mg⁺⁺ on complex formation.

5.4.3 Product Accumulation

As discussed in chapter 2, the reaction product between NO₂ and sulfite is a family of nitrogen-sulfur compounds. Since SO₃⁼ was consumed in the process, and the N-S products were largely acidic, the solution pH decreased with increasing NO₂ absorption. However, as the solution pH was controlled by both buffer and feeding of stock solution, the effect of reaction products on solution pH was minimized.

To investigate other possible effects of product accumulation on NO₂ absorption, experiments were performed by initially measuring NO₂ absorption rate under conditions of low NO₂ concentration. Afterwards, the NO₂ concentration was increased significantly and a high rate of NO₂ absorption was maintained over a long period a time to obtain a measurable level of product accumulation in the solution. The amount of product formed was calculated from nitrogen mass balance and checked with IC analysis. Finally, the NO₂

concentration was restored to its original value and the rate of NO_2 absorption was compared with that at the onset of the experiment. Any effect of product accumulation would be reflected in the discrepancies between the absorption rates.

Results of two of these experiments are plotted in Figure 5.5.

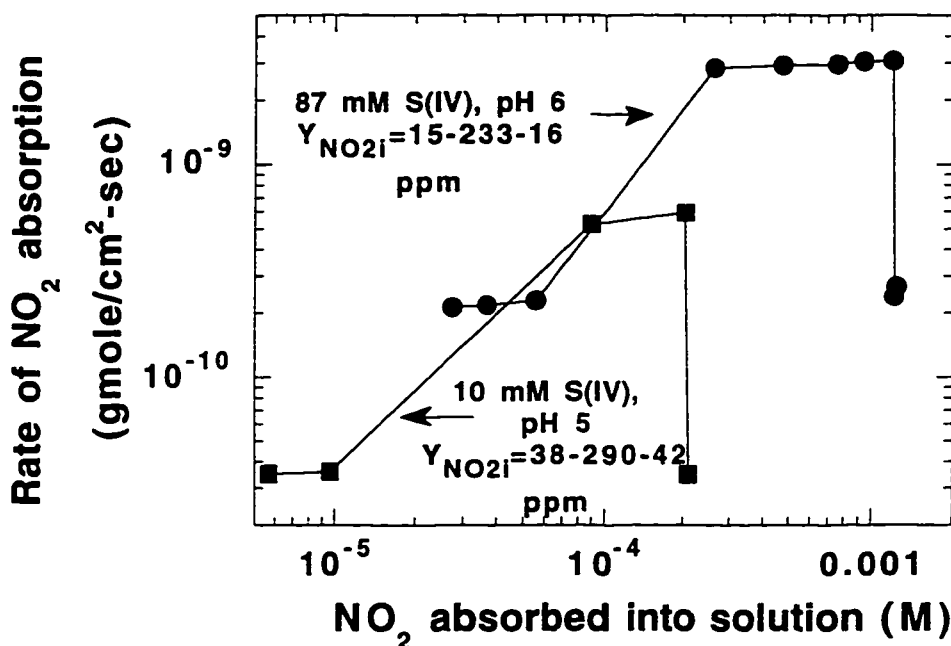


Figure 5.5 Effect of product accumulation on NO_2 absorption. Runs 5.1.20-5.1.22 and 5.1.30-5.1.32. 55 °C, 15% O_2 .

In both cases, the rate of NO_2 absorption returned to its original value after the NO_2 concentration was restored, indicating product accumulation up to a level of 1 mM had little effect on the rate of NO_2 absorption. IC analysis showed that

the final composition of the solution was quite similar in both cases, with an average of 21% hydroxylamine disulfonic acid, 62% amine disulfonic acid, 12% NO_3^- and the remaining 5% NO_2^- . Nitrogen recovery of over 92% was achieved in both cases.

5.4.4 Liquid Phase Agitation Speed

We looked briefly at the effect of liquid phase agitation speed on the rate of NO_2 absorption. Since SO_3^- was consumed at the gas liquid interface by reacting with NO_2 and by oxidation, the interfacial SO_3^- concentration was usually lower than that of the bulk. By increasing the liquid phase agitation speed, the liquid phase mass transfer increases, resulting in a faster rate of transport of SO_3^- from the bulk solution to the gas liquid interface, which in turn leads to a higher rate of NO_2 absorption. However, this effect is not expected to be very significant except for cases in which the depletion of SO_3^- at the interface is extremely high, i.e., high concentration of NO_2 .

An experiment was performed by varying the liquid phase agitation speed while keeping all other conditions constant. The rate of NO_2 absorption was plotted as a function of agitation speed and is given in figure 5.6.

As can be seen from figure 5.6, the rate of NO_2 absorption did increase with increasing liquid phase agitation. However, the increase in N_{NO_2} was significantly less than the increase in the liquid phase mass transfer coefficient.

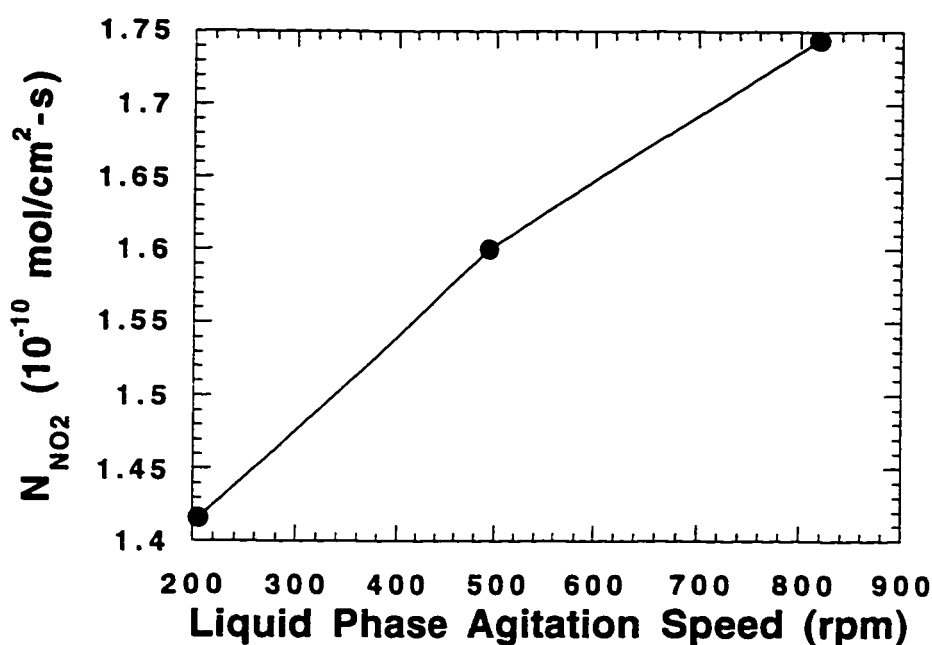


Figure 5.6 Effect of liquid phase agitation speed on NO₂ absorption. pH = 5.5, [S(IV)] = 10 mM, $Y_{\text{NO}_2,i}$ = 100 ppm, 55 °C, 15% O₂.

5.5 CHAPTER SUMMARY

This chapter discusses the results of NO₂ absorption experiments obtained by operating the stirred cell contactor in a continuous mode. From a large set of continuous experiments, the reaction rate constants between NO₂ and sulfite, bisulfite, thiosulfate, and water were regressed, and their values at 55 °C were

$1.12 \times 10^6 \text{ M}^{-1}\text{s}^{-1}$, $2.8 \times 10^4 \text{ M}^{-1}\text{s}^{-1}$, $5.4 \times 10^3 \text{ M}^{-1}\text{s}^{-1}$, and $1.6 \times 10^7 \text{ M}^{-1}\text{s}^{-1}$ respectively.

We also studied the effect of N_2 dilution and the presence of SO_2 on the rate of NO_2 absorption. The use of N_2 as diluent increased the rate of NO_2 absorption by minimizing sulfite oxidation, and the presence of SO_2 increased the interfacial concentration of sulfite when a buffer was also present.

The addition of thiosulfate enhanced NO_2 absorption by reducing the rate of sulfite oxidation, while the presence of Cl^- reduced the rate of NO_2 absorption by enhancing the rate of sulfite oxidation as well as causing the regeneration of NO_2 . The presence of Mg^{++} and Ca^{++} had little effect on NO_2 absorption, except by forming small amounts of complexes with SO_3^- that appeared to be unreactive toward NO_2 . We have verified that the accumulation of the reaction product in the solution up to 1 mM had little effect on the rate of NO_2 absorption, and we have shown that liquid phase agitation had moderate effect on the rate of NO_2 absorption..

Table 5.1 Results of continuous experiments, no additive, T = 55 °C.

Exp No.	[S(IV)] _b (mM)	pH	[SO ₃ ⁼] _l (mM)	Y _{NO₂,l} (ppm)	Y _{O₂} (%)	R _{g,exp} × 10 ⁻⁸ ($\frac{\text{mol}}{\text{cm}^2 \cdot \text{s} \cdot \text{atm}}$)	$\frac{R_{g,\text{mod}}}{R_{g,\text{exp}}}$	N _{ox} × 10 ⁻⁸ ($\frac{\text{mol}}{\text{cm}^2 \cdot \text{s}}$)	$\frac{N_{\text{ox,mod}}}{N_{\text{ox,exp}}}$	Na ₂ SO ₄ (M)	Succinate (M)
5.1.1	40.9	4.5	0.54	79.8	15	4.8	1.02	2.31	0.86	0.25	0.1
5.1.2	0	5.0	0	106	15	0.98	1.01	--	--	0.3	0.1
5.1.3	0	5.0	0	129	15	1.1	1.10	--	--	0.3	0.1
5.1.4	6.77	5.0	0.26	92	15	2.7	0.99	0.49	0.92	0.29	0.1
5.1.5	7.41	5.0	0	136	15	2.5	0.97	0.30	1.02	0.29	0.3
5.1.6	38.0	5.0	1.56	65	15	6.1	0.98	3.47	1.11	0.25	0.3
5.1.7	38.8	5.0	1.2	94	15	5.1	0.98	2.97	0.95	0.25	0.1
5.1.8	39.6	5.0	1.38	80	15	3.1	1.03	2.74	1.05	0.25	0.3
5.1.9	1.43	5.1	0	136	15	2.5	0.98	0.30	--	0.3	0.1
5.1.10	14.8	5.5	0.63	156	15	3.9	0.99	1.23	0.75	0.29	0.1
5.1.11	73.4	6.0	2.88	172	15	15.2	1.00	2.96	0.10	0.2	0.1
5.1.12	42.5	4.5	0.56	82.4	0	4.4	0.95	0.26	--	0.25	0.1
5.1.13	16.2	5.0	0.27	216	0	2.7	1.12	0.28	--	0.29	0.1
5.1.14	42.2	5.0	1.61	88	0	6.1	0.81	0.25	--	0.25	0.1
5.1.15	1.74	5.1	0	133	0	2.8	1.09	0.27	--	0.3	0.1
5.1.16	13.2	5.0	0.11	227	0	2.2	0.98	0.30	--	0.25	--
5.1.17	45.3	5.1	1.08	79	0	6.3	2.06	0.24	--	0.25	--
5.1.18	10	5.5	0.29	80	0	5.3	0.74	0.24	--	0.096	--
5.1.19	0	5.0	0	131	15	0.89	0.82	--	--	--	--
5.1.20	10	5.0	0	38	15	1.0	0.68	0.60	0.72	0.096	--
5.1.21	10	5.0	0	290	15	2.2	0.75	0.73	--	0.096	--
5.1.22	10	5.0	0	42	15	0.9	0.61	0.53	0.58	0.096	--
5.1.23	43.4	5.1	0.32	85	15	5.3	1.28	3.22	1.15	0.25	--
5.1.24	10.8	5.4	0	500	15	3.3	1.64	0.94	--	0.096	--
5.1.25	10	5.5	0	75	15	2.0	0.61	0.98	0.45	0.096	--
5.1.26	10	5.5	0	97	15	1.9	0.68	1.82	1.08	0.096	--

Table 5.1 (cont'd)

Exp No.	[S(IV)] _b (mM)	pH	[SO ₃] _l (mM)	Y _{NO₂,1} (ppm)	Y _{O₂} (%)	R _{g exp} × 10 ⁻⁶ ($\frac{\text{mol}}{\text{cm}^2 \cdot \text{s} \cdot \text{atm}}$)	$\frac{R_{g, \text{mod}}}{R_{g, \text{exp}}}$	N _{ox} × 10 ⁻⁶ ($\frac{\text{mol}}{\text{cm}^2 \cdot \text{s}}$)	$\frac{N_{\text{ox, mod}}}{N_{\text{ox, exp}}}$	Na ₂ SO ₄ (M)	Succinate (M)
5.1.27	10	5.5	0	105	15	1.6	0.52	1.30	0.77	0.096	--
5.1.28	10	5.5	0	116	15	1.3	0.59	0.66	--	0.096	--
5.1.29	10	6.0	0.16	65	15	4.3	1.53	1.02	0.10	0.096	--
5.1.30	87.0	6.0	3.2	15	15	15.4	1.24	4.76	1.28	0.2	--
5.1.31	87.0	6.0	0.73	233	15	12.3	0.79	8.20	1.22	0.2	--
5.1.32	87.0	6.0	0.65	16	15	18.1	0.85	10.8	1.78	0.2	--
5.1.33	8.32	4.9	0.14	85	15	7.5	0.39	0.68	--	0.29	0.1
5.1.34	6.76	5.7	1.05	58	15	2.1	1.35	0.96	1.12	0.25	0.1
5.1.35	6.96	5.58	0.66	53.3	15	2.63	1.31	0.50	--	0.25	0.1
5.1.36	6.77	5.58	0.84	52.2	5	3.06	1.13	0.38	1.51	0.25	0.1
5.1.37	6.68	5.64	0.82	35.3	1	5.21	1.20	0.26	0.99	0.25	0.1
5.1.38	7.73	5.52	0.78	45.8	10	3.53	0.85	0.85	0.92	0.25	0.1
5.1.39	80.7	5.38	8.32	52.1	15	9.72	1.18	5.96	1.06	0.20	0.2
5.1.40	46.8	5.46	5.74	69.1	15	4.70	1.86	4.16	0.87	0.25	0.15
5.1.41	9.887	5.48	1.04	245.1	15	3.43	1.28	1.91	0.09	0.25	0.1
5.1.42	42.22	5.52	4.82	350.2	15	7.28	1.21	7.43	1.30	0.25	0.15
5.1.43	72.1	9.87	54.0	168	15	9.2	1.32	14.5	--	0.15	--
5.1.44	76.8	9.96	70.5	24	15	19.3	1.15	9.63	--	0.2	--
5.1.45	81.1	9.91	75.2	34	15	20.0	1.14	11.6	--	0.2	--

*R_{g,mod} calculated from equation 2.44, using rate constants at 55 °C. NO₂-S₂O₃²⁻ reaction was excluded.

**N_{ox,mod} calculated from equation 6., using regressed values of C₁ and C₂.

Table 5.2 Results of continuous experiments with gas phase SO₂, T = 55 °C.

Exp No.	[S(IV)] _b (mM)	pH	[SO ₃ ⁼] _l (mM)	Y _{NO₂} _l (ppm)	Y _{O₂} (%)	R _{g,exp} × 10 ⁻⁸ ($\frac{\text{mol}}{\text{cm}^2 \cdot \text{s} \cdot \text{atm}}$)	$\frac{R_{g,\text{mod}}}{R_{g,\text{exp}}}$	N _{ox} × 10 ⁻⁸ ($\frac{\text{mol}}{\text{cm}^2 \cdot \text{s}}$)	$\frac{N_{\text{ox,mod}}}{N_{\text{ox,exp}}}$	Na ₂ SO ₄ (M)	Y _{SO₂} (ppm)	Succinate (M)
5.2.1	12.5	5.51	1.94	86.1	0	10.3	0.88	--	--	0.25	35.9	0.1
5.2.2	14.8	5.52	2.28	60.1	0	8.48	0.90	--	--	0.25	36.8	0.1
5.2.3	16.3	5.51	2.33	42.8	0	8.41	0.93	--	--	0.25	24.5	0.1
5.2.4	11.9	5.51	1.65	45.4	15	3.28	0.95	1.63	0.90	0.25	25.3	0.1
5.2.5	12.5	5.51	1.58	56.1	15	2.10	0.99	1.86	0.85	0.25	16.7	0.1
5.2.6	0.97	5.46	1.45	228.5	0	2.30	1.18	--	--	0.25	105.8	0.1
5.2.7	2.37	5.48	1.35	230.1	15	2.23	1.23	0.63	1.11	0.25	106.8	0.1
5.2.8	12.4	4.45	0.81	242	15	2.18	1.13	1.93	1.07	0.25	117	0.1
5.2.9	17.0	4.48	0.23	248	15	3.10	0.92	2.93	0.81	0.25	111	0.1
5.2.10	78.9	9.78	57.9	96	15	19.0	1.02	11.8	1.21	0.15	68	--

Table 5.3 Results of continuous experiments with thiosulfate, T = 55 °C.

Exp No.	[S(V)] _b (mM)	pH	[SO ₃ ⁼] _l (mM)	Y _{NO₂,l} (ppm)	Y _{O₂} (%)	R _{g,exp} × 10 ⁻⁸ ($\frac{\text{mol}}{\text{cm}^2 \cdot \text{s} \cdot \text{atm}}$)	$\frac{R_{g,\text{mod}}}{R_{g,\text{exp}}}$	N _{ox} × 10 ⁻⁸ ($\frac{\text{mol}}{\text{cm}^2 \cdot \text{s}}$)	$\frac{N_{\text{ox},\text{mod}}}{N_{\text{ox},\text{exp}}}$	N ₂ O ₃ × 10 ⁻⁸ ($\frac{\text{mol}}{\text{cm}^2 \cdot \text{s}}$)	[S ₂ O ₃ ⁼] (mM)
5.3.1	89.3	5.53	14.2	47.3	0	11.3	1.15	--	--	--	90
5.3.2	81.5	5.57	13.8	49.9	15	10.3	1.27	0.41	11.2	--	90
5.3.3	91	5.4	9.8	46.1	0	9.11	1.20	--	--	--	7.0
5.3.4	82.9	5.4	8.5	46.3	15	9.15	1.12	0.53	6.0	--	7.0
*5.3.5	0	5.63	0	91.2	0	2.31	--	--	--	--	88.7
*5.3.6	0	5.46	0	90.3	15	2.41	--	--	--	--	87
5.3.7	0	5.83	0	98.1	0	1.88	0.86	--	--	--	86.1
5.3.8	0	6.03	0	90.6	15	2.66	0.91	--	--	--	88.4
*5.3.9	86.0	6.11	33.3	63.1	0	7.67	--	--	--	--	8.2
5.3.10	79.4	6.14	31.8	68.7	15	6.42	--	0.37	--	--	6.7
5.3.11	98	7.71	85.8	17.2	15	36	0.83	3.19	6.8	0.14	103
5.3.12	84	7.70	74.5	150.7	15	24	1.05	2.86	16.1	0.33	99.2
5.3.13	103	7.45	82.5	21.0	15	33	0.90	3.52	6.3	0.035	10.2
5.3.14	81	7.35	60	185.7	15	19	1.14	4.10	9.1	0.046	9.2
5.3.15	9.9	7.65	7.5	15.2	15	10	0.90	0.43	3.7	0.019	10.3
5.3.16	6.2	7.49	3.3	190.1	15	4.3	1.12	0.81	4.3	0.033	9.5
5.3.17	10.7	7.81	9.6	17.5	15	12	0.84	0.32	7.5	0.12	103
5.3.18	8.6	7.86	7.7	177.1	15	6.1	1.24	0.46	10.3	0.29	104

*T = 25 °C. Our model of NO₂ absorption and sulfite oxidation do not apply to these runs.

Table 5.4 Results of continuous experiments with liquid phase additives, T = 55 °C, 15% O₂.

Exp No.	[S(IV)] _b (mM)	pH	[SO ₃ ⁼] (mM)	Y _{NO₂,I} (ppm)	R _{g,exp} × 10 ⁻⁸ ($\frac{\text{mol}}{\text{gH}_2\text{O} \cdot \text{s}}$)	$\frac{R_{g,\text{mod}}}{R_{g,\text{exp}}}$	N _{ox} × 10 ⁻⁸ ($\frac{\text{mol}}{\text{cm}^2 \cdot \text{s}}$)	$\frac{N_{\text{ox,mod}}}{N_{\text{ox,exp}}}$	Na ₂ SO ₄ (M)	Additive (mM)	Succinate (M)
5.4.1	5.6	5.0	0	500	3.1	1.05	0.88	0.93	0.096	1 NaI	--
5.4.2	5.0	5.4	0	500	4.7	1.24	1.74	0.81	0.096	200 NaCl	--
5.4.3	8.5	6.0	0.15	500	4.8	1.12	0.65	0.88	0.096	10 NaCl	--
5.4.4	37.7	5.0	1.56	73	4.4	1.33	1.42	0.72	0.25	300 NaCl	0.3
5.4.5	38.7	5.0	2.0	74	3.8	1.58	1.60	0.48	0.25	600 NaCl	0.1
5.4.6	36.1	5.0	1.1	70	4.2	1.05	2.79	0.94	0.25	300 MgSO ₄	0.3
5.4.7	37.8	5.1	1.57	82	2.1	1.11	0.40	0.88	0.25	500 MgSO ₄	0.3
5.4.8	7.58	5.0	0.22	22	2.1	1.20	0.52	0.84	0.29	50 MgCl ₂	0.1
5.4.9	33.3	5.2	1.38	85	2.1	1.64	1.68	0.52	0.25	300 MgCl ₂	0.1
5.4.10	9.94	5.1	0.31	19	2.8	1.18	0.63	0.85	0.29	50 CaCl ₂	0.1
5.4.11	4.8	5.0	1.29	89	3.2	1.60	0.88	0.44	0.29	300 CaCl ₂	0.1
5.4.12	7.18	5.0	1.29	93	5.1	1.38	0.19	0.70	0.25	150 CaCl ₂	0.1
5.4.13	7.35	5.0	1.17	89	4.0	1.44	0.23	0.66	0.05	150 CaCl ₂	0.1
5.4.14	7.12	5.0	2.21	87	7.1	1.66	0.41	0.48	0.30	150 MgSO ₄	0.1
5.4.15	6.0	5.0	0.22	79	1.6	1.70	0.51	0.55	0.29	300 CaCl ₂	0.1
5.4.16	6.43	5.65	0.96	64	3.2	1.31	0.71	0.74	0.25	300 MgCl ₂	0.1
5.4.17	7.15	5.61	1.05	0	0	1.15	0.30	0.67	0.25	0.02 Fe ⁺⁺	0.1
5.4.18	6.75	5.65	1.03	49.2	5.0	0.94	0.65	1.08	0.25	0.02 EDTA	0.1
5.4.19	7.16	5.52	0.91	0	0	0.78	0.13	1.21	0.25	0.02 EDTA	0.1
5.4.20	6.26	5.57	0.82	15.65	1.93	1.25	0.37	0.82	0.25	0.017 Fe ⁺⁺	0.1

Chapter 6

Sulfite Oxidation in the Presence of NO₂

This chapter presents the results of our study on sulfite oxidation in the presence of NO₂. We discover that the absorption of NO₂ into sulfite solutions catalyzes sulfite oxidation, and we propose a model to correlate the rate of sulfite oxidation to the rate of NO₂ absorption. This chapter also reports the effect of several important variables on the rate of sulfite oxidation, including gas phase SO₂ and O₂, and Fe⁺⁺, Ca⁺⁺, Mg⁺⁺, Cl⁻, and thiosulfate in the liquid phase.

6.1 SIGNIFICANCE OF SULFITE OXIDATION

When absorbing NO₂ into solutions of sulfite, there are two reaction steps that lead to the consumption of sulfite. As shown by equations 2.10-2.14, sulfite is consumed both by reaction with NO₂ and by reaction with free radicals formed in the presence of oxygen. The latter mechanism is known as sulfite oxidation.

The oxidation of sulfite in the presence of NO₂ follows a free radical mechanism (Huie and Neta, 1984; Huie and Neta, 1987). The initial reaction between NO₂ and SO₃⁼ leads to the formation of sulfite radicals (SO₃[•]), which, in the presence of O₂, can form various other radicals (e.g., SO₅[•], SO₄[•]). These radicals can either react with each other, or more frequently, react with more sulfite, until certain termination steps are reached. The net effect is for every mole of NO₂ absorbed, ten to hundreds of moles of sulfite may be oxidized to sulfate in the presence of oxygen. Therefore, the majority of sulfite in the

solution is consumed not by reaction with NO₂, but rather as a result of oxidation by air.

The reason why sulfite oxidation is important in limestone slurry scrubbing of NO_x is apparent. It is an unfavorable side reaction inside the scrubber. As sulfite is oxidized by air, there is less sulfite available to react with NO₂, and the NO₂ removal efficiency of the slurry scrubber suffers. On the other hand, the oxidation of sulfite is the desired reaction inside the liquid hold tank. In the hold tank, the sulfite is oxidized to sulfate by air via a forced oxidation mechanism; therefore, it will be desirable to discover ways of increasing the rate of sulfite oxidation. Our study of sulfite oxidation attempts to find ways of both enhancing and inhibiting sulfite oxidation.

6.2 SULFITE OXIDATION MEASUREMENT

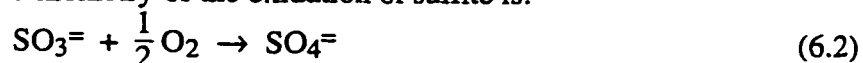
The rate of sulfite oxidation can be measured experimentally either by monitoring the change in gas phase O₂ concentration or liquid phase S(IV) concentration. In our study, we chose to measure the rate of sulfite oxidation by measuring the change in solution S(IV) concentration. The rate of sulfite oxidation, N_{ox}, in units of mol/cm²-s, was calculated from the following equation:

$$N_{ox} = \frac{V([S(IV)]_o - [S(IV)]_f) + V_{tit}[S(IV)]_{tit}}{A \Delta t} + N_{SO_2} \quad (6.1)$$

In equation 6.1, [S(IV)]_o and [S(IV)]_f are the initial and final concentrations of total S(IV) compounds measured via iodometric titration, Δt the time interval, and V and A the volume of the solution and the gas-liquid contacting area, respectively. The V_{tit}[S(IV)]_{tit} term takes into account the amount of S(IV) being fed into the contactor over the course of one experiment,

while the last term accounts for the additional sulfite formed by the absorption of SO₂ whenever SO₂ is present in the gas phase.

The stoichiometry of the oxidation of sulfite is:



Therefore, N_{ox} is related to the rate of oxygen absorption, N_{O2}, via the following equation:

$$N_{\text{ox}} = 2N_{\text{O2}} \quad (6.3)$$

In using the above expression, we have neglected the consumption of SO₃⁼ caused by the reaction between NO₂ and SO₃⁼. This simplification is valid for this study as in all cases the amount of sulfite depleted by reacting with NO₂ was less than 10% of total SO₃⁼ consumed. In some cases where it is desirable to eliminate the effect of gas phase O₂ concentration on the rate of sulfite oxidation, K_{g,O2}, the overall O₂ gas phase mass transfer coefficient, is used instead of N_{ox}. K_{g,O2} is defined as:

$$K_{\text{g,O2}} = \frac{N_{\text{O2}}}{P_{\text{O2 b}}} \quad (6.4)$$

6.3 MODEL OF SULFITE OXIDATION

The reaction mechanism we put forth in equations 2.10-2.14 suggests that the absorption of NO₂ could catalyze sulfite oxidation. Our experimental data (table 5.1 and 5.2) also support this conclusion. In figure 6.1, the rate of sulfite oxidation is given as a function of the rate of NO₂ absorption, normalized by P_{NO2,i}. It can be seen clearly that the rate of sulfite oxidation increases with the rate of NO₂ absorption, and the slope of the curve implies a dependence of the rate of sulfite oxidation on the square root of the rate of NO₂ absorption.

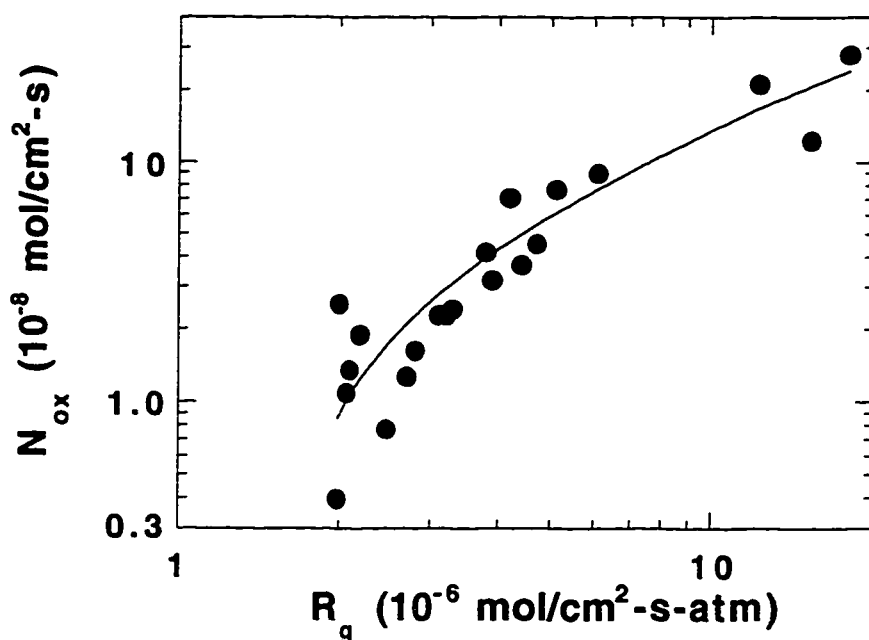


Figure 6.1 Effect of NO_2 absorption on sulfite oxidation. Runs 5.1.1-5.1.11, 5.1.19-5.1.35, and 5.1.39-5.1.45. 55 °C, 15% O_2 .

Based upon the mechanism in equations 2.10-2.14 and the square root relationship reflected in figure 6.1, we proposed that the rate of sulfite oxidation can be represented by the following relationship:

$$N_{ox} = C_1 \sqrt{N_{\text{NO}_2}} [\text{O}_2]_i + C_2 \sqrt{N_{\text{NO}_2}} [\text{SO}_3^{2-}]_i + k_1^{\circ} \text{O}_2 [\text{O}_2]_i \quad (6.5)$$

This is essentially an empirical correlation that gave the best fit of our experimental data. The first term on the right hand side of this equation denotes sulfite oxidation via free radical reaction with O_2 in the liquid phase, the second

term the free radical reaction with SO_3^\cdot , and the last term accounts for physical absorption of oxygen. $k_1^\circ \text{O}_2$, the liquid phase mass transfer coefficient of O_2 , is calculated by the calibration equation given in table 3.1. Runs 5.1.1-5.1.11, 5.1.29-5.1.35, and 5.1.39-5.1.45 in table 5.1 were used with BETAV3 to estimate the constants C_1 and C_2 . The results were:

$$C_1 = (3.7 \pm 0.63) \times 10^3 \text{ cm}^2/\text{mol}^{1/2}\text{-s}^{1/2}$$

$$C_2 = (0.093 \pm 0.022) \times 10^3 \text{ cm}^2/\text{mol}^{1/2}\text{-s}^{1/2}$$

Figure 6.2 gives the ratio of predicted rate of sulfite oxidation to the experimentally measured rate as a function of the NO_2 absorption rate.

82

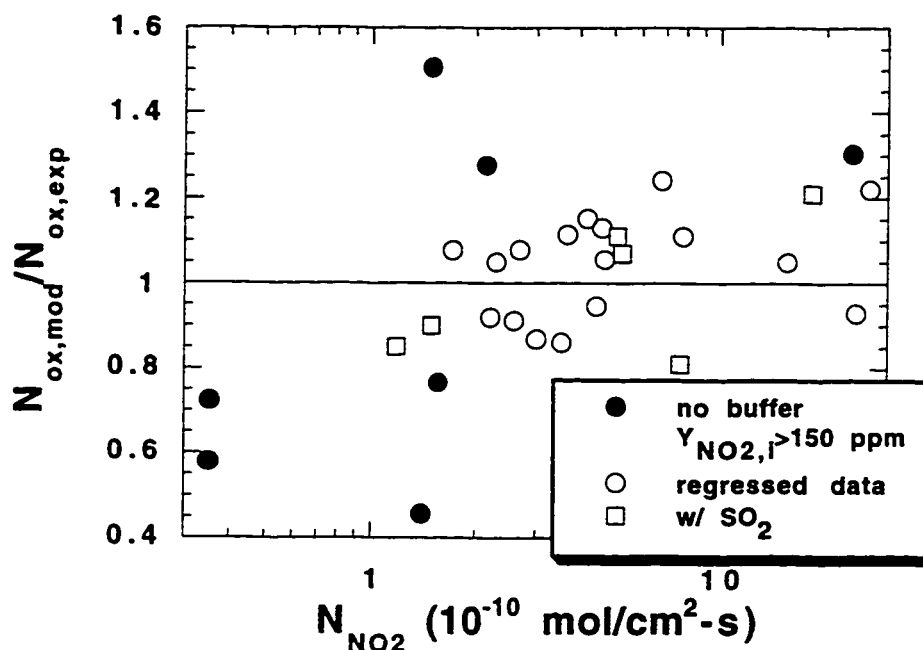


Figure 6.2 Model prediction of rates of sulfite oxidation. Runs 5.1.1-5.1.11, 5.1.29-5.1.35, 5.1.39-5.1.45, 5.2.4-5.2.5, and 5.2.7-5.2.10. 55 °C.

The overall fit of the data is reasonably good, with an average absolute deviation of 35% from the experimental oxidation rates. Therefore, the rate of sulfite oxidation is proven to increase with increasing NO_2 absorption rate as well as increasing sulfite and O_2 concentration. The data points showing the largest deviation from the model prediction were experiments with no buffer and relatively high concentration of NO_2 in the gas phase. Under these conditions, the depletion of $SO_3^{=}$ at the interface due to oxidation was extreme, and the

interfacial solution pH could be significantly below the model prediction, which in turn would lead to inaccurate prediction of $[\text{SO}_3^=]_i$ and the rate of sulfite oxidation by the model.

It was also noted that the first two terms on the right hand side of equation 6.5 were at least an order of magnitude greater than the third term under the conditions of our study. This indicates sulfite oxidation by physical absorption of O_2 is negligible when compared to the NO_2 catalyzed oxidation described in equations 2.10-2.14. However, in an actual scrubber where the k_1° is 5 to 10 times the value as in the stirred cell contactor, the physical absorption of O_2 will have a more significant contribution to the overall rate of sulfite oxidation.

To see how well equation 6.5 can predict oxidation rate based upon rates of NO_2 absorption, we generated several absorption curves from equation 6.5 with different $[\text{SO}_3^=]_i$, and compared them with the experimentally measured rates for a series of runs (figure 6.3).

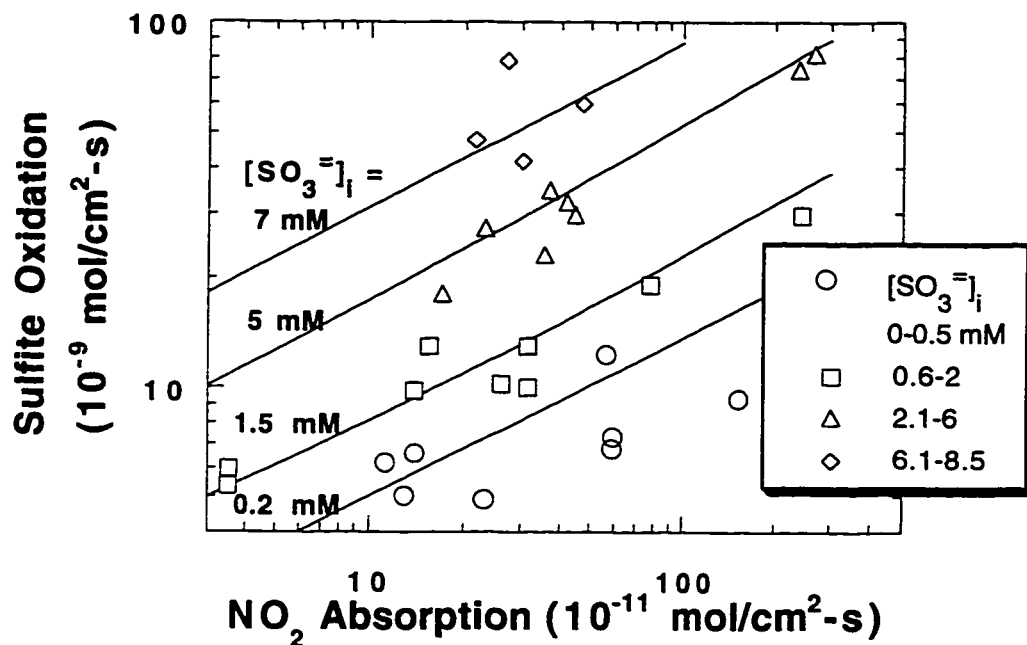


Figure 6.3 Model prediction of sulfite oxidation. Runs 5.1.1-5.1.11 and 5.1.19-5.1.29. pH = 5-7, 15% O₂, Y_{NO_{2,i}} = 30-350 ppm.

As can be seen from figure 6.3, our oxidation model did a good job in fitting the experimental data. The discrepancies between the measured and calculated rates of sulfite oxidation were due mainly to the difference in $[\text{SO}_3^=]_i$. A single value of $[\text{SO}_3^=]_i$ was used to generate the absorption curve, but the data contained $[\text{SO}_3^=]_i$ over a wide range. Some of the difference could also be due to the spread in the partial pressure of NO₂ in the experimental data.

6.4 EFFECT OF GAS PHASE VARIABLES ON SULFITE OXIDATION

6.4.1 Oxygen Partial Pressure

It has been shown in previous chapters that the rate of NO_2 absorption increases with no oxygen is present in the gas phase. On the other hand, equation 6.5 shows that the rate of sulfite oxidation increases with increasing oxygen concentration. Therefore, when the partial pressure of O_2 decreases, the rate of NO_2 absorption, N_{NO_2} , increases to partially compensate for the decrease in the rate of sulfite oxidation, and the net result is a fairly linear correlation between N_{ox} and $[\text{O}_2]_i$, as can be seen from figure 6.4.

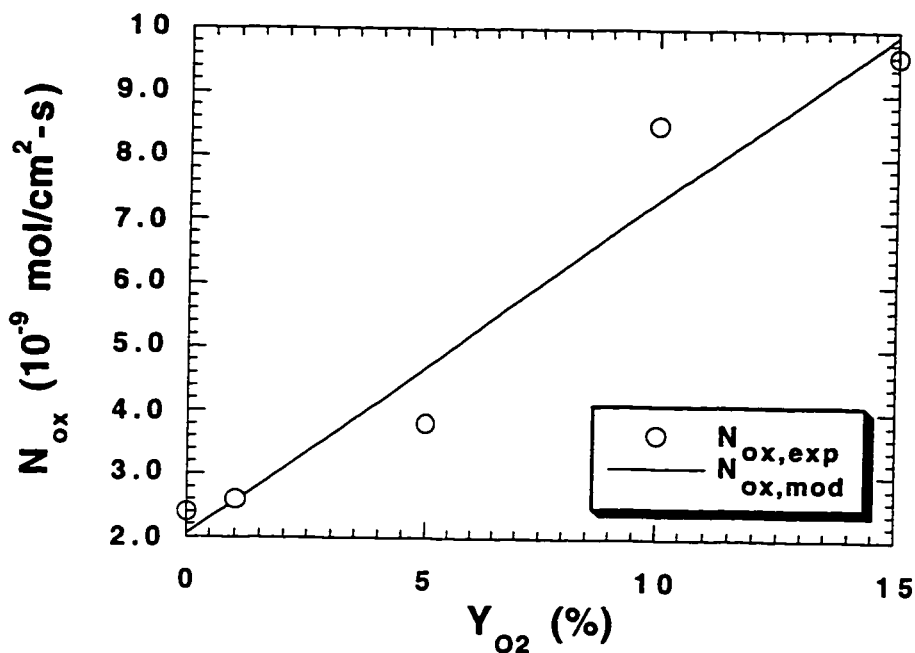


Figure 6.4 Effect of O_2 on sulfite oxidation. Runs 5.1.17, 5.1.34, and 5.1.36-5.1.38. $[SO_3]_i = 0.78-1.08$ mM, $Y_{NO_2,i} = 35-80$ ppm, $P_T = 1$ atm. $55^\circ C$.

6.4.2 Presence of SO_2

Figure 6.2 contains six experiments with gas phase SO_2 that were not used in the regression. The rate of sulfite oxidation of these runs were also predicted quite accurately by the oxidation model. This seems to suggest that the presence of SO_2 has no direct effect on the rate of sulfite oxidation, a conclusion also shared by Takeuchi et al. (1977). The absorption of SO_2 does lead to an increase

of interfacial $[S(IV)]$, but as our model uses the concentration of $SO_3^{=}$ at the interface, it is able to adequately account for this change in $[S(IV)]_i$.

In chapter 5 we have shown the effect of SO_2 on NO_2 absorption into sulfite solutions. The absorption of SO_2 into sulfite solutions leads to an increase in the interfacial $S(IV)$ concentration, which, in the presence of a buffer, results in a higher rate of NO_2 absorption as well as sulfite oxidation. On the other hand, when no buffer is present, SO_2 absorption leads to a decrease in interfacial solution pH, which in turn reduces the concentration of $SO_3^{=}$ at the interface, resulting in slower rates of NO_2 absorption and sulfite oxidation. The effect of SO_2 absorption with or without a buffer on the rate of sulfite oxidation is shown in figure 6.5.

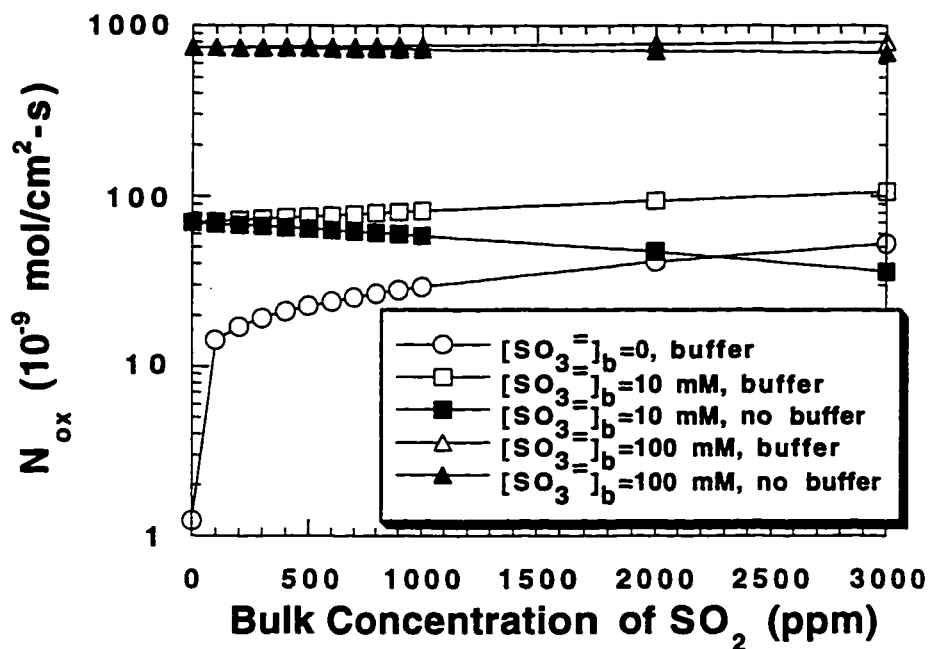


Figure 6.5 Effect of SO₂ absorption on rate of sulfite oxidation in stirred-cell contactor. Bulk solution pH assumed to be constant. Values of k_g and k_l are typical for the stirred-cell contactor..

6.5 EFFECT OF LIQUID PHASE VARIABLES ON SULFITE OXIDATION

6.5.1 Presence of Thiosulfate

Equations 2.15-2.19 show that thiosulfate functions as an oxidation inhibitor by providing an alternative route for the termination of the free radical reaction mechanism that consumes sulfite. Therefore, a significant reduction in

sulfite oxidation rate is to be expected with the addition of thiosulfate to the liquid phase.

Owens (1984) studied sulfite oxidation and thiosulfate degradation in FGD systems. He concluded that the addition of thiosulfate to a solution containing S(IV) could reduce the rate of sulfite oxidation. However, he also pointed out that because $S_2O_3^{2-}$ was involved directly in the reaction mechanism, it was being consumed at the same time. His results suggested that when the ratio of thiosulfate to S(IV) was greater than 0.1, the rate of thiosulfate degradation was independent of thiosulfate concentration, but increased with pH and decreased with the concentration of S(IV). Therefore, thiosulfate as an oxidation inhibitor was more effective at lower pH and higher concentration of S(IV), where it was consumed more slowly. Furthermore, he has also shown that O_2 in the gas phase had no significant effect on either thiosulfate degradation or inhibition of sulfite oxidation.

The experiments of sulfite oxidation in the presence of $S_2O_3^{2-}$ are given in table 5.3. Since $S_2O_3^{2-}$ was consumed with NO_2 absorption, a separate column in table 5.3, $N_{S_2O_3}$, reports the rate of $S_2O_3^{2-}$ depletion. In the presence of thiosulfate, N_{ox} is defined as the overall rate of S(IV) and $S_2O_3^{2-}$ consumption, which includes the depletion of SO_3^{2-} and $S_2O_3^{2-}$ both by reaction with NO_2 and by oxidation. A stoichiometry of 2 moles of SO_3^{2-} for every mole of NO_2 was assumed for the NO_2 - SO_3^{2-} reaction. Therefore, the amount of SO_3^{2-} consumed by reacting with NO_2 was simply twice the amount of NO_2 absorbed.

The free radical oxidation mechanism is initiated by the reaction between SO_3^{2-} and NO_2 (equation 2.15), and the rate of initiation is:

$$r_{ini} = k_{ini}[\text{NO}_2][\text{SO}_3^=] \quad (6.6)$$

The rate constant of the initiation reaction, k_{ini} , is the same as $k_{2,\text{SO}_3^=}$, which has a regressed value of $11.2 \times 10^5 \text{ M}^{-1}\text{s}^{-1}$ at 55°C . The termination step of the mechanism is the reaction between $\text{S}_2\text{O}_3^=$ and $\text{SO}_5^{\cdot-}$ (equation 2.17), and the rate of termination is:

$$r_t = k_t[\text{S}_2\text{O}_3^=][\text{SO}_5^{\cdot-}] \quad (6.7)$$

Assuming the rate of initiation equals the rate of termination, the steady-state concentration of $\text{SO}_5^{\cdot-}$ is:

$$[\text{SO}_5^{\cdot-}] = \frac{k_{ini}}{k_t} \frac{[\text{NO}_2][\text{SO}_3^=]}{[\text{S}_2\text{O}_3^=]} \quad (6.8)$$

The rate of oxidation is the rate of reaction between $\text{SO}_5^{\cdot-}$ and $\text{SO}_3^=$ (equation 2.12):

$$r_{ox} = k_{ox}[\text{SO}_5^{\cdot-}][\text{SO}_3^=] \quad (6.9)$$

Substituting the expression for $[\text{SO}_5^{\cdot-}]$ from equation 6.8 into equation 6.9, we have:

$$r_{ox} = \frac{k_{ox}k_{ini}}{k_t} \frac{[\text{SO}_3^=]^2[\text{NO}_2]}{[\text{S}_2\text{O}_3^=]} \quad (6.10)$$

To simplify the calculation, r_{ox} was assumed to be constant over the entire film thickness δ . The above expression was integrated over the entire thickness of δ , with the following boundary conditions:

$$@ x = 0, [\text{O}_2] = [\text{O}_2]_i \text{ and } \text{O}_2 \text{ flux} = N_{ox};$$

$$@ x = \delta, [\text{O}_2] = 0$$

Finally we have:

$$N_{ox} = \sqrt{2D_{\text{O}_2}[\text{O}_2]_i \frac{k_{ox}k_{ini}}{k_t} \frac{[\text{SO}_3^=]_i^2[\text{NO}_2]_i}{[\text{S}_2\text{O}_3^=]}} \quad (6.11)$$

D_{O_2} is the diffusivity of O_2 , with a value of $4.79 \times 10^{-5} \text{ cm}^2/\text{s}$ at 55°C , and N_{ox} is the measured rate of sulfite oxidation. Runs 5.3.2, 5.3.4, and 5.3.11-5.3.18 from table 5.3 were used to regress the ratio of k_{ox} to k_t , and at 55°C , the regressed ratio is:

$$\frac{k_{ox}}{k_t} = 3.43$$

The derivation of equation 6.11 and the regression of $\frac{k_{ox}}{k_t}$ are given in Appendix H. Owens (1984) reported a value of 4 for the above ratio at 50°C . The difference in temperature may account for the small difference between Owens' result and the result of this study. A plot of the measured rate of sulfite oxidation versus the oxidation rate predicted from equation 6.11 is given in figure 6.6.

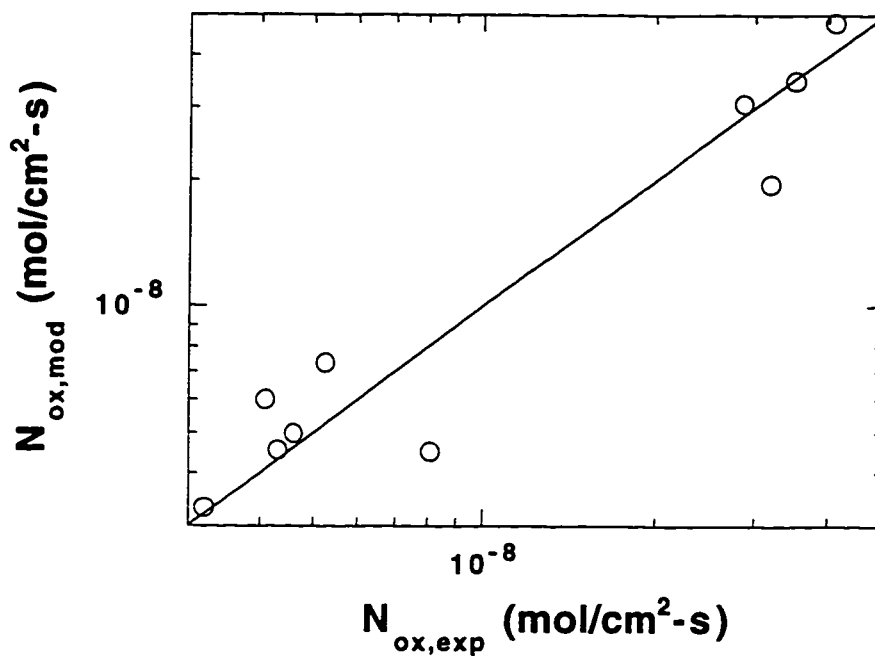


Figure 6.6 Model fit of rate of sulfite oxidation in the presence of thiosulfate. Runs 5.3.2, 5.3.4, and 5.3.11-5.3.18. pH = 5.5 & 7.5, $[\text{SO}_3^{2-}]_i = 7\text{-}90$ mM, $[\text{S}_2\text{O}_3^{2-}] = 7\text{-}105$ mM, $Y_{\text{NO}_2,i} = 15\text{-}200$ ppm. 55 °C, 15% O_2 .

To relate the rate of sulfite oxidation to more fundamental variables in equation 6.11, the predicted and measured rates of sulfite oxidation were compared at various levels of $Y_{\text{NO}_2,i}$ in figure 6.7.

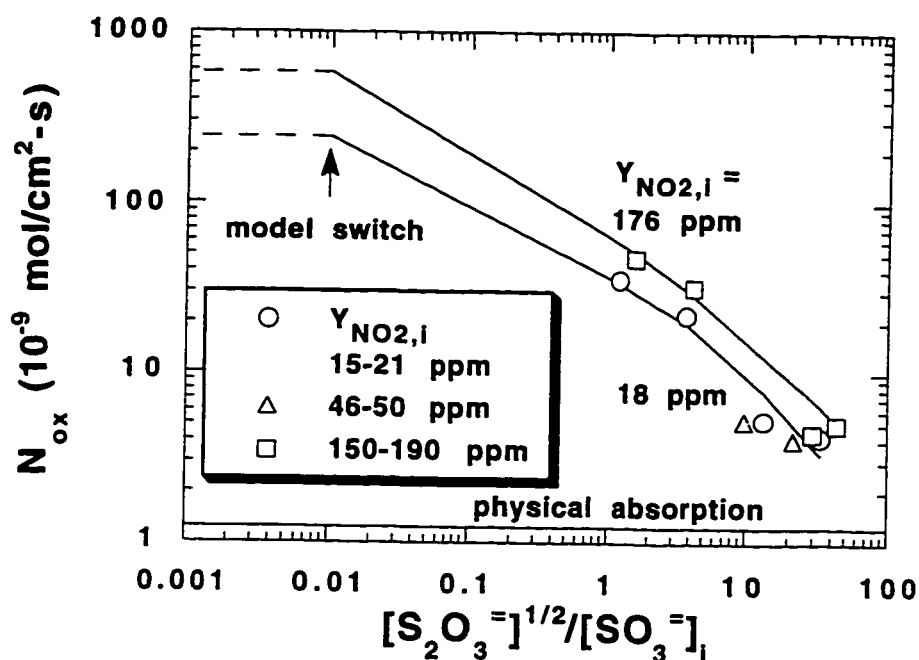


Figure 6.7 Model prediction of rates of sulfite oxidation with thiosulfate. Runs 5.3.2, 5.3.4, and 5.3.11-5.3.18. 15% O_2 , 55 °C.

It can be seen from figure 6.7 that the rate of sulfite oxidation decreases with increasing ratio of the square root of $[S_2O_3^{=}]$ to $[SO_3^{=}]_i$ but increases with $Y_{NO_2,i}$. An order of magnitude increase in the concentration of interfacial NO_2 leads to a factor of 3 increase in N_{ox} , consistent with the expression in equation 6.11. Furthermore, even with $\frac{\sqrt{[S_2O_3^{=}]}}{[SO_3^{=}]_i}$ of 40, the rate of sulfite oxidation was still 3-4 times higher than that of physical absorption, indicating that certain levels

of sulfite oxidation was unavoidable with NO_2 absorption, even with the addition of thiosulfate. Noticeable deviation from the model is observed with runs 5.3.2 and 5.3.4 (46-50 ppm $\text{NO}_{2,i}$). This is due to the fact that the solution pH for these two runs was around 5.5. At this pH, the oxidation of HSO_3^- started to become significant (Owens, 1984). All other runs in figure 6.7 had $\text{pH} > 7.5$.

Figure 6.7 also shows the continuity between our model of sulfite oxidation without thiosulfate (equation 6.5) and the model of sulfite oxidation in the presence of thiosulfate (equation 6.11). When $\frac{\sqrt{[\text{S}_2\text{O}_3^{2-}]}}{[\text{SO}_3^{2-}]_i}$ is greater than 0.01, the rate of sulfite oxidation can be predicted from equation 6.11. When $\frac{\sqrt{[\text{S}_2\text{O}_3^{2-}]}}{[\text{SO}_3^{2-}]_i}$ is less than 0.01, equation 6.5 should be used to predict the rate of sulfite oxidation. The curves representing the two models intersected at $\frac{\sqrt{[\text{S}_2\text{O}_3^{2-}]}}{[\text{SO}_3^{2-}]_i} = 0.01$ for both NO_2 concentrations shown in figure 6.7.

It has also become possible to estimate the number of moles of S(IV) oxidized for every mole of NO_2 absorbed in the presence of thiosulfate. The ratio of moles S(IV) oxidized to moles NO_2 absorbed can be expressed as the ratio of the rate of sulfite oxidation to the rate of NO_2 absorption. In the presence of $\text{S}_2\text{O}_3^{2-}$, the rate of sulfite oxidation is given by equation 6.11, and the rate of NO_2 absorption is:

$$N_{\text{NO}_2} = \frac{P_{\text{NO}_2,i}}{H_{\text{NO}_2}} \sqrt{D_{\text{NO}_2}(k_{2,\text{SO}_3^{2-}}[\text{SO}_3^{2-}]_i + k_{2,\text{S}_2\text{O}_3^{2-}}[\text{S}_2\text{O}_3^{2-}]_i)} \quad (6.12)$$

The reaction between NO_2 and water is negligible under these conditions and is not included in equation 6.12. On the other hand, when the concentration of $\text{S}_2\text{O}_3^{2-}$ is high, the contribution of the NO_2 - $\text{S}_2\text{O}_3^{2-}$ reaction to the overall rate of

NO₂ absorption is significant; therefore it is necessary to include it in equation 6.12. The ratio of N_{ox} to N_{NO2} can now be written as:

$$\frac{N_{ox}}{N_{NO2}} = \frac{\sqrt{2D_{O2}[O2]_i \frac{k_{ox}k_{ini}}{k_t} \frac{[SO_3^{=}]_i^2 [NO_2]_i}{[S_2O_3^{=}]}}}{\frac{P_{NO2,i}}{H_{NO2}} \sqrt{D_{NO2}(k_{2,SO3}=[SO_3^{=}]_i + k_{2,S2O3}=[S_2O_3^{=}]_i)}} \quad (6.13)$$

Figure 6.8 gives the above ratio as a function of [SO₃⁼]_i to the square root of [S₂O₃⁼] at several interfacial NO₂ concentrations.

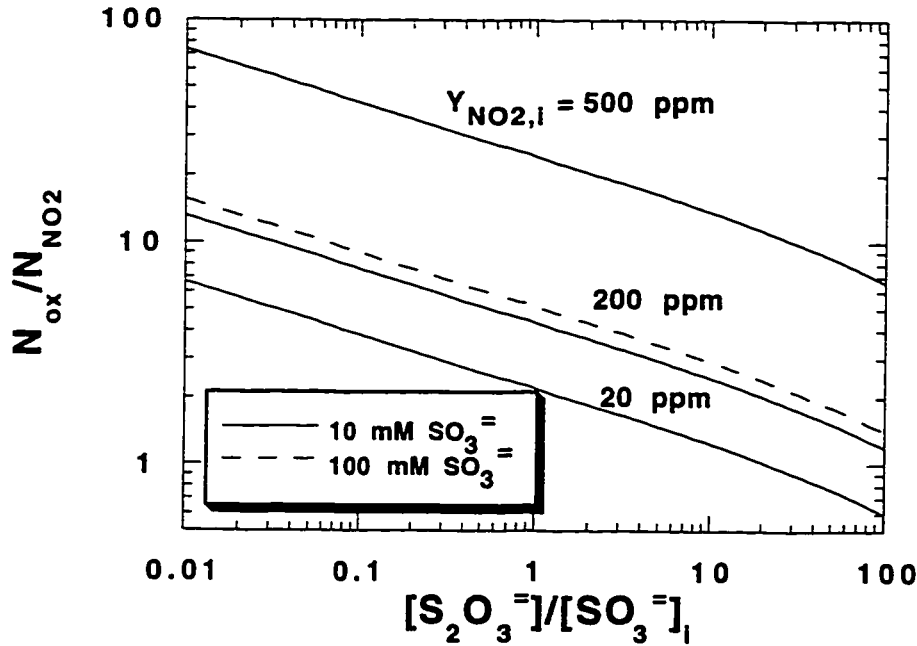


Figure 6.8 Calculated effect of NO₂ concentration on the ratio of sulfite oxidation to NO₂ absorption. pH>6.8, [SO₃⁼]_i = 10 mM, 15% O₂, 55 °C.

At low ratios of thiosulfate to sulfite, (i.e., relatively lower concentrations of $\text{S}_2\text{O}_3^{2-}$), the amount of oxidation occurred for every mole of NO_2 absorbed was higher. On the other hand, when the concentration of $\text{S}_2\text{O}_3^{2-}$ was higher than that of SO_3^{2-} , the rate of sulfite oxidation decreased significantly. The ratio of sulfite oxidation to NO_2 absorption increases with NO_2 concentration, as NO_2 concentration has a more significant impact on sulfite oxidation than on NO_2 absorption. Finally, the ratio of N_{ox} to N_{NO_2} was more strongly affected by the concentration of NO_2 than by the concentration of SO_3^{2-} , as an order of magnitude increase in $Y_{\text{NO}_2,i}$ led to a factor of 5 increase in $\frac{N_{\text{ox}}}{N_{\text{NO}_2}}$, but an order of magnitude increase in $[\text{SO}_3^{2-}]$ only led to a 20% increase in the above ratio.

The data in table 5.3 shows that although the total number of moles of S(IV) consumed per mole of NO_2 absorbed varied with $[\text{SO}_3^{2-}]_i$ and $P_{\text{NO}_2,i}$, the number of moles of $\text{S}_2\text{O}_3^{2-}$ depleted per mole of NO_2 absorbed remained fairly constant. In fact, a stoichiometry of 4 moles of $\text{S}_2\text{O}_3^{2-}$ consumed for every 3 moles of NO_2 absorbed was determined from the data in table 5.3. Figure 6.9 shows the contribution of NO_2 reaction and $\text{S}_2\text{O}_3^{2-}$ oxidation to the overall rate of S(IV) depletion.

Since a stoichiometry of 2 moles of SO_3^{2-} consumed for every mole of NO_2 absorbed was assumed for the NO_2 - SO_3^{2-} reaction, the contribution of NO_2 reaction to the overall rate of S(IV) depletion was constant. Furthermore, the contribution of $\text{S}_2\text{O}_3^{2-}$ oxidation to the overall rate of S(IV) depletion was relatively small and constant. This implies that SO_3^{2-} oxidation could not be stopped completely by adding more $\text{S}_2\text{O}_3^{2-}$. Above a certain ratio of $\text{S}_2\text{O}_3^{2-}$ to SO_3^{2-} , further addition of thiosulfate has little effect on sulfite oxidation.

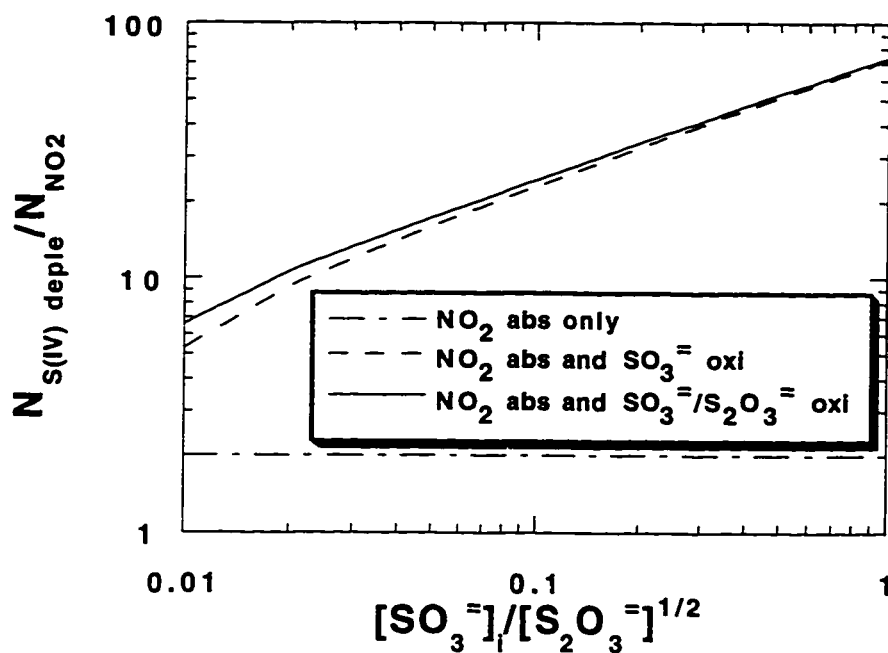


Figure 6.9 Calculated contribution of NO_2 reaction and $\text{S}_2\text{O}_3^{2-}$ oxidation to overall rate of S(IV) depletion. $Y_{\text{NO}_2, i} = 20$ ppm, $[\text{SO}_3^{2-}]_i = 10$ mM, $\text{pH} > 6.8$, 15% O_2 , 55 °C.

6.5.2 Other Additives

Ferrous ion (Fe^{++})

Ulrich (1983) has studied the effect of various additives on the rate of sulfite oxidation under typical scrubbing conditions. His results showed that ferrous ion was a powerful catalyst for sulfite oxidation. Even background levels

of Fe^{++} could lead to significant enhancement on the rate of sulfite oxidation. Since a trace amount of Fe^{++} , introduced as impurities in Na_2SO_4 and Na_2SO_3 solids, was always present in our study, we performed a series of experiments to quantify the effect of $[\text{Fe}^{++}]$ on the rate of sulfite oxidation in our system.

In this set of experiments, Fe^{++} was introduced into the solution in the form of dilute FeSO_4 solution, and the concentration of total dissolved iron was analyzed by atomic absorption. The concentration of Fe^{++} in the solution was analyzed both before and after each experiment. Typical background $[\text{Fe}^{++}]$ in a solution of 0.3 M Na_2SO_4 and 0.01 M Na_2SO_3 was 0.005 mM. For experiments in which a zero effective $[\text{Fe}^{++}]$ was desired, sufficient $\text{Na}_2\text{-EDTA}$ (sodium ethylenediaminetetraacetate, 0.02 mM) was added to chelate all the background Fe^{++} .

Three sets of data are plotted in figure 6.10. One set of three experiments was performed without NO_2 , another set with 50 ppm interfacial NO_2 , and the last experiment with 15 ppm NO_2 .

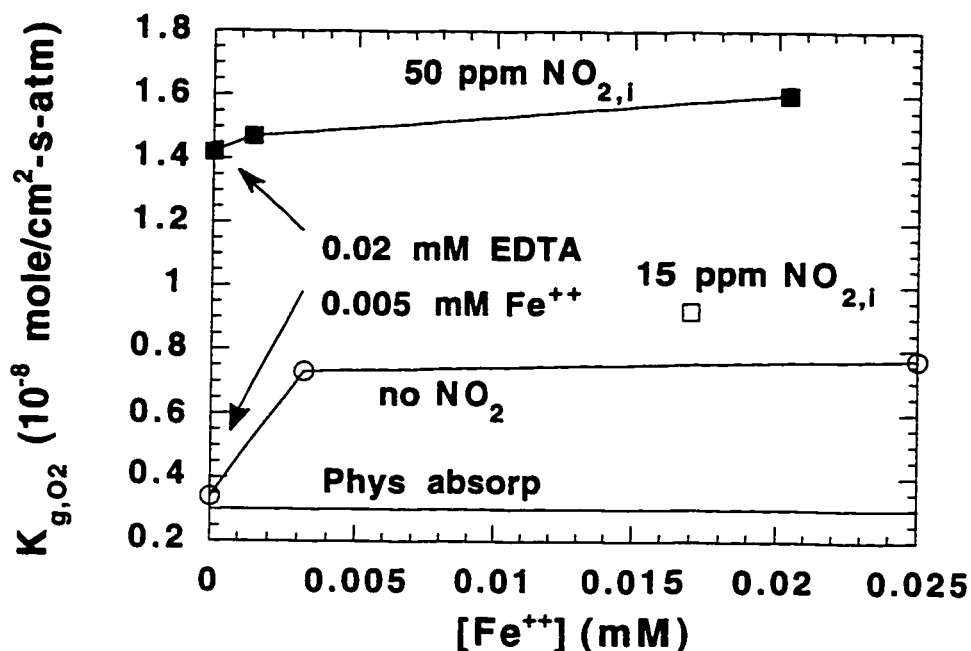


Figure 6.10 Effect of Fe⁺⁺ on sulfite oxidation. Runs 5.4.16-5.4.20. pH 5.5, [SO₃⁼]_i = 0.8-1.1 mM. 55 °C, 15% O₂.

From figure 6.10, it can be seen that although the rate of sulfite oxidation did increase with increasing [Fe⁺⁺], the increase was not significant between the range of 0 to 0.02 mM [Fe⁺⁺], especially when NO₂ was also present to catalyze oxidation. A solution containing four times the background [Fe⁺⁺], i.e., 0.02 mM, had an oxidation enhancement factor of 2 in the absence of NO₂, and an enhancement factor of only 1.1 with 50 ppm NO₂. Therefore, it seems

appropriate to conclude that when relatively higher concentration of NO₂ was present to provide free radicals to catalyze oxidation, the contribution of low concentrations of Fe⁺⁺ to the experimentally measured rates of sulfite oxidation was not significant. Figure 6.10 also shows the catalytic effect of NO₂ on sulfite oxidation, as the rate of oxidation increased with increasing concentration of NO₂, even in the presence of Fe⁺⁺.

Chloride ion (Cl⁻)

Clarke and Radojevic (1982) studied the effect of chloride salts such as NaCl, MgCl₂, and CaCl₂ on the rate of sodium sulfite oxidation. They observed that the oxidation was enhanced with >10⁻³ M chloride and the effect increased with increasing Cl⁻ concentration. The additional oxidation in the presence of Cl⁻ can be summarized as the following:



We made a similar study but with NO₂ present in the gas phase. NO₂ was absorbed into solutions of Na₂SO₃/Na₂SO₄ and various additives such as NaCl, MgCl₂, and CaCl₂. The expected rates of sulfite oxidation were calculated from equation 6.5, and they were compared with the experimentally measured rates of sulfite oxidation. The results are given in figure 6.11.

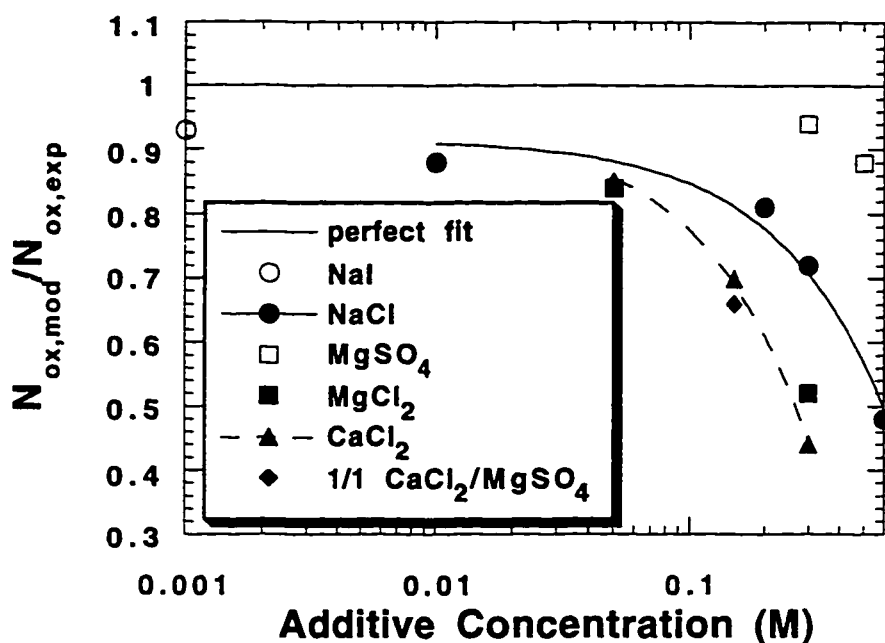


Figure 6.11 Effect of additive on rate of sulfite oxidation. Runs 5.4.1-5.4.15. All additive concentrations were nominal. 55 °C, 15% O₂.

It can be seen from figure 6.11 that the same trend as observed by Clarke and Radojevic was observed here in the presence of NO₂. In all cases with chloride additive, the experimental oxidation rates exceeded the predicted rates, and the difference increased with increasing chloride concentration, as indicated by the two curves with NaCl and CaCl₂. Our study has also shown that I⁻ has small catalytic effect on sulfite oxidation. Similar observation was made by Clarke and Radojevic (1982) with Br⁻ and F⁻.

Calcium ion (Ca^{++}) and Magnesium ion (Mg^{++})

Clarke and Radojevic (1982) also studied the effect of metal ions such as Mg^{++} , Na^+ , Ca^{++} on the rate of Na_2SO_3 oxidation. They did not observe any significant effect of these cations on the rate of sulfite oxidation. They believed that these metal ions, unlike transition metal ions such as Mn^{++} , were less likely to be involved in electron transfer reactions. On the other hand, Bassett and Parker (1951) did observe a small effect of MgSO_4 and ZnSO_4 on sulfite oxidation. But the effect is much less significant when comparing to Fe^{++} and Mn^{++} at similar concentrations.

As can be seen from figure 6.11, the result of our study showed better agreement with the observation of Bassett and Parker. The addition of MgSO_4 did lead to a slightly higher rate of sulfite oxidation than the model prediction. However, this catalytic effect is not at all significant when comparing to the effect of Cl^- or I^- , as 0.3 M of MgSO_4 had the same effect on sulfite oxidation as 0.001 M of I^- .

6.5.3 Liquid Phase Agitation Speed

As discussed in section 5.4.4, increasing liquid phase agitation increases the transport of $\text{SO}_3=$ from bulk solution to the gas liquid interface. Since the rate of sulfite oxidation had a stronger dependence on $[\text{SO}_3=]_i$ than the rate of NO_2 absorption, increasing liquid phase agitation speed had a stronger affect on No_x than it did on NNO_2 , as reflected in figure 6.12.

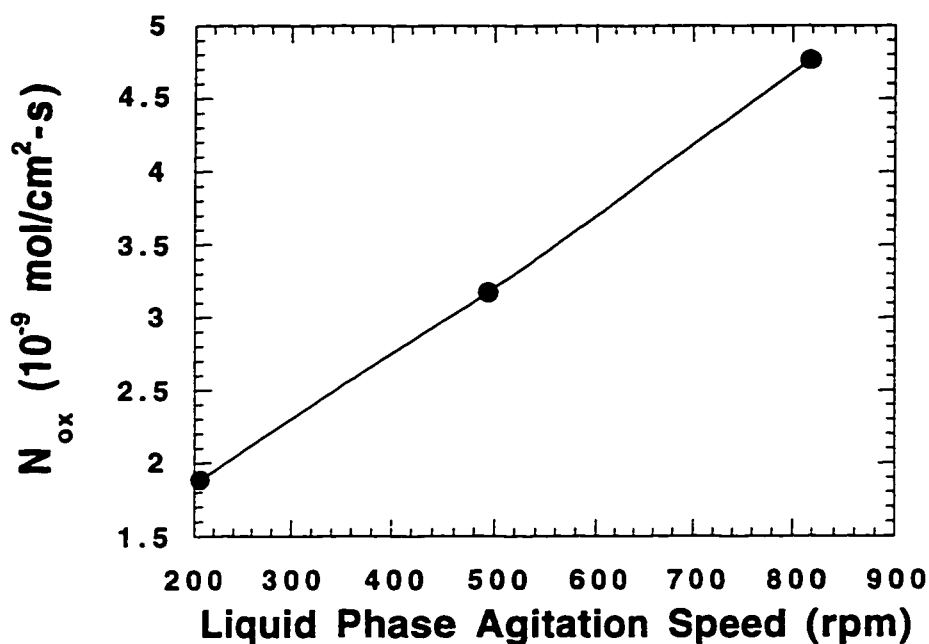


Figure 6.12 Effect of liquid phase agitation on sulfite oxidation. pH = 5.5, [S(IV)] = 10 mM, $Y_{NO_2,i}$ = 100 ppm, 55 °C, 15% O₂.

6.6 CHAPTER SUMMARY

This chapter presents the results of our study on sulfite oxidation in the presence of gas phase NO₂. It is an important reaction both for the absorption of NO₂ inside a limestone slurry scrubber and the oxidation of SO₃⁼ to SO₄⁼ in the hold tank.

We proposed a model to relate the rate of sulfite oxidation to the rate of NO_2 absorption, the concentration of sulfite at the liquid boundary, and the concentration of O_2 in the solution. This model gives fairly good predictions of sulfite oxidation rates for most cases.

We have shown that the rate of sulfite oxidation increases with increasing $[\text{SO}_3^{2-}]$ and P_{O_2} , while the presence of gas phase SO_2 has no significant effect on sulfite oxidation. We have also shown that the addition of thiosulfate can significantly inhibit sulfite oxidation, and we have derived a fundamental model that quantifies the effect of thiosulfate on sulfite oxidation. Furthermore, we have observed that both Fe^{++} and Cl^- are potent catalysts for sulfite oxidation, while Mg^{++} and Ca^{++} have much smaller effects. Finally, we have shown that liquid phase agitation had a noticeable effect on the rate of sulfite oxidation.

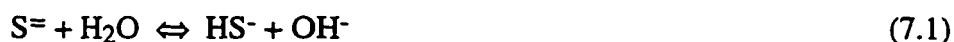
Chapter 7

NO₂ Absorption in Aqueous Na₂S

During the course of our study, we investigated other possible reagents that reacted with NO₂ at a rate fast enough to cause substantial NO₂ removal. Aqueous sodium sulfide (Na₂S) emerged as a likely candidate because: 1) It has been used on an industrial scale to scrub NO₂ and has been proven a very efficient reagent; and 2) Our preliminary study has shown Na₂S to be at least as reactive toward NO₂ as Na₂SO₃ at room temperature (figure 4.2). Therefore, we devoted a part of our research to studying the reaction between NO₂ and sulfide, or S(-II), at 55 °C. Our objective was to understand how the rate of NO₂ absorption into aqueous Na₂S was affected by the concentration of S(-II) in the solution, the partial pressure of NO₂ in the gas phase, and the NO₂ catalyzed air oxidation of S(-II).

7.1 LITERATURE REVIEW

Under most solution pH conditions, Na₂S, dissolved in water, hydrolyzes more or less completely (Stahl and Jordon, 1987), viz.



Giggenbach (1971) reported a value of 1.15×10^{17} as the equilibrium constant K for the above reaction. Therefore, S(-II) exists almost exclusively as bisulfide, or HS⁻, and aqueous Na₂S is often referred to as "solutions of HS⁻" in the literature (Stahl and Jordon, 1987).

Kuropka and Gostomczyk (1981) absorbed NO₂ into solutions of Na₂S in a gas liquid contactor, and they varied the inlet NO₂ concentration from 1 to 4 g/m³, and the S(-II) concentration from 0.1 to 1.0 M. They performed the same absorption experiments with Na₂SO₃, and compared the fraction NO₂ removal obtained in both cases. Their results showed that higher NO₂ removal was obtained with Na₂S, indicating that the reaction rate was faster for S(-II) than SO₃⁼. Furthermore, they observed a slightly higher than first order dependence of the reaction rate on NO₂ concentration, as the fractional NO₂ removal increased with increasing NO₂ concentration.

The removal of NO₂ by aqueous Na₂S scrubbing has been attempted on an industrial scale. Shen (1990) documented NO₂ scrubbing by a mixture of 5% Na₂S and 3% NaOH in a whirlwind plate tower. He reported an average NO₂ removal of >90% over a period of 2 years, with inlet NO₂ concentration as high as 14200 ppm and a gas rate of 4000 m³/hr. He also observed that the Na₂S /NaOH mixture was more efficient in removing NO₂ than a mixture of Na₂SO₃/NaOH.

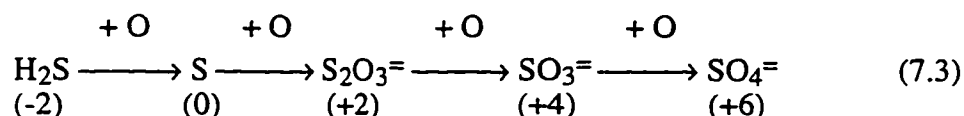
Seel and Wagner (1988) studied the reactions of NaHS, Na₂S₂, and Na₂S₄ with NO by UV-visible and NMR spectroscopy. The formation of N-nitrosohydroxylamine monosulfonate, ONNOSO₃⁼ was confirmed, via the reaction:



They also observed that unstable orange-yellow perthionitrite, ONSS⁻, formed temporarily.

It is known that aqueous sulfide is oxidized by air. Kuhn et al. (1983) reviewed the literature dealing with the air oxidation of aqueous sulfide solutions,

and they concluded that the rate of sulfide oxidation was first order in O₂ partial pressure. They also reported a first order dependence of oxidation rate on the concentration of S(-II), while other researchers reported a reaction order of 1.3 for S(-II) (Lefers et al., 1978). Kuhn et al. (1983) found that the rate of sulfide oxidation increased dramatically with temperature, and the effect of pH on the rate of oxidation was very complex, going through two maxima and one minimum. Perhaps their most important discovery was that the product of sulfide oxidation depended on the ratio of molecular oxygen to S(-II) concentration. They proposed the following possible reaction scheme:



Chen and Morris (1972) observed that at pH>8.5, thiosulfate was the main oxidation product, and the oxidation of sulfite to sulfate was inhibited by the presence of S(-II). Polysulfides, formed by the reaction between elemental sulfur and sulfide, existed at very low concentrations, and elemental sulfur was virtually non-existent.

7.2 NO₂-S(-II) REACTION

The reaction between NO₂ and HS⁻ is likely to involve charge transfer that leads to a free radical mechanism. The following reaction is likely to occur in the liquid boundary and enhances NO₂ absorption:



The result of our batch experiments has shown that the rate of the reaction was first order in $[\text{NO}_2]$ (figure 4.2); therefore the rate expression for the above reaction can be written as:

$$r_{\text{HS}^-} = k_{2,\text{HS}^-} [\text{HS}^-]_i [\text{NO}_2]_i \quad (7.5)$$

The NO_2 absorption flux expression was given in equation 2.43. By neglecting the NO_2 -water reaction and using the normalized NO_2 flux R_g , equation 2.43 can be written in its linear form as:

$$\frac{R_g^2 \text{HNO}_2^2}{D_{\text{NO}_2}} = k_{2,\text{HS}^-} [\text{HS}^-]_i \quad (7.6)$$

In the above equation, the values of HNO_2 and D_{NO_2} at 55 °C were taken from table 2.1. $[\text{HS}^-]_i$, the interfacial concentration of bisulfide, was calculated from the following equation:

$$[\text{HS}^-]_i = [\text{HS}^-]_b - \frac{N_{\text{ox}}}{k_{l^{\circ}\text{HS}^-}} \quad (7.7)$$

$[\text{HS}^-]_b$, the bulk solution HS^- concentration, was measured by titrating with AgNO_3 solution. $k_{l^{\circ}\text{HS}^-}$, the liquid phase mass transfer coefficient of HS^- , was taken to be 4.04×10^{-3} cm/s at 55 °C. The rate of S(-II) oxidation, N_{ox} , was calculated by:

$$N_{\text{ox}} = \frac{V([\text{S}(-\text{II})]_o - [\text{S}(-\text{II})]_f) + V_{\text{tit}}[\text{S}(-\text{II})]_{\text{tit}}}{A \Delta t} \quad (7.8)$$

In this equation, $[\text{S}(-\text{II})]_o$ and $[\text{S}(-\text{II})]_f$ were the initial and final concentrations of HS^- measured via titration, Δt the time interval, and V and A the volume of the solution and the gas-liquid contacting area, respectively. The $V_{\text{tit}}[\text{S}(-\text{II})]_{\text{tit}}$ term took into account the amount of S(-II) being fed into the contactor over the course of an experiment.

Table 7.1 lists all experiments of NO₂ absorption into S(-II) solutions. Since H₂S was likely to form when the solution pH fell below 9.0, the pH was monitored and controlled carefully with the additional of fresh Na₂S/NaOH solution. In three of the experiments where a pH of 9.0±0.2 was desired, 0.2 M NaHCO₃ was added to the solution as a buffer to minimize the formation of H₂S. All experiments listed in table 7.1, with the exception of three experiments without NO₂, were used to regress the reaction rate constant between NO₂ and HS⁻, using equation 7.6 and BETAV3. The reaction rate constant, k_{2,HS-}, at 55 °C, was determined to be:

$$k_{2,HS-} = (26.4 \pm 4.2) \times 10^5 \text{ M}^{-1}\text{s}^{-1}$$

This rate constant was twice as large as the reaction rate constant between NO₂ and SO₃⁼, which at 55 °C has a regressed value of:

$$k_{2,SO_3=} = (11.2 \pm 0.3) \times 10^5 \text{ M}^{-1}\text{s}^{-1}$$

Therefore, our study reached the same conclusion as Shen (1990) and Kuropka et al. (1981), that HS⁻ is more reactive toward NO₂ than SO₃⁼, even at elevated temperatures.

Figure 7.1 gives the ratio of the predicted NO₂ absorption rate to the experimentally measured rate as a function of [HS⁻] at the interface:

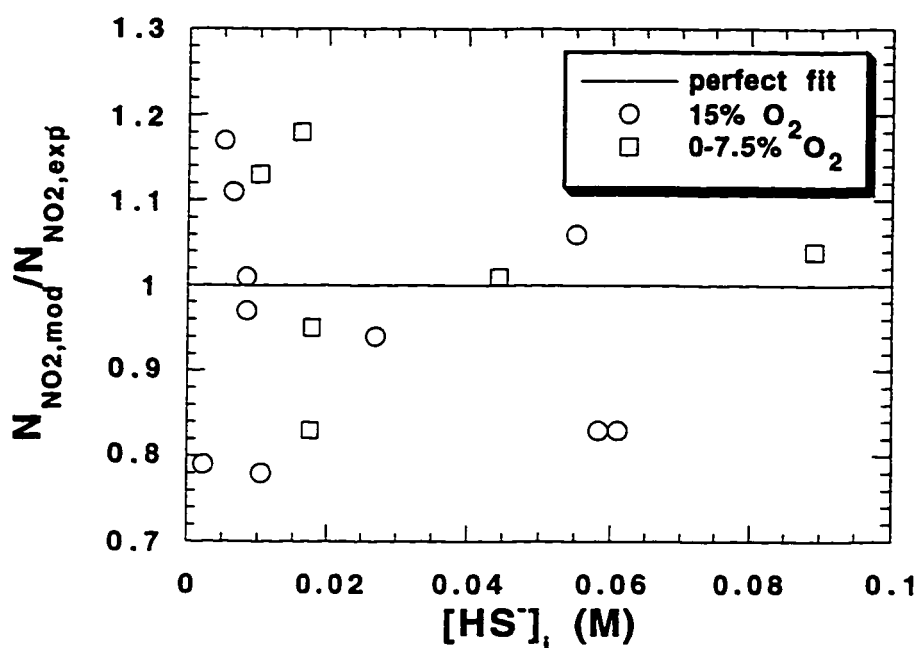


Figure 7.1 Model fit of rate of NO_2 absorption. Runs 7.1.2, 7.1.4, 7.1.6-7.1.7, 7.1.9-7.1.12, 7.1.14-7.1.15, and 7.1.17-7.1.22. 55 °C, $Y_{\text{NO}_2, i} = 40\text{-}500$ ppm.

Since the model did an equally good job in fitting the 15% O_2 data as the 0-7.5% O_2 data, we could conclude that our method of taking into account S(-II) oxidation by reporting an interfacial HS^- concentration (equation 7.7) was correct and adequate to account for the effect of HS^- depletion via oxidation.

Figure 7.2 shows the effect of interfacial partial pressure on NO_2 absorption.

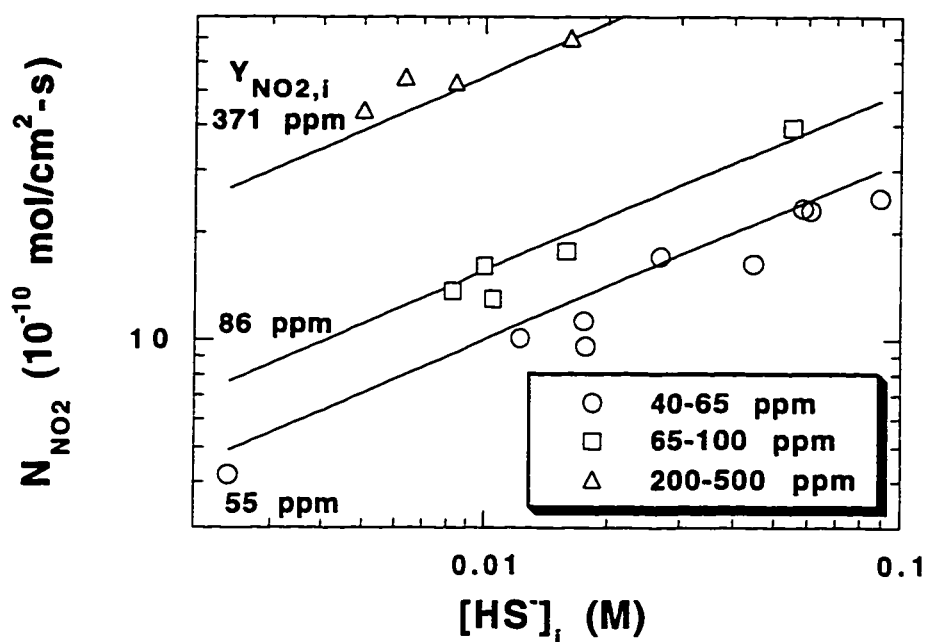
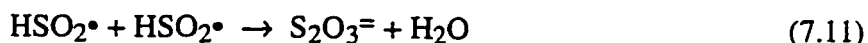


Figure 7.2 Effect of $Y_{\text{NO}_2,i}$ on rate of NO_2 absorption. Runs 7.1.2, 7.1.4, 7.1.6-7.1.7, 7.1.9-7.1.12, 7.1.14-7.1.15, and 7.1.17-7.1.22. 55 °C, pH = 8.8-13.1.

Three sets of data, each with a different range of interfacial NO_2 concentration, were plotted in the above figure. An average $Y_{\text{NO}_2,i}$ for each data set was calculated and used to generate the absorption curves from equation 2.43. Despite the spread in NO_2 concentration, the curves did a great job in fitting the corresponding sets of data.

7.3 S(-II) OXIDATION IN THE PRESENCE OF NO₂

We have shown that S(-II) is oxidized by O₂. In the presence of NO₂, HS• is produced by the reaction between NO₂ and HS⁻, and the oxidation mechanism may follow the following path:



This mechanism is consistent with the findings of Kuhn et al. (1983), whom have observed that the rate of sulfide oxidation was first order in S(-II) concentration and O₂ partial pressure, and that S₂O₃²⁻ was the main oxidation product.

Since the oxidation of S(-II) follows a free radical mechanism similar to the oxidation of SO₃²⁻, NO₂ is expected to have a catalytic effect on the oxidation mechanism. Furthermore, the presence of an oxidation inhibitor such as thiosulfate should reduce the rate of S(-II) oxidation. It is interesting to note that since S₂O₃²⁻ is itself a product of S(-II) oxidation, the oxidation of S(-II) should be self-inhibiting. However, due to the relatively short duration of the experiments in this study, the amount of S₂O₃²⁻ accumulated in the solution as oxidation product was too small to significantly affect the rate of S(-II) oxidation, and consequently the self-inhibiting behavior of S(-II) oxidation had not been observed.

Since NO₂ can catalyze S(-II) oxidation by a mechanism similar to that of sulfite oxidation, we propose a parallel expression for the rate of S(-II) oxidation:

$$N_{ox} = C_1\sqrt{N_{NO_2}} + C_2\sqrt{N_{NO_2}}[O_2]_i + C_3[HS^-]_i[O_2]_i + k_1^{\circ}O_2[O_2]_i \quad (7.12)$$

The first term on the right hand side is used to directly correlate NO_2 absorption rate to the rate of sulfide oxidation, the second term accounts for the free radical reaction with O_2 . The third term accounts for the baseline oxidation of sulfide when no NO_2 is present, and the last term represents the physical absorption of O_2 . The experiments in table 7.1 were used with BETAV3 to estimate the three constants C_1 , C_2 , and C_3 .

$$C_1 = (3.4 \pm 0.84) \times 10^{-4} \text{ mol}^{1/2}/\text{cm-s}^{1/2}$$

$$C_2 = (1.3 \pm 0.36) \times 10^3 \text{ cm}^2/\text{mol}^{1/2}\text{-s}^{1/2}$$

$$C_3 = (9.7 \pm 1.4) \times 10^3 \text{ cm}^4/\text{mol-s}$$

Figure 7.3 gives the ratio of the predicted rate of S(-II) oxidation to the experimentally measured rate as a function of the rate of NO_2 absorption.

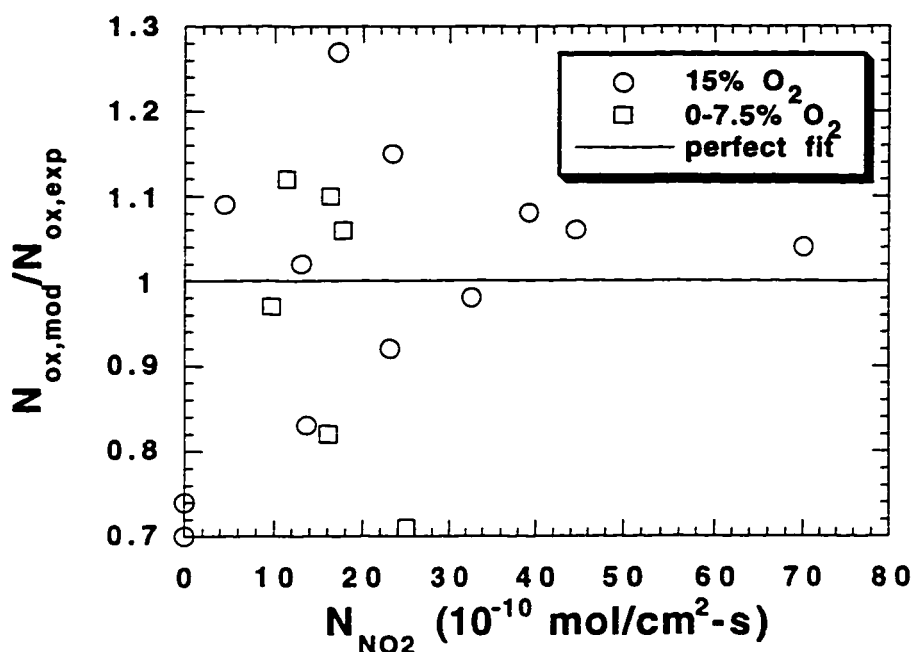


Figure 7.3 Model fit of S(-II) oxidation rate. Runs 7.1.2, 7.1.4, 7.1.6-7.1.7, 7.1.9-7.1.12, 7.1.14-7.1.15, and 7.1.17-7.1.22. 55 °C, $[HS^-]_i = 4\text{-}90$ mM, $Y_{NO_2,i} = 40\text{-}500$ ppm.

As can be observed from the plot above, our model did a reasonably good job in fitting the experimental data, with an absolute average deviation of 22%. Therefore, the rate of S(-II) oxidation was proven to increase with increasing NO_2 absorption rate as well as increasing S(-II) and O_2 concentration.

To see how well equation 7.12 can predict oxidation rate based upon rates of NO_2 absorption, we generated several oxidation curves from equation 7.12

with different $[\text{HS}^-]_i$, and compared them with the experimentally measured oxidation rates for a series of runs from table 7.1 (figure 7.4).

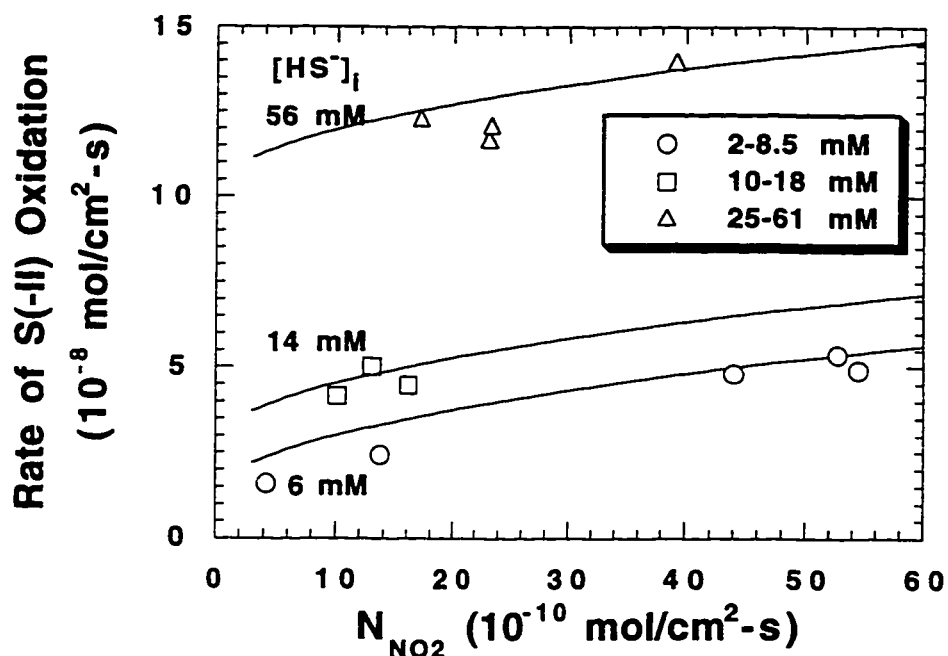


Figure 7.4 Model prediction of S(-II) oxidation. Runs 7.1.2, 7.1.4, 7.1.6-7.1.7, 7.1.9-7.1.10, 7.1.14-7.1.15, 7.1.17-7.1.18, and 7.1.20-7.1.22. 55 °C, 15% O_2 , pH = 8.8-13.1.

As can be seen from figure 7.4, our oxidation model did a good job in fitting the experimental data. Whatever discrepancy there was between the measured and calculated rates of S(-II) oxidation was due mainly to the difference in $[\text{HS}^-]_i$. A single value of $[\text{HS}^-]_i$ was used to generate the oxidation curve, but

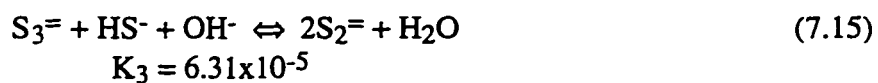
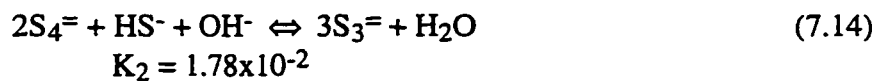
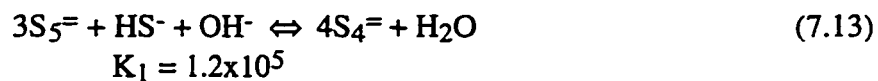
the data contained $[\text{HS}^-]_i$ over a wide range. Some of the difference could also be due to the spread in the partial pressure of NO_2 in the experimental data.

As mentioned earlier, S(-II) oxidation follows a free radical mechanism, therefore an oxidation inhibitor such as thiosulfate should be able to reduce the rate of S(-II) oxidation. To test this hypothesis, we performed two experiments to study the effect of $\text{S}_2\text{O}_3^{2-}$ on the rate of S(-II) oxidation, with and without the presence of NO_2 (runs 7.1.12 and 7.1.15). The rate of S(-II) oxidation was experimentally measured in each case, and the results were compared to other runs without thiosulfate but under otherwise similar conditions. The outcome of this study clearly indicates that thiosulfate inhibits S(-II) oxidation. The presence of 40 mM $\text{S}_2\text{O}_3^{2-}$ reduced the oxidation rate by a factor of 30, even when high concentration (500 ppm) of NO_2 was present in the gas phase to catalyze oxidation. Furthermore, when no NO_2 was present, the presence of mere 10 mM $\text{S}_2\text{O}_3^{2-}$ reduced the oxidation rate to the level to be expected from pure physical absorption of O_2 .

7.4 NO_2 REACTION WITH POLYSULFIDE

As discussed in previous sections, polysulfides (S_n^{2-}) are potential products of air oxidation of sulfide. We performed a preliminary study to determine which of the polysulfides was most likely to be present in the liquid phase and if it could react with NO_2 .

Giggenbach (1974) studied the equilibria involving polysulfide ions in aqueous sulfide solutions, and based upon his findings, we calculated the equilibrium constants at 55 °C for the following reactions:



By using the above equilibrium constants, we calculated the equilibrium concentrations of HS^- and various polysulfides in a solution initially containing 20 mM $S(-II)$ at 55 °C, but in the absence of NO_2 . The result is given in figure 7.5.

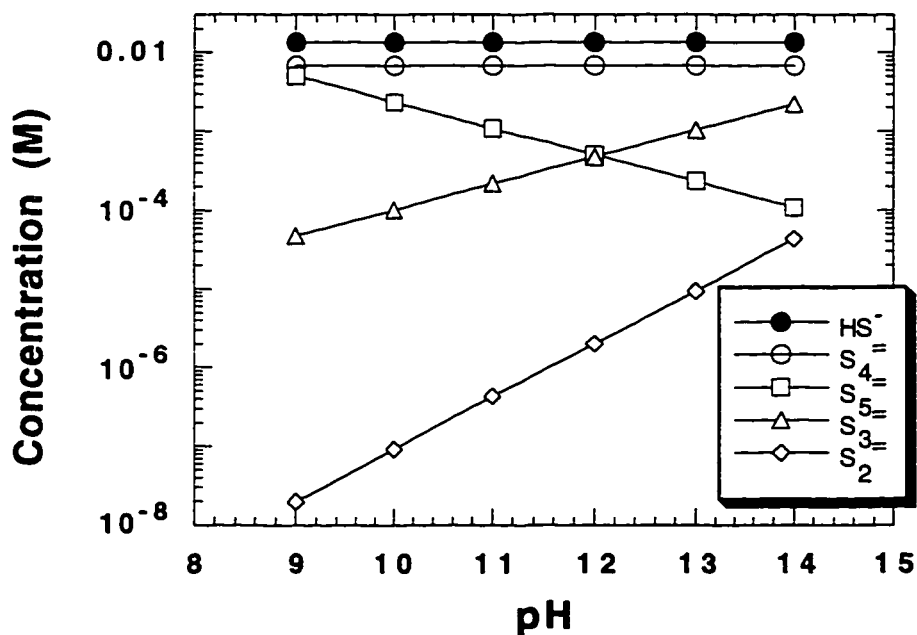


Figure 7.5 Equilibrium composition of HS^- and polysulfides. 55 °C, total concentration of sulfur species = 20 mM.

From the above plot, it can be seen that between pH 9 and 13, the only polysulfide species that had the potential to accumulate to a high enough concentration to interfere with the HS⁻/NO₂ reaction was tetrasulfide, or S₄⁼. However, when NO₂ is present, the rate of S(-II) oxidation is greatly enhanced, and the main oxidation product is thiosulfate. Polysulfide, if exists at all, will be of much lower concentration. Therefore, unless S₄⁼ can react with NO₂ at a much faster rate than HS⁻, it will not have any significant effect on NO₂ absorption.

Table 7.2 lists the series of experiments of NO₂ absorption into solutions of Na₂S₄. As Na₂S₄ cannot be titrated with AgNO₃, the concentrations of S₄⁼ reported below were nominal concentrations not determined by actual measurements. For the same reason, the depletion of S₄⁼ during the experiment was not measured, and no oxidation data was reported. The second order rate constant for the reaction between NO₂ and S₄⁼, k_{2,S4=}, was calculated for each experiment.

Table 7.2 NO₂ absorption into aqueous Na₂S₄. 55 °C, 15% O₂.

Exp No.	[S ₄ ⁼] _b (mM)	[HS ⁻] _b (mM)	pH	PNO _{2,i} (ppm)	NNO ₂ (10 ⁻⁹ mol/cm ² -s)	k _{2,S4=} (10 ⁶ M ⁻¹ s ⁻¹)
7.2.1	20	0	7.5	83	1.03	1.05
7.2.2	20	0	10.8	68	1.66	1.88
7.2.3	6.7	13.3	11.3	65	1.58	1.59
7.2.4	20	0	13.0	62	1.83	2.45

Figure 7.6 gives the second order rate constant as a function of the bulk solution pH.

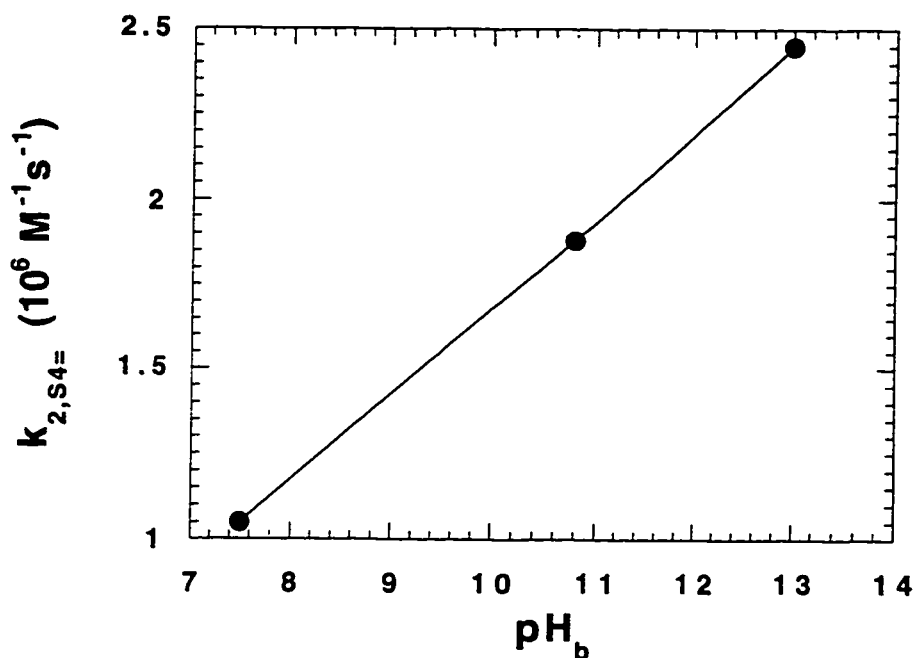


Figure 7.6 Effect of pH on second order rate constant. Run 7.2.1-7.2.2 and 7.2.4. 55 °C, 15% O₂.

The plot above shows that the second order rate constant increases with solution pH. This could be due to the fact that the $k_{2,S4=}$ was calculated by assuming all $S_4^{=}$ added initially stayed as $S_4^{=}$, while in actuality various other polysulfides might form via equilibrium, and they were not as reactive toward NO_2 as $S_4^{=}$. Since higher pH favors the formation of $S_4^{=}$, the amount of polysulfide that existed as $S_4^{=}$ increased with pH, which in turn led to the increase in the rate of NO_2 absorption. Furthermore, it should be noted that even

at pH 13, the $k_{2,S_4^{2-}}$ reported in table 7.2 was lower than the actual k_2 , since our calculation did not account for S_4^{2-} depletion and used the nominal concentration of S_4^{2-} , which was always greater than the actual concentration of S_4^{2-} . However, even in the most extreme cases, the calculated $k_{2,S_4^{2-}}$ could be lower than the actual k_2 by no more than 50%, and since the calculated $k_{2,S_4^{2-}}$ was about the same as that of k_{2,HS^-} , it was safe to conclude that S_4^{2-} did not react with NO_2 significantly faster than HS^- . Therefore, the contribution of S_4^{2-}/NO_2 reaction to the overall rate of NO_2 absorption into aqueous Na_2S was not significant.

7.5 CHAPTER SUMMARY

In this chapter, we present the result of our preliminary study of NO_2 absorption into solutions of S(-II). The phenomenon of S(-II) oxidation by O_2 in the presence of NO_2 was studied, and we briefly investigated the reaction between NO_2 and tetrasulfide.

Our study determined the reaction rate constant for the NO_2/HS^- reaction to be $2.64 \times 10^6 \text{ M}^{-1}\text{s}^{-1}$ at 55 °C, and it was shown that NO_2 reacts with HS^- at a faster rate than with sulfite. The reaction is first order in the concentrations of HS^- and NO_2 .

We have shown that NO_2 absorption catalyzes S(-II) oxidation, and we proposed a model to correlate the rate of S(-II) oxidation with the rate of NO_2 absorption, the interfacial concentration of HS^- , and the concentration of dissolved O_2 . The addition of thiosulfate to the solution was shown to reduce the rate of S(-II) oxidation.

Our preliminary study of the $\text{NO}_2/\text{S}_4^{=}$ reaction shows that NO_2 reacts with $\text{S}_4^{=}$ at a rate similar to that of HS^- , and in the presence of NO_2 , the reaction between NO_2 and $\text{S}_4^{=}$ did not contribute significantly to the overall rate of NO_2 absorption into solutions of $\text{S}(-\text{II})$.

Table 7.1 Summary of Experiments with S(-II), T = 55 °C.

Exp No.	[HS ⁻]b (mM)	[HS ⁻]i (mM)	Y _{NO₂,i} (ppm)	pH	Y _{O₂} (%)	N _{NO₂} × 10 ⁹ ($\frac{\text{mol}}{\text{cm}^2 \cdot \text{s}}$)	$\frac{N_{\text{NO}_2, \text{mod}}}{N_{\text{NO}_2, \text{exp}}}$	N _{ox} × 10 ⁹ ($\frac{\text{mol}}{\text{cm}^2 \cdot \text{s}}$)	$\frac{N_{\text{ox}, \text{mod}}}{N_{\text{ox}, \text{exp}}}$	Additive (mM)
7.1.1	**100	89.2	42	12.3	0	2.50	1.04	*3.13	1.00	--
7.1.2	**100	61.0	59	12.4	15	2.31	0.83	*1.17	1.00	--
7.1.3	**50	44.4	50	11.9	0	1.63	1.01	*2.40	1.00	--
7.1.4	**50	26.9	63	11.7	15	1.71	0.94	*123.1	1.00	--
7.1.5	16.6	15.9	76	11.8	0	1.77	1.18	*2.82	1.00	--
7.1.6	14.3	8.3	88	11.6	15	1.37	1.01	24.4	0.83	--
7.1.7	15.5	10.5	82	10.3	15	1.30	0.78	50.1	1.02	--
7.1.8	13.6	10.0	89	10.2	7.5	1.61	1.13	44.7	0.82	--
7.1.9	17.2	8.4	214	11.8	15	5.27	0.97	53.6	0.98	--
7.1.10	16.0	6.3	315	11.7	15	5.45	1.11	49.1	1.06	--
7.1.11	4.9	4.1	0	10.1	15	--	--	3.17	0.70	--
7.1.12	5.2	4.8	0	10.0	15	--	--	1.35	--	8.8 S ₂ O ₃ =
7.1.13	18.2	17.5	54	11.1	0	1.13	0.83	2.67	1.12	--
7.1.14	16.9	5.0	471	11.0	15	4.40	1.17	48.0	1.04	--
7.1.15	17.7	16.2	486	11.1	15	7.01	--	3.10	--	37.5 S ₂ O ₃ =
7.1.16	18.8	17.7	48	11.1	1	0.96	0.95	4.64	0.97	--
7.1.17	18.1	15.4	55	11.0	15	0.39	--	5.42	--	25 °C
7.1.18	4.7	2.4	58	9.2	15	0.42	0.79	15.9	1.09	NaHCO ₃
7.1.19	4.9	4.0	0	9.0	15	--	--	3.64	0.74	NaHCO ₃
7.1.20	88.2	58.3	61	8.8	15	2.33	0.83	121	1.15	NaHCO ₃
7.1.21	18.1	12.3	56	13.1	15	1.01	--	41.6	--	100 NaOH
7.1.22	89.7	55.1	96	12.2	15	3.92	1.06	140	1.08	--

*Oxidation rates estimated from equation 7.12, not measured.

**Nominal concentration, not measured.

Chapter 8

Industrial Implications

This chapter discusses the potential areas of application of the results of our study. We evaluate NO₂ removal by conventional limestone slurry scrubbers and by aqueous Na₂SO₃ and Na₂S scrubbers, and we present the results on hold tank depth reduction by NO₂ injection.

8.1 NO₂ REMOVAL BY CONVENTIONAL LIMESTONE SLURRY SCRUBBING

The performance of a scrubber in removing NO₂ can be evaluated by the following equation:

$$\ln \frac{Y_{\text{NO}_2 \text{ in}}}{Y_{\text{NO}_2 \text{ out}}} = \frac{K_g A}{G} = N_G \quad (8.1)$$

Y_{NO_2} is the mole fraction of NO₂, N_G the total number of mass transfer units, A the gas-liquid contact area, G the gas flow rate, and K_g the overall gas phase mass transfer coefficient, calculated by:

$$\frac{1}{K_g} = \frac{1}{k_g} + \frac{1}{m\Phi k_l^\circ} \quad (8.2)$$

In the above equation, k_l° is the liquid phase mass transfer coefficient, with a value of 0.01 cm/s for a typical scrubber. Φ is the enhancement factor, determined by the following equation:

$$\Phi = \frac{\sqrt{k_l D_{\text{NO}_2}}}{k_l^\circ} \quad (8.3)$$

N_G is related to the number of gas transfer units, N_g , by the following equation:

$$\frac{1}{N_G} = \frac{1}{N_g} + \frac{G}{Am\Phi k_l^\circ} \quad (8.4)$$

N_g is defined by the following equation:

$$N_g = \frac{k_g A}{G} \quad (8.5)$$

For a typical limestone slurry scrubber that achieves 95% SO_2 removal,

$$N_g = 6.9$$

and

$$\frac{k_l^\circ}{k_g} = 292 \frac{\text{atm}\cdot\text{ml}}{\text{gmol}} \quad (\text{Agarwal, 1995})$$

Therefore, a typical k_g is 3×10^{-5} mol/cm²-s-atm, and from equation (8.5), the value of A/G was calculated to be 2×10^5 atm-cm²-s/gmol.

When evaluating the fraction NO_2 removal by a limestone slurry scrubber, the results of our study entered into the calculation in the form of the enhancement factor, Φ , as defined by equation (8.3). In this equation,

$$k_1 = k_{2,SO_3} [SO_3^{2-}]_i + k_{2,HSO_3} [HSO_3^-] + \frac{2k_2 H_2O P_{NO_2} i}{3H_{NO_2}} \quad (8.6)$$

When the total concentration of S(IV) and the pH at the interface were given, the Bechtel-Modified Radian Equilibrium Program (Epstein, 1975) was used to determine the concentration of SO_3^{2-} and HSO_3^- at the interface. With the concentration of NO_2 , an enhancement factor for NO_2 absorption could be calculated from equation (8.3), from which N_G was calculated from equation (8.4), and the fraction NO_2 removal was calculated from equation (8.1). A sample of this calculation is given in Appendix I.

Figure 8.1 plots the fraction NO_2 removal as a function of $[S(IV)]_i$ in a typical limestone slurry scrubber.

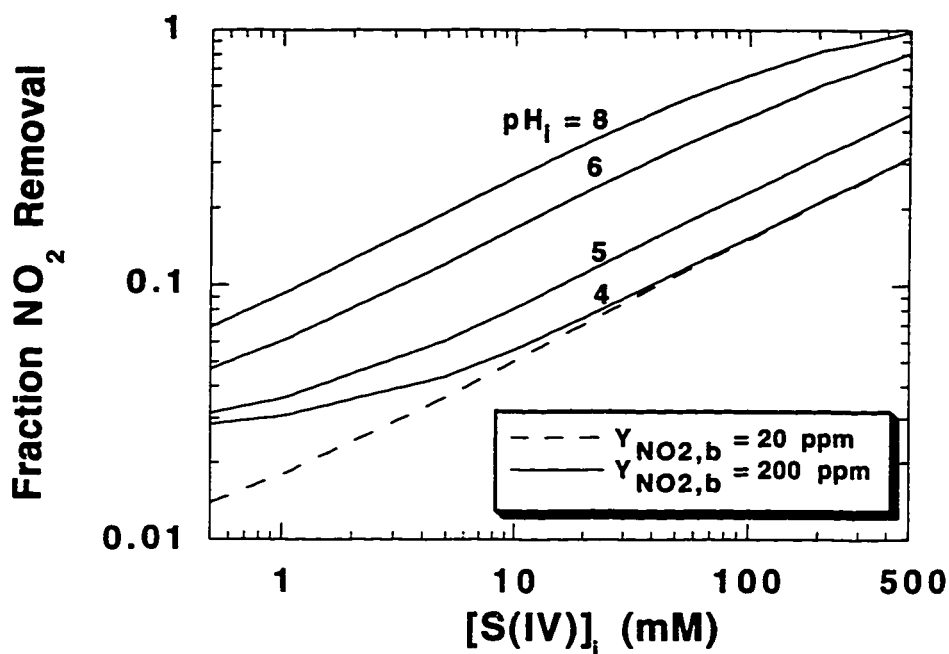


Figure 8.1 NO_2 removal in a typical limestone slurry scrubber. $N_g = 6.9$, $k_g = 3.4 \times 10^{-5} \text{ mol/cm}^2\text{-s-atm}$. Difference between solid and dotted line reflects the effect of NO_2 concentration on fraction NO_2 removal.

With typical conditions for limestone slurry, 10 mM total dissolved $[\text{S(IV)}]$ and pH 5-6, the estimated NO_2 removal is significantly less than 90-95%. This is because the amount of free $\text{SO}_3^{=}$ in the solution was determined by the dissolution of CaSO_3 , and when the slurry was saturated with CaSO_4 , the highest concentration of free $\text{SO}_3^{=}$ in the solution was 1 mM. Since $\text{SO}_3^{=}$ was responsible for the bulk of NO_2 removal, 1 mM of $\text{SO}_3^{=}$ was not sufficient to

achieve the level of NO₂ removal desired. Therefore, an acceptable level of NO₂ removal by a conventional limestone slurry scrubber is not probable.

8.2 NO₂ REMOVAL BY AQUEOUS SCRUBBING

8.2.1 Scrubbing with Na₂SO₃ Solution

The procedure for estimating the fraction NO₂ removal in an aqueous scrubber was much the same as described in the previous section. However, in an aqueous Na₂SO₃ scrubber, there is no limitation on the amount of free sulfite that can be present in the solution. Sulfite concentration can be adjusted by adding fresh Na₂SO₃ solution. pH can be raised with the addition of NaOH so that the majority of S(IV) in the solution will be in the form of SO₃⁼, and thiosulfate can be added to minimize oxidation. Therefore, it is expected that aqueous Na₂SO₃ scrubbing should achieve a higher level of NO₂ removal.

For aqueous Na₂SO₃ scrubbing with pH>7.5, k_1 in equation (8.3) is:

$$k_1 = k_{2,\text{SO}_3=}[\text{SO}_3^=]_i + k_{2,\text{S}_2\text{O}_3=}[\text{S}_2\text{O}_3^=] + \frac{2k_2 \text{H}_2\text{O}^{\text{PNO}_2} i}{3\text{HNO}_2} \quad (8.7)$$

Figure 8.2 shows the fraction NO₂ removal in an aqueous scrubber at variable bulk S(IV) concentrations.

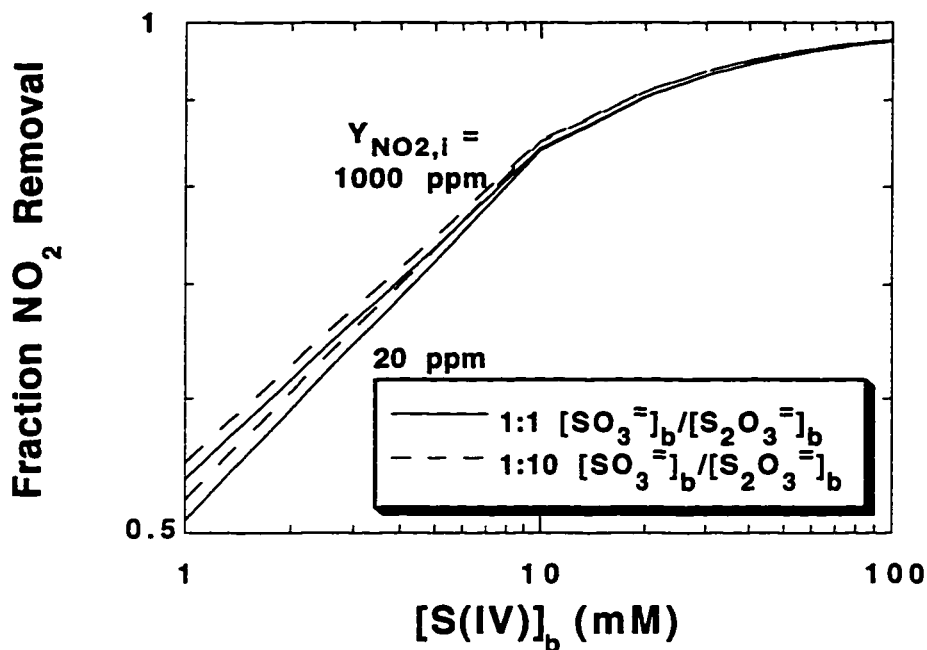


Figure 8.2 NO_2 removal in an aqueous Na_2SO_3 scrubber. $N_g = 6.9$, $\text{pH} > 7.5$, $k_g = 3.4 \times 10^{-5} \text{ mol/cm}^2\text{-s-atm}$. 55°C , 15% O_2 .

As can be seen from figure 8.2, at pH 7.5, 80 mM or more total dissolved sulfite and at least a molar ratio of 1 to 1 thiosulfate to sulfite are necessary for 90% removal of NO_2 . Increasing the ratio of thiosulfate to sulfite does not lead to significant enhancement in NO_2 removal, but it would reduce the rate of sulfite oxidation and minimize the consumption of SO_3^{2-} .

8.2.2 Scrubbing with Na₂S Solution

An alternative to aqueous Na₂SO₃ scrubbing is to scrub NO₂ with Na₂S solution. This technology has been demonstrated effective in removing NO₂ on an industrial scale (Shen, 1990). As the formation of H₂S becomes a problem whenever the solution pH falls below 9.0, NaOH is usually added to the scrubbing solution to maintain a high pH. Thiosulfate can also be added to the solution to minimize S(-II) oxidation if desired.

When scrubbing with Na₂S solution, the expression for k_1 is:

$$k_1 = k_{2,HS^-} [HS^-]_i \quad (8.8)$$

Figure 8.3 shows the fraction NO₂ removal in an aqueous scrubber at variable bulk S(-II) concentrations.

Due to the fast rate of reaction between NO₂ and HS⁻, it is not difficult to achieve 90-95% NO₂ removal with a moderate concentration of HS⁻ in the scrubbing solution. The fraction NO₂ removal at each [HS⁻]_b decreases with increasing NO₂ partial pressure. This is due to the faster rate of S(-II) oxidation at higher P_{NO₂,i}, which in turn lead to lower concentration of HS⁻ at the liquid boundary. This effect can be minimized with the addition of thiosulfate.

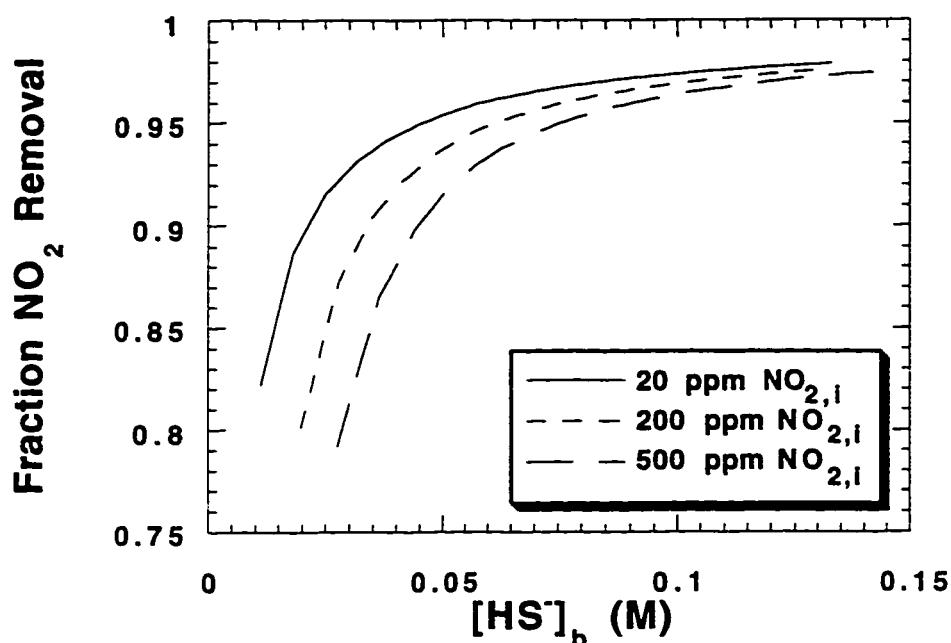


Figure 8.3 NO₂ removal in an aqueous Na₂S scrubber. pH > 9.5, N_g = 6.9, k_g = 3.4×10⁻⁵ mol/cm²-s-atm. 55 °C, 15% O₂.

8.3 HOLD TANK DEPTH REDUCTION BY NO₂ INJECTION

In a limestone slurry scrubbing process, air is typically added to the hold tank to oxidize sulfite to sulfate via a mechanism of forced oxidation. Since our study has shown that the absorption of NO₂ can catalyze sulfite oxidation, it may be feasible to reduce the liquid depth in the hold tank by injecting NO₂. NO₂ can be mixed with air and sparged into the hold tank, and oxidation in the hold tank

will increase, resulting in considerable reduction of required liquid depth in the tank.

We performed the calculation for a baseline case. By assuming a liquid depth of 30 ft in the hold tank was required to oxidize 50% of the oxygen in the inlet air via physical absorption, we wrote the following equation:

$$\int_{0.2}^{0.1} G dY_{O_2} = \int_0^{30\text{ft}} N_{\text{ox,phy}} A' dx \quad (8.9)$$

Y_{O_2} is the mole fraction of O_2 , G the gas flow rate in units of mol/s, A' is the contact area per unit depth, and $N_{\text{ox,phy}}$ the rate of oxidation by physical absorption of O_2 , defined as:

$$N_{\text{ox,phy}} = \frac{k_l^{\circ} O_2 P_T Y_{O_2}}{H_{O_2}} \quad (8.10)$$

$k_l^{\circ} O_2$ is the liquid phase mass transfer coefficient of O_2 , with a typical value of 0.02 cm/s. P_T is the total pressure, and H_{O_2} is the Henry's constant of O_2 , its value taken to be 6.085×10^4 atm/mol frac at 55 °C (Perry and Green, 1984).

By integrating both sides of equation (8.7), a value of 1.9×10^4 cm-s/mol for A'/G was obtained. With the addition of NO_2 at the bottom of the hold tank, the following expression could be written:

$$\int_{0.2}^{0.1} G dY_{O_2} = \int_0^{D\text{ft}} N_{\text{ox}} A' dx \quad (8.11)$$

D is the new liquid depth required to achieve the same level of oxygen absorption, and N_{ox} is the rate of sulfite oxidation catalyzed by NO_2 , as given in equation (6.5). A numerical integration of the above equation gave the value of D . A sample of this calculation is given in Appendix J.

Figure 8.4 gives the new liquid depth required at several different concentrations of injected NO_2 .

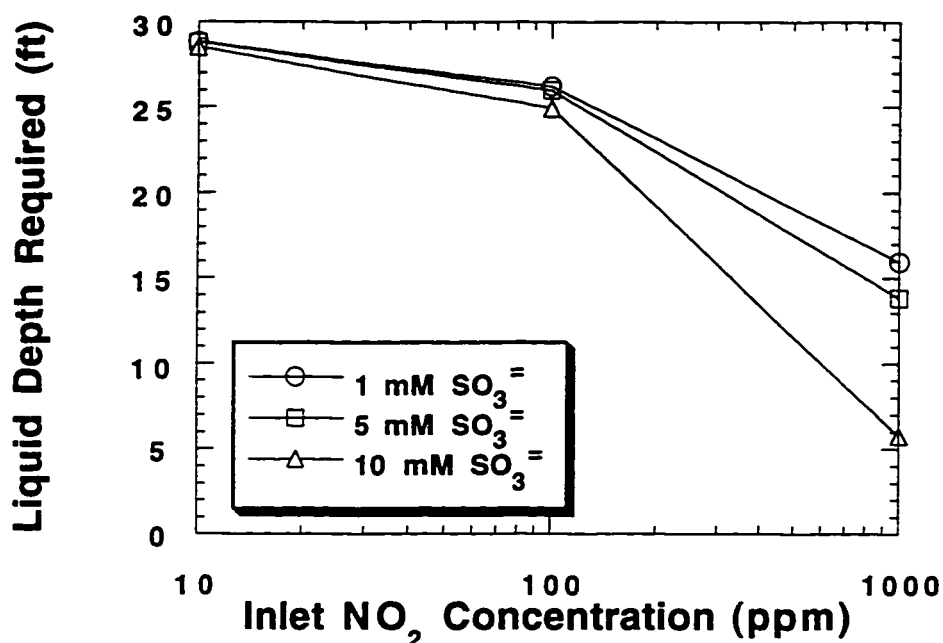


Figure 8.4 Hold tank liquid depth reduction by NO_2 injection. $Y_{\text{O}_2, \text{in}} = 0.2$, $Y_{\text{O}_2, \text{out}} = 0.1$. 55°C .

As can be seen from the above plot, significant reduction in hold tank liquid depth can be achieved by injecting 1000 ppm NO_2 at the bottom of the hold tank. This represents 1 mole of NO_2 injected for every 100 moles of O_2 absorbed. This ratio of NO_2 to O_2 absorbed was necessary because the NO_2 was rapidly consumed by reaction with sulfite and thus was only able to catalyze oxidation in a small segment of the liquid. The catalytic effect of NO_2 absorption on sulfite

oxidation at different liquid depths is shown in figure 8.5. In this plot, the number of moles of O_2 consumed per mole of NO_2 absorbed at several liquid depth is given as a function of inlet NO_2 concentration. The higher the ratio of moles O_2 to mole NO_2 , the more effective the injected NO_2 is in catalyzing sulfite oxidation.

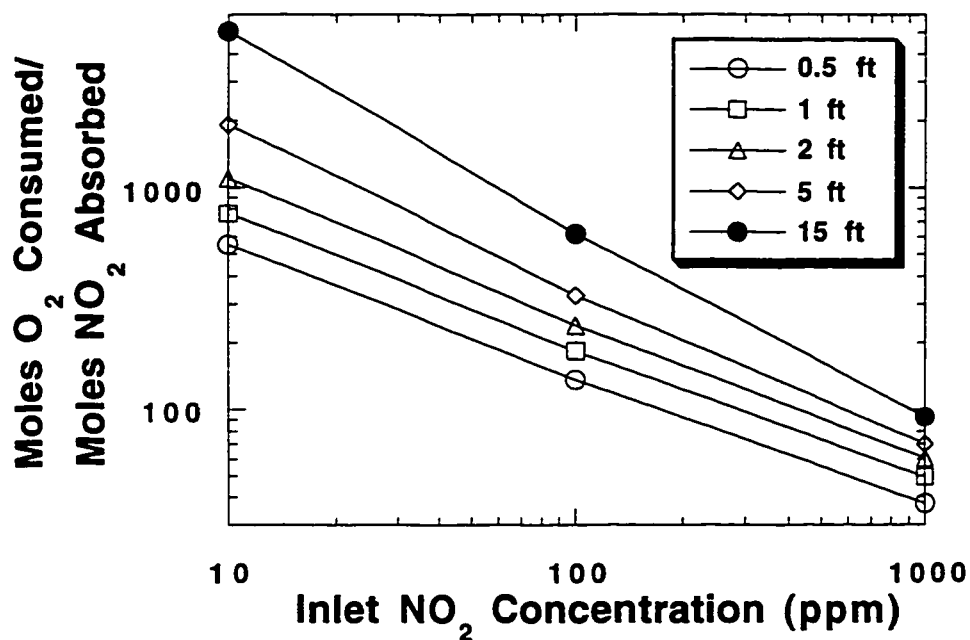


Figure 8.5 Sulfite oxidation catalyzed by NO_2 absorption. $[SO_3^{2-}] = 1 \text{ mM}$.

An alternative application of this study was to maintain the hold tank liquid depth but reduce the amount of oxidizing air with the injection of NO_2 . As the rate of sulfite oxidation increases with NO_2 injection, less air is required to

achieve the same level of oxidation, therefore an air stoichiometry of 1 may be sufficient where 2 to 2.5 is being used currently.

Chapter 9

Conclusions and Recommendations

This chapter summarizes the important conclusions we have reached by studying the absorption of NO_2 into solutions of S(IV) and S(-II). Areas in which more work is required in order to reach a better understanding of the subject are listed at the end of the chapter.

9.1 CONCLUSIONS

9.1.1 NO_2 Absorption into S(IV) Solutions

Among the various S(IV) species, sulfite is the most effective reagent in reacting with NO_2 . Bisulfite and thiosulfate are less reactive toward NO_2 , and water is even less reactive. However, the rate of NO_2 absorption into water is much higher than that of pure physical absorption, indicating that chemical reaction between NO_2 and water is significant.

Surface renewal theory, applied together with a reaction mechanism that accounts for the reaction between NO_2 and $\text{SO}_3^{=}$, HSO_3^- , NO_2 and $\text{S}_2\text{O}_3^{=}$ (when present), is adequate in predicting the rate of NO_2 absorption. The reactions between NO_2 and $\text{SO}_3^{=}$, HSO_3^- and $\text{S}_2\text{O}_3^{=}$ are first order with respect to both reactants, while the reaction between NO_2 and water is second order in NO_2 .

The presence of oxygen in the gas phase reduces the rate of NO_2 absorption into S(IV) solutions by oxidizing the $\text{SO}_3^{=}$ in the solution and

interface. The presence of SO_2 increases the concentration of total S(IV) at the interface while reducing the pH of the solution.

The addition of thiosulfate can enhance NO_2 absorption by inhibiting sulfite oxidation. The presence of Cl^- , Mg^{++} and Ca^{++} hinders NO_2 absorption, while the accumulation of sulfur-nitrogen compounds in the solution has little effect on NO_2 absorption.

9.1.2 S(IV) Oxidation in the Presence of NO_2

The absorption of NO_2 catalyzes sulfite oxidation via a free radical mechanism. A semi-empirical model that relates the rate of sulfite oxidation to the rate of NO_2 absorption and the concentration of O_2 and SO_3^- at the interface is successful in fitting most of the experimental results.

Thiosulfate inhibits sulfite oxidation by providing an alternative route for the termination of the oxidation mechanism. A fundamental model that relates the rate of sulfite oxidation to the interfacial concentrations of SO_3^- , NO_2 , and $\text{S}_2\text{O}_3^{2-}$ is successful in fitting the experimental results.

The presence of SO_2 has no significant effect on sulfite oxidation, while Cl^- , Fe^{++} , Mg^{++} , and Ca^{++} in the solution enhance sulfite oxidation.

9.1.3 NO_2 Absorption into S(-II) Solutions

Bisulfide reacts with NO_2 at a rate twice that of sulfite at 55 °C, and the reaction rate is first order with respect to HS^- and NO_2 . S_4^{2-} reacts with NO_2 at a rate similar to that of HS^- at 55 °C. Surface renewal theory, applied together with a reaction mechanism that accounts for the reaction between NO_2 and HS^- , is successful in fitting the experimental results.

NO_2 absorption catalyzes the oxidation of HS^- . A semi-empirical model that relates the rate of S(-II) oxidation to the rate of NO_2 absorption and the interfacial concentration of HS^- and O_2 is successful in fitting the experimental data. The addition of thiosulfate reduces the rate of S(-II) oxidation.

9.1.4 Industrial Implications

Acceptable level of NO_2 removal by a conventional limestone slurry scrubber is not probable. However, aqueous scrubbing of NO_2 by Na_2SO_3 and Na_2S solutions are viable options. Furthermore, significant reduction in hold tank liquid depth and/or oxidizing air stoichiometry is possible by NO_2 injection.

9.2 RECOMMENDATIONS

To have a more complete understanding of the absorption of NO_2 into solutions of S(IV) and S(-II), further study in the following areas is recommended:

1. Develop a more fundamental model of sulfite oxidation in the presence of NO_2 . This consists of solving the relevant sets of reaction/diffusion equations with the appropriate boundary conditions. The objective is to be able to predict the rate of sulfite oxidation based upon reaction kinetics and interfacial concentrations of S(IV), NO_2 and O_2 .
2. Perform additional experiments of NO_2 absorption into water, both at 25 °C and 55 °C. To obtain better results, a more reliable way of controlling solution pH (especially the pH at the interface) is required. This may help to explain the observed difference in the NO_2 -water reaction rate constants among various researchers (this study included).

3 Quantify the effect of Cl^- , Ca^{++} , and Fe^{++} on NO_2 absorption and sulfite oxidation in S(IV) solutions. This requires a better understanding of the interaction between these species and the NO_2 -S(IV) reaction mechanism. The objective is to develop a more fundamental model that predicts the effect of additives on the rate of NO_2 absorption and sulfite oxidation.

4 Develop analytical procedure for polysulfides and other products of NO_2 - HS^- reaction and HS^- oxidation. This will help us confirm the reaction mechanism and find ways to minimize undesirable side reactions.

5 Perform preliminary economic study on aqueous Na_2SO_3 and Na_2S scrubbing of NO_2 and hold tank depth reduction with NO_2 injection. The cost of the aqueous scrubbing processes should be compared with other NO_2 emission control technology (Appendix A) to determine whether they are economically feasible. The savings in hold tank depth reduction should be compared with the additional costs involved in NO_2 injection to see if it is worthwhile.

Appendix A

Review of Post Combustion Methods for NO_x Emissions Control

The following is a review of processes used in post combustion NO_x emissions control (Rosenberg et al., 1980). The processes are divided into either simultaneous NO_x and SO₂ removal or NO_x removal alone, and each category is further divided into wet and dry processes.

A1 SIMULTANEOUS REMOVAL OF NO_x AND SO₂

1. Wet Processes
 - a. Absorption of NO_x and SO₂ by liquids with liquid-phase reduction of NO_x to N₂ by SO₃⁼
 - b. Absorption of NO_x and SO₂ by liquids with liquid-phase oxidation to NO₃⁻ and SO₄⁼
 - c. Gas phase oxidation to NO or recycle of NO₂ followed by absorption of NO_x and SO₂ by liquids
 - 1) liquid-phase reduction of NO₂ to N₂ by SO₃⁼
 - 2) liquid-phase oxidation of NO_x to NO₃⁻
2. Dry Processes
 - a. Sorption of NO_x and SO₂ by solids
 - b. Selective catalytic reduction of NO_x by NH₃ with simultaneous sorption of SO₂
 - 1) reaction of SO₂ with copper oxide
 - 2) adsorption of SO₂ by activated carbon

- c. Electron beam radiation

A2 REMOVAL OF NO_x ALONE

1. Wet Processes

- a. Absorption of NO_x by liquids with liquid-phase reduction to NH₄⁺
- b. Absorption of NO_x by liquids with liquid-phase oxidation to NO₂⁻/NO₃⁻
- c. Gas phase oxidation of NO or recycle of NO₂ followed by absorption by liquids
 - 1) liquid-phase reduction to N₂
 - 2) liquid-phase oxidation to NO₂⁻/NO₃⁻

2. Dry Processes

- a. Catalytic decomposition of NO_x
- b. Sorption by solids
- c. Catalytic reduction to N₂
 - 1) selective with NH₃
 - 2) nonselective with reducing gases
- d. Homogeneous reduction to N₂ with NH₃

Appendix B

Rate Constants of Sulfur-Nitrogen Reactions

The following table gives the reaction rate constants for the formation of various sulfur-nitrogen compounds at 25 °C (Chang et al., 1982). Units are M for aqueous species and atm for gaseous species.

Table B1 Rate constants of sulfur-nitrogen reactions

Reaction	k (25 °C)	ΔE_a (kcal/mol)
$\text{HNO}_2 + \text{HSO}_3^- \rightarrow \text{NOSO}_3^- + \text{H}_2\text{O}$	2.43	12.1
$\text{NOSO}_3^- + \text{HSO}_3^- \rightarrow \text{HON}(\text{SO}_3)_2^-$ HADS	fast	--
$\text{HON}(\text{SO}_3)_2^- + \text{H}_2\text{O} \rightarrow \text{HONHSO}_3^- + \text{HSO}_4^-$ HADS HAMS	1.52×10^{-6}	23.0
$\text{HON}(\text{SO}_3)_2^- + \text{HSO}_3^- \rightarrow \text{N}(\text{SO}_3)_3^{3-} + \text{H}_2\text{O}$ HADS ATS	2.02×10^{-4}	19.5
$\text{HON}(\text{SO}_3)_2^- + \text{HSO}_3^- \rightarrow \text{HN}(\text{SO}_3)_2^- + \text{HSO}_4^-$ HADS ADS	1.22×10^{-4}	18.0
$\text{HONHSO}_3^- + \text{HSO}_3^- \rightarrow \text{HN}(\text{SO}_3)_2^- + \text{H}_2\text{O}$ HAMS ADS	1.50×10^{-5}	24.5
$\text{HONHSO}_3^- + \text{HSO}_3^- \rightarrow \text{H}_2\text{NSO}_3^- + \text{HSO}_4^-$ HAMS Sulfamic Acid	6.44×10^{-6}	24.5
$\text{N}(\text{SO}_3)_3^{3-} + \text{H}^+ + \text{H}_2\text{O} \rightarrow \text{HN}(\text{SO}_3)_2^- + \text{HSO}_4^-$ ATS ADS	fast	--
$\text{HN}(\text{SO}_3)_2^- + \text{H}^+ + \text{H}_2\text{O} \rightarrow \text{H}_2\text{NSO}_3^- + \text{HSO}_4^-$ ADS Sulfamic Acid	9.85×10^{-4}	23.5

Appendix C

Sample Calculation of Iodometric Titration

C1 IODOMETRIC TITRATION OF SULFITE ALONE

The following sample calculation is for the iodometric titration of a solution containing a nominal of 0.01 M sulfite.

Concentration of standard Iodine solution = 1 N

Factor of dilution = $\frac{250 \text{ ml}}{5 \text{ ml}} = 50$

Concentration of titrating iodine solution, $n_{I_2} = \frac{1 \text{ N}}{50} = 0.02 \text{ N}$

Concentration of standard thiosulfate solution = 1 N

Factor of dilution = $\frac{250 \text{ ml}}{5 \text{ ml}} = 50$

Concentration of titrating thiosulfate solution, $n_{S_2O_3} = \frac{1 \text{ N}}{50} = 0.02 \text{ N}$

Initial iodine solution volume reading = 4.3 ml

Final iodine solution volume reading = 10.67 ml

Iodine solution used, $V_{I_2} = 10.67 \text{ ml} - 4.3 \text{ ml} = 6.37 \text{ ml}$

Initial thiosulfate solution volume reading = 3.61 ml

Final thiosulfate solution volume reading = 5.35 ml

Thiosulfate solution used, $V_{S_2O_3} = 5.35 \text{ ml} - 3.61 \text{ ml} = 1.74 \text{ ml}$

Sulfite sample volume, $V_s = 5 \text{ ml}$

$$\begin{aligned} \text{Sulfite concentration} &= \frac{V_{I_2} n_{I_2} - V_{S_2O_3} n_{S_2O_3}}{V_s} \times \frac{1 \text{ M}}{2 \text{ N}} \\ &= \frac{6.37 \text{ ml} \times 0.02 \text{ N} - 1.74 \text{ ml} \times 0.02 \text{ N}}{5 \text{ ml}} \times \frac{1 \text{ M}}{2 \text{ N}} \\ &= 0.00926 \text{ M} \end{aligned}$$

C2 IODOMETRIC TITRATION OF SULFITE/THIOSULFATE MIXTURE

The following is a sample calculation of iodometric titration of a solution containing nominally 0.01 M sulfite and 0.01 M thiosulfate.

Concentration of titrating iodine solution, $n_{I_2} = 0.02 \text{ N}$

Concentration of titrating thiosulfate solution, $n_{S_2O_3^{2-}} = 0.02 \text{ N}$

Sample 1 contained both sulfite and thiosulfate.

Sample 1 volume, $V_{s1} = 5 \text{ ml}$

Iodine solution used with sample 1, $V_{I_2,1} = 11.17 \text{ ml} - 1.97 \text{ ml} = 9.2 \text{ ml}$

Thiosulfate solution used with sample 1, $V_{S_2O_3^{2-},1} = 5.61 \text{ ml} - 4.3 \text{ ml} =$

1.31 ml

$$\begin{aligned} [SO_3^{2-}] + \frac{1}{2} [S_2O_3^{2-}] &= \frac{V_{I_2,1} n_{I_2} - V_{S_2O_3^{2-},1} n_{S_2O_3^{2-}}}{V_{s1}} \times \frac{1 \text{ M}}{2 \text{ N}} \\ &= \frac{9.2 \text{ ml} \times 0.02 \text{ N} - 1.31 \text{ ml} \times 0.02 \text{ N}}{5 \text{ ml}} \times \frac{1 \text{ M}}{2 \text{ N}} \\ &= 0.01578 \text{ M} \end{aligned}$$

Sample 2 contained only thiosulfate. All sulfite present has reacted with formaldehyde and is no longer reactive toward iodine.

Sample 2 volume, $V_{s2} = 5 \text{ ml}$

Iodine solution used with sample 2, $V_{I_2,2} = 15.23 \text{ ml} - 11.17 \text{ ml} = 4.06 \text{ ml}$

Thiosulfate solution used with sample 2, $V_{S_2O_3^{2-},2} = 7.03 \text{ ml} - 5.61 \text{ ml} =$

1.42 ml

$$\begin{aligned} [S_2O_3^{2-}] &= \frac{V_{I_2,2} n_{I_2} - V_{S_2O_3^{2-},2} n_{S_2O_3^{2-}}}{V_{s2}} \times \frac{1 \text{ M}}{1 \text{ N}} \\ &= \frac{4.06 \text{ ml} \times 0.02 \text{ N} - 1.42 \text{ ml} \times 0.02 \text{ N}}{5 \text{ ml}} \times \frac{1 \text{ M}}{1 \text{ N}} \\ &= 0.01056 \text{ M} \end{aligned}$$

$$[SO_3^{2-}] = 0.01578 \text{ M} - \frac{1}{2} \times 0.01056 \text{ M} = 0.0105 \text{ M}$$

Appendix D

Sample Calculation for Batch Experiments

At the early stage of this study, a series of experiments were performed by operating the stirred cell contactor in the batch mode. The concentration of S(IV) species in these experiments was not measured, instead a nominal concentration was assumed. Furthermore, as nitrogen was used as diluent instead of air, the rate of sulfite oxidation was not measured, therefore a bulk solution S(IV) concentration was reported instead of the interfacial S(IV) concentration. These batch experiments were not used to regress the reaction rate constant. Instead, for every experiment, a second order rate constant, k_2 , was calculated. The following shows how this calculation was performed.

D1 SAMPLE CALCULATION OF SULFITE EXPERIMENTS

The following is a sample calculation for a batch experiment of NO_2 absorption into a solution containing Na_2SO_3 with N_2 dilution at 25 °C. The same procedure was used for batch experiments of NO_2 absorption into solutions of NaHSO_3 , Na_2S , and $\text{Na}_2\text{S}_2\text{O}_3$.

Gas liquid contact area, $A = 81 \text{ cm}^2$

Inlet NO_2 concentration, $Y_{\text{NO}_2,\text{in}} = 506 \text{ ppm}$

Outlet NO_2 Concentration, $Y_{\text{NO}_2,\text{out}} = 110.1 \text{ ppm}$

NO_2 flow rate, $G = 1 \text{ SLM}$

Temperature, $T = 25 \text{ }^\circ\text{C} = 298.15 \text{ K}$

Pressure, $P_T = 1 \text{ atm}$

$$\text{Inlet NO}_2 \text{ rate, } n_{\text{NO}_2,\text{in}} = \frac{P_{\text{NO}_2,\text{in}} G}{RT} = \frac{P_T G}{RT} Y_{\text{NO}_2,\text{in}}$$

$$\text{Outlet NO}_2 \text{ rate, } n_{\text{NO}_2,\text{out}} = \frac{P_T G}{RT} Y_{\text{NO}_2,\text{out}}$$

$$\text{NO}_2 \text{ absorption flux, } N_{\text{NO}_2} = \frac{\frac{P_T G}{RT} (Y_{\text{NO}_2,\text{in}} - Y_{\text{NO}_2,\text{out}})}{A}$$

$$= \frac{1 \text{ atm} \times 1 \frac{1}{\text{min}} \times \frac{1 \text{ min}}{60 \text{ s}}}{0.0820567 \frac{\text{atm-l}}{\text{mol-K}} \times 298.15 \text{ K} \times 81 \text{ cm}^2} \times \frac{506 \text{ ppm} - 110.1 \text{ ppm}}{10^6 \text{ ppm}}$$

$$= 3.33 \times 10^{-9} \frac{\text{mol}}{\text{cm}^2\text{-s}}$$

$$\text{Gas agitation speed} = 717 \text{ rpm}$$

$$\text{Gas phase mass transfer coefficient, } k_g$$

$$= \frac{4.95 \times 10^{-5} \times (717)^{0.76} \times \frac{1.01325 \text{ bar}}{1 \text{ atm}}}{81 \text{ cm}^2}$$

$$= 9.16 \times 10^{-5} \frac{\text{mol}}{\text{cm}^2\text{-s-atm}}$$

$$\text{Interfacial NO}_2 \text{ concentration, } Y_{\text{NO}_2,i}$$

$$= Y_{\text{NO}_2,\text{out}} - \frac{N_{\text{NO}_2}}{k_g}$$

$$= 110.1 \text{ ppm} - \frac{3.33 \times 10^{-9} \frac{\text{mol}}{\text{cm}^2\text{-s}}}{9.16 \times 10^{-5} \frac{\text{mol}}{\text{cm}^2\text{-s-atm}} \times 1 \text{ atm}} \times 10^6 \text{ ppm}$$

$$= 73.7 \text{ ppm}$$

$$\text{Interfacial NO}_2 \text{ partial pressure, } P_{\text{NO}_2,i} = \frac{73.7 \text{ ppm}}{10^6 \text{ ppm}} \times 1 \text{ atm}$$

$$= 7.37 \times 10^{-5} \text{ atm}$$

$$\text{Normalized NO}_2 \text{ flux of absorption, } R_g$$

$$= \frac{N_{\text{NO}_2}}{P_{\text{NO}_2,i}} = \frac{3.33 \times 10^{-9} \frac{\text{mol}}{\text{cm}^2\text{-s}}}{7.37 \times 10^{-5} \text{ atm}}$$

$$= 4.52 \times 10^{-5} \frac{\text{mol}}{\text{cm}^2\text{-s-atm}}$$

Henry's constant of NO₂, H_{NO2}, at 25 °C = $2.44 \times 10^4 \frac{\text{cm}^3\text{-atm}}{\text{mol}}$

Diffusion coefficient of NO₂, D_{NO2}, at 25 °C = $2.16 \times 10^{-5} \frac{\text{cm}^2}{\text{s}}$

Nominal concentration of sulfite in solution, [SO₃⁼] = $0.085 \frac{\text{mol}}{\text{l}}$

Second order rate constant, k₂

$$\begin{aligned}
 &= \frac{R_g^2 H_{\text{NO}_2}^2}{D_{\text{NO}_2} [\text{SO}_3^=]} \\
 &= \frac{(4.52 \times 10^{-5} \frac{\text{mol}}{\text{cm}^2\text{-s-atm}})^2 \times (2.44 \times 10^4 \frac{\text{cm}^3\text{-atm}}{\text{mol}})^2}{2.16 \times 10^{-5} \frac{\text{cm}^2}{\text{s}} \times 0.085 \frac{\text{mol}}{\text{l}}} \\
 &= 6.62 \times 10^5 \frac{1}{\text{M-s}}
 \end{aligned}$$

D2 SAMPLE CALCULATION OF WATER EXPERIMENT

The procedure for calculating the reaction rate constant between NO₂ and water is much the same as given in D1, up to the point of obtaining the normalized flux of NO₂, R_g. Afterward, however, the formula for calculating k₂ is slightly different due to the second order dependence of the reaction rate on the concentration of NO₂. The following gives a sample of this part of the calculation. The temperature is 25 °C.

$$Y_{\text{NO}_2,i} = 128.53 \text{ ppm}$$

$$P_{\text{NO}_2,i} = \frac{128.53 \text{ ppm}}{10^6 \text{ ppm}} \times 1 \text{ atm} = 0.00012853 \text{ atm}$$

$$N_{\text{NO}_2} = 3.33 \times 10^{-10} \frac{\text{mol}}{\text{cm}^2\text{-s}}$$

$$R_g = \frac{3.33 \times 10^{-10} \frac{\text{mol}}{\text{cm}^2\text{-s}}}{0.00012853 \text{ atm}} = 2.59 \times 10^{-6} \frac{\text{mol}}{\text{cm}^2\text{-s-atm}}$$

For the reaction between NO₂ and water:

$$\frac{R_g^2 H_{\text{NO}_2}^2}{D_{\text{NO}_2}} = \frac{2}{3} \frac{k_2 P_{\text{NO}_2,i}}{H_{\text{NO}_2}}$$

therefore,

$$\begin{aligned}
 k_2 &= \frac{3}{2} \frac{R_g^2 H_{\text{NO}_2}^3}{P_{\text{NO}_2} i D_{\text{NO}_2}} \\
 &= \frac{3}{2} \frac{(2.59 \times 10^{-6} \frac{\text{mol}}{\text{cm}^2 \cdot \text{s} \cdot \text{atm}})^2 (2.44 \times 10^4 \frac{\text{cm}^3 \cdot \text{atm}}{\text{mol}})^3}{0.00012853 \text{ atm} \cdot 2.16 \times 10^{-5} \frac{\text{cm}^2}{\text{s}}} \times \frac{1 \text{ l}}{1000 \text{ cm}^3} \\
 &= 5.27 \times 10^7 \frac{1}{\text{M} \cdot \text{s}}
 \end{aligned}$$

Appendix E

Sample Calculation of Rate of S(IV) Oxidation

The rate of sulfite oxidation was calculated from the change in solution S(IV) concentration as determined by iodimetric titration. The following is a sample of such calculation.

[S(IV)] at the beginning of the run, $[S(IV)]^o = 0.0088 \text{ M}$

[S(IV)] at the end of the run, $[S(IV)]_f = 0.0075 \text{ M}$

Run time, $\Delta t = 185 \text{ min} = 11100 \text{ s}$

[S(IV)] of the stock solution, $[S(IV)]_{tit} = 0.09 \text{ M}$

Volume of stock solution fed into the contactor, $V_{tit} = 84.6 \text{ ml} = 0.0846 \text{ l}$

Volume of solution in the contactor, $V = 1 \text{ l}$

Gas-liquid contact area, $A = 81 \text{ cm}^2$

Bulk gas phase O_2 concentration, $Y_{O_2,b} = 15 \%$

Total pressure, $P_T = 1 \text{ atm}$

The rate of S(IV) oxidation, is calculated by:

$$\begin{aligned}
 N_{ox} &= \frac{V([S(IV)]^o - [S(IV)]_f) + V_{tit}[S(IV)]_{tit}}{A \Delta t} \\
 &= \frac{1 \text{ l} \times (0.0088 - 0.0075) \frac{\text{mol}}{\text{l}} + 0.0846 \text{ l} \times 0.09 \frac{\text{mol}}{\text{l}}}{81 \text{ cm}^2 \times 11100 \text{ s}} \\
 &= \frac{0.0013 \text{ mol} + 0.007614 \text{ mol}}{81 \text{ cm}^2 \times 11100 \text{ s}} \\
 &= 9.91 \times 10^{-9} \frac{\text{mol}}{\text{cm}^2 \cdot \text{s}}
 \end{aligned}$$

The overall O_2 gas phase mass transfer coefficient, K_{g,O_2}

$$= \frac{N_{ox}}{Y_{O_2,b} \times P_T}$$

$$\begin{aligned}
 &= \frac{9.91 \times 10^{-9} \frac{\text{mol}}{\text{cm}^2 \cdot \text{s}}}{0.15 \times 1 \text{ atm}} \\
 &= 6.61 \times 10^{-8} \frac{\text{mol}}{\text{cm}^2 \cdot \text{s} \cdot \text{atm}}
 \end{aligned}$$

Temperature, $T = 55^\circ\text{C}$

Liquid agitation speed = 700 rpm

$$\begin{aligned}
 k_l^\circ \text{SO}_2 &= 8.84 \times 10^{-2} \times (700)^{0.65} \\
 &= 6.25 \left(\times 10^{-5} \frac{\text{m}}{\text{s}} \right) \\
 &= 6.25 \times 10^{-3} \frac{\text{cm}}{\text{s}}
 \end{aligned}$$

$$\begin{aligned}
 k_l^\circ \text{S(IV)} &= k_l^\circ \text{SO}_2 \times \sqrt{\frac{D_{\text{S(IV)}}}{D_{\text{SO}_2}}} \\
 &= 6.25 \times 10^{-3} \frac{\text{cm}}{\text{s}} \times \sqrt{\frac{1.84 \times 10^{-5} \frac{\text{cm}^2}{\text{s}}}{3.83 \times 10^{-5} \frac{\text{cm}^2}{\text{s}}}} \\
 &= 4.33 \times 10^{-3} \frac{\text{cm}}{\text{s}}
 \end{aligned}$$

Interfacial concentration of S(IV), $[\text{S(IV)}]_i$

$$\begin{aligned}
 &= [\text{S(IV)}]_b - \frac{N_{\text{ox}}}{k_l^\circ \text{S(IV)}} \\
 &= 0.0075 \text{ M} - \frac{9.91 \times 10^{-9} \frac{\text{mol}}{\text{cm}^2 \cdot \text{s}}}{4.33 \times 10^{-3} \frac{\text{cm}}{\text{s}}} \times \frac{1000 \text{ cm}^3}{1 \text{ l}} \\
 &= 0.0075 \text{ M} - 0.0023 \text{ M} \\
 &= 0.0052 \text{ M}
 \end{aligned}$$

Appendix F

FORTTRAN Program for Equilibrium Speciation Calculation

This section lists the FORTRAN program used to calculate the equilibrium concentration of various species at bulk solution and interfacial conditions. The solution initially containing Na_2SO_3 , Na_2SO_4 , and occasionally $\text{Na}_2\text{S}_2\text{O}_3$ and a buffer.

F1 FORTRAN PROGRAM FOR BULK SOLUTION EQUILIBRIUM

This program is written to calculate the equilibrium concentration of various species at bulk solution condition. The input required includes: concentration of total S(IV) in bulk solution, bulk solution pH, bulk solution concentration of $\text{SO}_4^{=}$, ionic strength of bulk solution, and bulk concentration of any additives (e.g., Na^+ , Mg^{++} , Ca^{++} , Cl^-). The output includes bulk solution concentration of $\text{SO}_3^{=}$, HSO_3^- , dissolved SO_2 , H^+ , and other S(IV) complexes such as MgSO_3 , CaSO_3 , and NaSO_3° .

The following is a sample of a typical calculation. The inputs were:

$$[\text{S(IV)}] = 0.0095 \text{ M}$$

$$[\text{SO}_4^{=}] = 0.25 \text{ M}$$

$$[\text{Na}^+] = 0.52 \text{ M}$$

$$I = 0.78$$

$$\text{pH} = 5.5$$

The following is the FORTRAN code.

- c This program performs equilibrium calculation for solutions containing
- c sulfite ($\text{SO}_3^{=}$) and sulfate ($\text{SO}_4^{=}$). The species whose equilibrium

```

c   concentration is calculated by this progeam include  $\text{SO}_3^{=}$ ,  $\text{SO}_4^{=}$ ,  $\text{HSO}_3^{-}$ ,
c   dissolved  $\text{SO}_2$ ,  $\text{H}^{+}$ ,  $\text{MgSO}_3$ ,  $\text{CaSO}_3$ ,  $\text{NaSO}_3^{\circ}$ .
c
c   program sulfiteequilibrium
c   real cna, ch, chso3, cso3, cso4, cs4, cso2, i, ka1, ka2, ah, rso3
c   real rhso3, rso2, rh, T, A1, A2, ra1, ra2, frac
c   real rmaso3, cnaso3, ka3, ra3, a3, rna, cnacal, cnadif, rmg,rmgso3
c   real cmg, ccl, cmgso3, ka4, ra4, a4, cso3eff, cca, ccase3,ka5,ra5,a5
c   real rca, rcaso3, cmgso4, ccase4, r6, r7, ka6, ka7, a6, a7, rmgso4
c   real rcaso4
c
c   Input total concentration of S(IV) species.
c   cs4=0.0095
c
c   Input ionic strength of solution.
c   I=0.78
c
c   Calculate activity coefficient of  $\text{SO}_3^{=}$ ,  $\text{HSO}_3^{-}$ ,  $\text{SO}_2$ ,  $\text{H}^{+}$ ,  $\text{NaSO}_3^{\circ}$ ,  $\text{Na}^{+}$ ,
c    $\text{Mg}^{++}$ ,  $\text{MgSO}_3$ ,  $\text{SO}_4^{=}$ ,  $\text{Ca}^{++}$ ,  $\text{CaSO}_4$ , and  $\text{CaSO}_3$ .
c   rso3=10.**((0.5434*4.0*(-sqrt(I)/(1.+0.3358*4.5*sqrt(I))))
c   rhso3=10.**((0.5434*1.0*(-sqrt(i)/(1.+0.3358*4.5*sqrt(i))))
c   rso2=10.**((0.076*i)
c   rh=10.**((0.5434*1.0*(-sqrt(i)/(1.+0.3358*6.0*sqrt(i))+0.4*I))
c   rmaso3=10.**((0.5434*1.0*(-sqrt(I)/(1.0+0.3358*4.5*sqrt(I))))
c   rna=10.**((0.5434*1.0*(-sqrt(I)/(1.0+0.3358*5.0*sqrt(I))+0.1*I))
c   rmg=10.**((0.5434*4.0*(-sqrt(i)/(1.+0.3358*4.5*sqrt(i))+0.1*i))
c   rmgso3=10.**((0.076*i)
c   rmgso4=rmgso3
c   rso4=10.**((0.5434*4.0*(-sqrt(I)/(1.+0.3358*3.0*sqrt(i))))
c   rcaso4=rmgso3
c   rca=rmg
c   rcaso3=rmgso3
c
c   Input concentration of  $\text{Na}^{+}$ , introduced into the solution as  $\text{Na}_2\text{SO}_3$  and
c    $\text{Na}_2\text{SO}_4$ .
c   cna=0.52
c
c   Input concentration of  $\text{Mg}^{++}$ ,  $\text{Cl}^{-}$ ,  $\text{Ca}^{++}$ , if any.
c   cmg=0.
c   ccl=0.
c   cca=0.
c
c   Input initial concentration of  $\text{SO}_4^{=}$ .
c   cso4=0.25
c
c   Input initial solution pH.

```



```

ph=5.5
c
c   Define output file.
open(unit=6, file='eqoutnew', status='new')
c
c   Write output column headings
write(6,7)
7   format(1x,'frac',6x,'pH',3x,['SO3'],3x,['HSO3'],3x,['SO4'],3x,['SO2]',
&       3x,['H'], 3x,['NaSO3'], 3x,['Na'])
c
c   Define activities based upon activity coefficients.
ah=10.**(-ph)
a1=ah*rso3/rhso3
a2=ah*rhso3/rso2
a3=ma*rso3/rmaso3
a4=rmg*rso3/rmgso3
a5=rca*rso3/rcaso3
a6=rmg*rso4/rmgso4
a7=rca*rso4/rcaso4
ch=ah/rh
c
c   Calculate equilibrium constants.
ka1=10.**((6.3386e2/296.15-9.3320)
ka2=10.**((8.4367e2/296.15-4.7171)
ka3=10.**((2.41e2/296.15-1.529)
ka4=10.**((4.325e2/296.15-4.3715)
ka5=10.**((5.048e2/296.15-5.0910)
ka6=10.**((1.0579e3/296.15-5.795)
ka7=10.**((-2.5721e3/296.15-2.315e1*log(296.15)+63.6)
ra1=ka1/a1
ra2=ka2/a2
ra3=ka3/a3
ra4=ka4/a4
ra5=ka5/a5
ra6=ka6/a6
ra7=ka7/a7
c
c   Solve for equilibrium concentrations of various species.
cso3=cs4/(1./ra1+1./(ra1*ra2)+1.+cna/ra3+cmg/ra4+cca/ra5)
chso3=cso3/ra1
cso2=chso3/ra2
cnaso3=cna*cso3/ra3
c   cso4=(i-3.*cso3-chso3-0.5*cnaso3-3*cmgso3-3*ccaso3)/3.
cmgso3=cmg*cso3/ra4
ccaso3=cca*cso3/ra5
cmgso4=cmg*cso4/ra6
ccaso4=cca*cso4/ra7

```

```

c   cnacal=chso3+2.*cso3+2.*cso4+cnaso3+ccl-2.*cmg-ch-2*cca
c   cso3eff=cso3+cnaso3+cmgso3+ccaso3
c   frac=cso3/cs4
c   cnadif=cnacal-cna
c
c   Write equilibrium concentrations under respective headings.
c   write(6,5) frac,ph,cso3,chso3,cso4,cso2,ch,cnaso3,cna,cmgso3,cso3eff,
&      ccl,ccaso3
5   format(1x,f7.5,1x,f4.1,1x,f12.7,1x,f15.9,1x,f7.5,1x,f9.7,1x,f9.7,
&      1x,f12.7,1x,f9.7,1x,f9.7,1x,f9.7,1x,2f9.7)
c   write(6,*) ka1, ka2, ka3
c   stop
c   end

```

The output of the FORTRAN program gave the following results:

$$[\text{SO}_3^-] = 7.1 \times 10^{-4} \text{ M}$$

$$[\text{HSO}_3^-] = 8.5 \times 10^{-3} \text{ M}$$

$$[\text{SO}_2 (\text{aq})] = 3.2 \times 10^{-6} \text{ M}$$

$$[\text{NaSO}_3^\circ] = 3.2 \times 10^{-4} \text{ M}$$

F2 FORTRAN PROGRAM FOR INTERFACIAL EQUILIBRIUM

The interfacial equilibrium speciation is done by using BMREP. The following subroutine, mdiva, developed by Agarwal (1995), was used to call BMREP to perform the necessary calculation. In addition to the above required input, it is also necessary to know the rate of sulfite depletion in order to determine the interfacial concentration of S(IV) and pH.

The following is the subroutine mdiva.

```

C ***** COMMENT USED BEFORE PROGRAM
TAD*****
C           PROGRAM
TAD(INPUT,OUTPUT,TTY,TAPE5=INPUT,TAPE6=OUTPUT,TAPE7=TTY)
C*****
***** C***** THIS ROUTINE CALLS BEQ TO DETERMINE AQUEOUS
C           SOLUTION EQUILIBRIA FOR THE SYSTEM
CA,MG,NA,K,SO3,SO4,CO3,CL.

```

```

C          (NITRATES ASSUMED ZERO FOR INPUT/OUTPUT
CONVENIENCE)
C
C***** FOR JS=1 AND SPECIFIED PPCO2, SOLIDS ARE ALSO
DETERMINED.    C
C          PROGRAM USES BEQ EXEC .
C*****
*****
subroutine mdiva(rklkg1,mtusp1,dba1,xscale,u1,iest)
    implicit integer*4 (i-n)
    implicit real*8 (a-h,o-z)
    REAL*8 NL
    REAL*8 K(50)
    REAL*8 NTUSP,mtusp1
    integer*4 ios,rmssts,rmsstv
    CHARACTER*5 CMP(10)
    DIMENSION X(50),CM(10),PP(2),SS(3),XMW(10)
    DIMENSION BPP(3),D(50),PHI(50),phi1(50)
    common/model1/mtusp
    COMMON /ID/IDENT(20), CCM(10), CW(10)
    COMMON /INPUT/ PPSO2, PPCO2, SS1,SS2, SS3, KK1, JJS,
    PPH
    COMMON /STAGE/JSTAGE
    COMMON /INPUTSP/SO2IN,FSP,NTUSP
    COMMON /CONST/K,FFLUX
    COMMON /GAMMA/GAM(50)
    COMMON /PPRESS/BPP,RKLKG,BPPI(3),NDIFF
    COMMON /INPUT2/RLG,XKSP(3,2),EF,NMIX
    COMMON /CAAD/CKCAAD
    COMMON /LIMER/P1,P2,D1,D2
    COMMON /RTIME/TAUSC,TAUHT,DELAVE
    COMMON /DI/D
    COMMON
    /HTPRINT/POUT(2),PIN(2),RSCASO3,RSCASO4,COLD,COUT(4)
    COMMON /TANKPAR/RLG2,CXKSP(2,2),E,NL,RD
    COMMON /NEW/RATEK
    COMMON
    /CC3/SOLIDIN(4),SOLID(4),DSOLID(4),SOLIDSP(4)
    COMMON /DIFLUX/FLUXCA,DFCASO3,DFCASO4,RSO3SO4
C      this block added to provide a first estimate to [H+]b
COMMON/BULKSP/BH,BOH,BCO2,BHCO3,BCO3,BSO2,BHSO3,BS
O3,BHSO4,BSO4, 1
    BH2A,BHA,BA,BCA,BCL,BPH
C      this block added to provide a first estimate to [H+]i
COMMON /INFACE/
    H,OH,CO2,HCO3,CO3,SO2,HSO3,SO3,HSO4,SO4,H2A,HA,A
    common/casedata/u2,ph1,s1,ox1,pin1,pout1,cs1(9)

```

```

        write(*,*)'*****starting mdiva'
        write(10,*)'at the begining of mdiva, rntusp1=',rntusp1
c      components and their molecular weights
        DATA CMP /'CA++', 'MG++', 'NA+', 'K+', 'SO3--',
          1 'SO4', 'CO3', 'CL-', 'H2AD', ' ' /
        DATA XMW /40.08,24.31,22.99,39.10,80.06,96.06,60.01,35.45,
          1 146.,0.0/

C
C      XPR  = 0= NO PRINTOUT FROM SUBROUTINE BPR
C              1= FULL PRINTOUT
C              2= SHORT FORM PRINTOUT
C
C      K1   = 1= INPUT CONCS IN PPM
C              2= INPUT CONCS IN G-MOLE/LITER
C
C      JS   = 0= NO SOLIDS
C              = 1= SOLIDS MAY BE PRESENT. PPCO2
C                  SPECIFIED.
C
C      TK   =      SLURRY TEMPERATURE, DEGREES KELVIN
C
C      PP   =      PARTIAL PRESSURES OF SO2,CO2 IN ATM
C
C      SS(1)=      RELATIVE SATURATION OF CASO3 AT
C                  WHICH
C      CRYSTALLIZATION OCCURS. USE VALUE OF 1.00
C                  FOR NORMAL RADIANT
C      EQUILIBRIUM.
C
C      SS(2)      APPLIES TO CACO3
C      SS(3)      APPLIES TO CASO4
C
C      PH   = 0= PH NOT SPECIFIED
C              1= PH IS SPECIFIED
C
C      PH   =      SLURRY PH (FOR INPUT, SET = 0. IF NOT
SPECIFIED)
C
C      CCM  =      INPUT DATA CONCS
CA,MG,NA,K,SO3,SO4,CO3,CL
C      IN THAT ORDER.
C
C      CM   =      CONCS OF
SO3,CO3,SO4,NO3,CA,MG,(NA+K),CL
C      N THAT ORDER, GMOL/LITER
C

```

```

C          this lines provide first guesses for [H+]b in EQUIL and [H+]i in
CONVER      BH=1.d-4
            H=1.d-4
100 CONTINUE
C          READ A NEW CASE = INPUT DATA FROM FILE BEQ DATA
.
            READ(17,110,END=200) IDENT
110 FORMAT( 20A4)
            WRITE (11,115) IDENT
115 FORMAT(1H , 5X, 20A4)
c          INFLAG indicates input format; NDIFF chooses the O.D.E. solver
            READ(17,*) INFLAG,NDIFF
            write(*,*)'reading k1,tk,ph'
c          use ssmfgd defaults (inflag=1) or input all information (inflag=2)
            write(*,*)'inflag=',inflag
            IF(INFLAG.EQ.1) THEN
                READ(17,*) K1, TK, PH
                write(*,*)'reading k1,tk,ph',k1,tk,ph XPR = 0.0
                SJ = 0.0
                PP(1) = 0.0
                PP(2) = 0.
            write(*,*)'setting some to zero' SS(1) = 0.55d0
                SS(2) = 1.0d0
                SS(3) = 1.0d0
                XIPH = 1.0 d0
            ELSE
                5 READ (17,*) XPR, K1, SJ, TK, PP(1), PP(2), SS(1),
1 SS(2),SS(3), XIPH, PH
            END IF
c*****
            write(*,*)'setting ph=ph1'
            if(iest.eq.1)then
                ph = ph1
            else
            endif
c*****
c          concentrations, in order: Ca, Mg, Na, K, SO3, SO4, CO3, Cl, H2Ad:
            READ (17,*) (CCM(I),I=1,9)
c*****
            if(iest.eq.1)then
                do 15 i=1,9
                    ccm(i)=cs1(i)
                    write(*,*)'ccm=',ccm(i)
15                continue
            else

```

```

endif
c*****
guess for outlet partial pressures; mtc ratio
READ (17,*) BPP(1),BPP(2),BPP(3),RKLKG
c*****
if(iest.eq.1)then
    rklkg = rklkg1
    write(*,*)'bpp(1)=',bpp(1)
else
endif
c*****
write(10,*)'from mdiva, rklkg=',rklkg
c    scrubber liquid to gas ratio and enhancement factor
READ(17,*) RLG,EF
c    dissolution rate parameters for CaSO3, gypsum
READ(17,*) XKSP(1,1),XKSP(2,1)
c    inlet pp SO2, NTU, single/multistage, co/countercurrent
READ(17,*) FSP,NTUSP,NFLAG,NFLAG2
    if (iest.eq.1)then
        fsp = pin1
        ntusp = ntusp1
        write(10,*)'ntusp=',ntusp
        write(10,*)'adipic acid=',ccm(9)
    else
    endif
c    # of stages, eq. const. at scrubber temp of Ca anion with buffer
READ(17,*) NMIX,CKCAAD
JSTAGE=0
c    PSD calculated or given, utilization percent
READ(17,*)LA,U
    write(*,*)'u=',u1,u
c    calculate the solids composition
read(17,*)s,o
c*****
if(iest.eq.1)then
    u = u2
    s = s1
    o = ox1
    write(*,*)u,o,s,'u-o-s'
else
endif
c*****
call calcsol(u,s,o)
    write(*,*)'***** u=*****=',u
c    scrubber and hold tank residence times
READ(17,*)TAUSC,TAUHT,B
write(1,*)'tauht=',tauht

```

```

        write(3,*)'tauht=',tauht
        write(11,*)'tauht=',tauht
c        hold tank inlet partial pressures of CO2, O2 (atm)
        READ(17,*) PIN(1), PIN(2)
c        hold tank RLG, chrystallization constants for CaSO3, gypsum
        READ(17,*) RLG2, CXKSP(1,2), CXKSP(2,2)
c        limestone rate K (surf. kinetics), const. by which to reduce
        reactivity
        READ(17,*) RATEK, RD
c        hold tank oxidation enhancement factor; liq. phase trans
        units
        READ(17,*) E, NL
c        data for particle size distribution
        IF(LA.NE.0) THEN
            READ(17,*) N
            write(10,*)'scale=',xscale
            DO 21 I=1,N
                READ(17,*) D(I),PHI(I)
                d(i) = xscale*d(i)
21            CONTINUE
            ELSE
35            READ(17,*) P1,D1,P2,D2
            END IF
c*****
c        statement added for rewinding the date file
            rewind(unit=17)
            rewind(unit=5)
c*****
            DO 103 I= 1,3
                BPPI(I)=BPP(I)
103 CONTINUE
120 FORMAT(11(F5.0))
        NOPR = XPR
        CCMCL=CCM(8)
c        check input data
        DO 3 I= 1,9
            IF (CCM(I).LT.0.) THEN
                WRITE (11,170) CMP(I), CCM(I)
170 FORMAT(1H0,'INPUT ERROR; CONCN OF ',A8, ' IS NEGATIVE=
',F12.5/
1            6X, 'SKIP TO NEXT CASE.')
                GO TO 100
            END IF
3            CONTINUE
c        calculate concns in gmol/l (K1=1: given in ppm; K1=2 given in gmol/l)
105 ICOUNT=1
        L=0

```

```

                F(K1.EQ.1) GO TO 20
113 CONTINUE
IF(L.GT.0.) CCM(1)=CM(5)
                DO 10 I=1,9
                CW(I) = 1000.d0 * CCM(I) * XMW(I) 10 CONTINUE
                GO TO 40
20 CONTINUE
                DO 30 I = 1,9
                CW(I) = CCM(I)
                CCM(I) = 0.001d0 * CCM(I) / XMW(I)
30          CONTINUE
40 CONTINUE
C          DO MODIFIED RADIAN CALC=
                EPS = 1.0d-8
                JS = SJ
                IPH = XIPH
                PPSO2 = PP(1)

PPCO2 = PP(2)
SS1 = SS(1)
SS2 = SS(2)
SS3 = SS(3)
KK1 = K1
JJS = JS
PPH = PH

                IF(TK.LT.253.d0) THEN
                        WRITE (11,175) TK
175          FORMAT( 1H0, 'INPUT TEMP OF ', F6.1, ' K IS TOO LOW
FOR',
1 ' RADIAN CALC;' / 6X, 'SKIP TO NEXT CALC. ')
GO TO 100
45 END IF
c          CCM values used in common blocks; CM values used by BEQ
CM(1) = CCM(5)
CM(2) = CCM(7)
CM(3) = CCM(6)
CM(4) = 0.
CM(5) = CCM(1)
CM(6) = CCM(2)
CM(7) = CCM(3)+CCM(4)
CM(8) = CCM(8)
CM(9) = CCM(9)
EPSNA = 1.d-10          !d
FNA=0.0
c          fna is the Na/(Na+K) ratio
                IF(CM(7).GT.EPSNA) FNA = CCM(3)/CM(7)
IOPT = 0
IF(PP(2).GT.EPS)

```



```

IOPT = 2
IF(PP(1).GT.EPS)
IOPT = IOPT+1
write(*,*)'calling bew*****'
c          call Radian modified equilibrium program
CALL BEQ (NOPR,JS,IOPT,TK,X,CM,PP,SS,IPH,PH,FNA)
L=L+1
IF(L.EQ.12) GO TO 230 !convergence count for charge balance
c          calculate charge error
          CALL CHARBL(X,CM,CHERR)
          IF(CHERR.GT.0.003) GO TO 123 !repeat loop
          IF(ICOUNT.EQ.2) GO TO 107 !completed
IF(CHERR.LT.0.003d0) NOPR=1 !do one more loop, full printout
          ICOUNT=ICOUNT +1
c          reset values for BEQ
123 SS(2)=1.0d0
          SS(3)=1.0d0
          SS(1)=0.55d0
          PP(2)=PPCO2
          PP(1)=PPSO2
          GO TO 113
c          evaluate pseudo-equilibrium constants, diffusivities and
concentrations
          107 CALL PSEUDO(X,TK,1)
write(*,*)'*****calling pseudo'
write(*,*)'before calling react'
write(*,*)'u=',u
write(*,*)'n=',n
write(*,*)'phi=',phi(1)
write(*,*)'la=',la,'b=',b
c          evaluate limestone reactivity
          CALL REACT(U,N,PHI,LA,B)
c          evaluate flux of dissolving CaCO3
          IFLAG=1
          CALL LISTONE(IFLAG)
c          evaluate flux of dissolving CaSO3
          CALL CASO3DI
c          again evaluate properties of the pseudo solution
          CALL PSEUDO(X,TK,2)
c          conver evaluates the gas driving force for SO2 absorption
          FFLUX=0.01d0
          write(7,*) 'calling conver from mdiva'
          CALL CONV99(DELCH)
c          model integration
          CALL SCRINT(NFLAG,NFLAG2)
c          parameter estimation

```

```

c          CALL GREGINTT
(NOPR,JS,IOP,T,K,X,CM,PP,SS,IPH,PH,FNA,NFLAG,NFLAG2
c          & U,N,PHI1,LA,B1 )
          write (*,*) 'R U N   C O N C L U D E D'
          return
c          GO TO 100
230 CONTINUE
          WRITE(11,33)
33 FORMAT(//,'CONVERGENCE FOR CHARGE BALANCE EXCEED 8TH
ITERATION')
GO TO 100
160 CONTINUE
WRITE (11,180)
180 FORMAT( 1H0, 'INPUT DATA INCOMPLETE FOR THIS CASE.')
200 CONTINUE
WRITE(11,210)
210 FORMAT(1H0,'END OF DATA')
c
STOP
return
END

```

Appendix G

Rate Constant Estimation by BETAV3

The reaction rate constants between NO_2 and SO_3^- , HSO_3^- , H_2O , S_2O_3^- , HS^- and the constants in the oxidation model were regressed by using BETAV3. The following sample shows how the three rate constants (between NO_2 and SO_3^- , HSO_3^- , and H_2O) were estimated by BETAV3 from a small group of 6 data points. The actual estimation of reaction rate constants was done on a much larger set of data.

As given in Chapter 2, the linearized form of the NO_2 absorption model is:

$$\frac{R_g^2 \text{HNO}_2^2}{D_{\text{NO}_2}} = k_2 \text{SO}_3^- [\text{SO}_3^-]_i + k_2 \text{HSO}_3^- [\text{HSO}_3^-]_i + \frac{2}{3} \frac{k_2 \text{H}_2\text{O} P_{\text{NO}_2 i}}{\text{HNO}_2} \quad (\text{G.1})$$

When applying BETAV3, the above equation can be represented as:

$$Y = B(1) * (X1) + B(2) * (X2) + B(3) * (X3) \quad (\text{G.2})$$

where $B(1)$, $B(2)$, and $B(3)$ are the three rate constants. $X1$ and $X2$ are the interfacial concentrations of SO_3^- and HSO_3^- , given in units of M. $X3$ is the value of $\frac{2}{3} \frac{P_{\text{NO}_2 i}}{\text{HNO}_2}$, divided by 1000 to have the same order of magnitude as the other X 's.

The data file for this calculation, datain.dat, is given as following:

X1	X2	X3	Y
1'	1	0.0006287	0.008866
2'	2	0.0015584	0.02805
3'	3	0.	0.
4'	4	0.0002569	0.005179

```
' 5' 5 0. 0. 3.7806e-3 7.6310e1 1.0
' 6' 6 0.0005367 0.03425 2.3387e-3 1.6148e3 1.0
END
```

BETAV3 was called to perform the parameter estimation by the following command:

```
Run BETAV3_TV.EXE;1
```

The output from BETAV3 was given in a file named dataout.dat. The following lists some of the important information contained in dataout.dat.

Rate Constant Esti

PROBLEM HAS ONE EQUATION

DATA READ VIA STANDARD FREE FORMAT

EQUATION GOES THROUGH ORIGIN

NAMES OF INDEPENDENT VARIABLES AND DEPENDENT VARIABLE

```
      X1      X2      X3      Y
```

DATA INPUT ORDER = 3 INDEPENDENT VARIABLE(S) 1

DEPENDENT VARIABLE

WEIGHT OF OBSERVATION

Obsv	Seq	X1	X2	X3	Y	WEIGHT
1	0	6.2870E-04	8.8660E-03	4.5719E-03	1.0528E+03	1.0000E+00
2	0	1.5584E-03	2.8050E-02	1.9050E-03	2.5756E+03	1.0000E+00
3	0	0.0000E+00	0.0000E+00	2.1687E-03	6.3790E+01	1.0000E+00
4	0	2.5690E-04	5.1790E-03	2.6962E-03	5.0460E+02	1.0000E+00
5	0	0.0000E+00	0.0000E+00	3.7806E-03	7.6310E+01	1.0000E+00
6	0	5.3670E-04	3.4250E-02	2.3387E-03	1.6148E+03	1.0000E+00

COLUMN TOTALS

```
2.9807E-03 7.6345E-02 1.7461E-02 5.8879E+03
```

c This matrix is to determine whether any of the independent variables are
c related

SIMPLE CORRELATION COEFFICIENTS, R(I,I PRIME)

```
1 1.0000E+00
2 7.2117E-01 1.0000E+00
3 -2.9044E-01 -4.4216E-01 1.0000E+00
```

c These are the three coefficients regressed from the data. $B(0) = 0$ implies
 c that there is no intercept.

IND.VAR(I) NAME COEF.B(I)

B(0) = 0

1	X1	1.11865E+06
2	X2	2.77463E+04
3	X3	1.54930E+04

NO. OF OBSERVATIONS	6
NO. OF IND. VARIABLES	3
RESIDUAL DEGREES OF FREEDOM	3
MULT. CORREL. COEF. SQUARED	1.0000

SOURCE
 OF DEVIATION DEGREES OF FREEDOM SUM OF THE SQUARES
 VARIANCE VARIANCE
 E RATIO
 (BETWEEN)

REGRESSION LINE					
AND GRAND MEAN	3	0.483615E+07	0.161205E+07	0.309001E+05	
REGRESSION LINE					
AND DATA	3	0.156509E+03	0.521696E+02		
SUB-TOTAL	6	0.483630E+07			

ANALYSIS OF VARIANCE

VARIABLES REMOVED DEGREES OF FREEDOM SUM OF THE
 SQUARES VARIANCE
 VARIANCE RATIO

X(1)	1	0.1019307500E+07	0.1019307500E+07
0.1953833008E+05			
X(2)	1	0.4292498438E+06	0.4292498438E+06
0.8227963867E+04			
X(3)	1	0.8770321289E+04	0.8770321289E+04
0.1681116180E+03			

CONFIDENCE LIMIT OF B
 WITH LIMITS OF 95 PERCENT

B(1) = 1118654.0000000000 +/- 25380.8535156250
 B(2) = 27746.2519531250 +/- 1066.5611572266
 B(3) = 15492.9580078125 +/- 10937.8046875000

STUDENTIZED

IDENT.	OBSV.	RESIDUAL	RESIDUAL	V(Y)/SSR	V(R)/SSR	V(Y)/V(R)
1	1	32.672	9.6	0.7768	0.2232	3.5
2	2	24.493	14.2	0.9434	0.0566	16.7
3	3	30.190	6.8	0.6260	0.3740	1.7
4	4	31.748	5.1	0.2651	0.7349	0.4
5	5	17.737	3.1	0.3915	0.6085	0.6
6	6	27.876	73.9	0.9973	0.0027	365.3

c This shows the variance for each data point.

VARIANCE OF Y

 VARIANCE ON Y(1) = 40.5240631104
 VARIANCE ON Y(2) = 49.2144508362
 VARIANCE ON Y(3) = 32.6573944092
 VARIANCE ON Y(4) = 13.8314056396
 VARIANCE ON Y(5) = 20.4239959717
 VARIANCE ON Y(6) = 52.0272178650

CONFIDENCE LIMITS OF PREDICTED Y WITH LIMITS OF 95 PERCENT

ION	O/O	DEVIAT
Y(1) =	1020.1283569336 +/-	20.2593212128
8945	3.1033	32.671691
Y(2) =	2551.1069335938 +/-	22.3261947632
0625	0.9510	24.493164
Y(3) =	33.5995788574 +/-	18.1869201660
0581	47.3278	30.190422
Y(4) =	472.8522033691 +/-	11.8359069824
7344	6.2917	31.747802
Y(5) =	58.5726776123 +/-	14.3826446533
9463	23.2438	17.737319
Y(6) =	1586.9240722656 +/-	22.9553375244
5625	1.7263	27.875976

THE AVERAGE ABSOLUTE DEVIATION IS 13.7740 PERCENT

From the above output, it is determined that the three rate constants, with their respective 95% confidence limits, are:

$$k_{2,\text{SO}_3=} = (11.2 \pm 0.3) \times 10^5 \text{ M}^{-1}\text{s}^{-1}$$

$$k_{2,\text{HSO}_3-} = (2.8 \pm 0.1) \times 10^4 \text{ M}^{-1}\text{s}^{-1}$$

$$k_{2\text{ H}_2\text{O}} = (1.6 \pm 1.1) \times 10^7 \text{ M}^{-1}\text{s}^{-1}$$

Appendix H

Model of Sulfite Oxidation with Thiosulfate

H1 DERIVATION OF EXPRESSION FOR N_{Ox}

Material balance on O_2 gives:

$$-D_{O_2} \frac{d^2[O_2]}{dx^2} = r_{ox} \quad (H.1)$$

Assuming r_{ox} does not change with depth, integration of H.1 gives:

$$-D_{O_2} \frac{d[O_2]}{dx} = r_{ox}x + a \quad (H.2)$$

Integrating the above expression gives:

$$-D_{O_2}[O_2] = \frac{r_{ox}}{2}x^2 + ax + b \quad (H.3)$$

Applying

B.C. 1: @ $x = 0$, O_2 flux = N_{Ox}

to H.2, gives:

$$a = N_{Ox}$$

Applying

B.C. 2: @ $x = \delta$, O_2 flux = 0

to H.2 gives:

$$d = \frac{a}{r_{ox}} = \frac{N_{Ox}}{r_{ox}}$$

Applying

B.C. 3: @ $x = \delta$, $[O_2] = 0$

to H.3 gives:

$$\frac{r_{ox}}{2}\delta^2 + N_{Ox}\delta + b = 0$$

$$b = \frac{N_{Ox}^2}{2r_{ox}}$$

Applying

B.C. 4: @ $x = 0$, $[O_2] = [O_2]_i$

to H.3 gives:

$$D_{O_2}[O_2]_i = \frac{N_{ox}^2}{2r_{ox}}$$

Solving for N_{ox} yields:

$$\begin{aligned} N_{ox} &= \sqrt{2r_{ox}D_{O_2}[O_2]_i} \\ &= \sqrt{2D_{O_2}[O_2]_i \frac{k_{ini}k_{ox}}{k_t} \frac{[SO_3^{=}]_i^2[NO_2]_i}{[S_2O_3^{=}]}} \end{aligned} \quad (H.4)$$

H2 DERIVATION OF RATIO $\frac{K_{ox}}{K_T}$

Results from a set of 10 experiments were chosen to regress the ratio of the rate constants k_{ox} to k_t at 55 °C. In all 10 experiments, NO_2 was absorbed into solutions containing $SO_3^{=}$ and $S_2O_3^{=}$ in the presence of 15% gas phase O_2 and the rate of sulfite oxidation was experimentally measured. The natural log of both sides in equation H.4 was taken to linearize the O_2 flux expression, and the value of $\sqrt{2D_{O_2}[O_2]_i \frac{k_{ini}k_{ox}}{k_t}}$ was regressed by BETAV3. The output of BETAV3 indicates:

$$\ln\left(\sqrt{2D_{O_2}[O_2]_i \frac{k_{ini}k_{ox}}{k_t}}\right) = -8.25$$

Therefore:

$$\frac{1}{2} \ln(2 \times 4.79e-5 \times 0.00018547 \times \frac{k_{ini}k_{ox}}{k_t} \times 1e-6) = -8.25$$

or

$$\frac{k_{ini}k_{ox}}{k_t} = 3.84 \times 10^6 \text{ M}^{-1}\text{s}^{-1}$$

$$k_{ini} = k_{2,SO_3^{=}} = 1.12 \times 10^6 \text{ M}^{-1}\text{s}^{-1} \text{ at } 55^\circ\text{C}$$

Therefore:

$$\text{at } 55\text{ }^{\circ}\text{C}, \frac{k_{\text{ox}}}{k_{\text{t}}} = 3.43$$

Appendix I

Sample Calculation of NO₂ Removal in Typical Scrubber

The following sample calculation shows the procedure to determine the fraction NO₂ removal in an actual scrubber based upon the kinetics of reaction between NO₂ and various S(IV) species.

For a typical limestone slurry scrubber that achieves 95% SO₂ control,

$$\begin{aligned} N_g &= 6.9 \\ \frac{k_l}{k_g} &= 292 \frac{\text{atm}\cdot\text{ml}}{\text{gmol}} \\ k_l^\circ &= 0.01 \frac{\text{cm}}{\text{s}} \end{aligned}$$

Therefore,

$$\begin{aligned} k_g &= \frac{0.01 \frac{\text{cm}}{\text{s}}}{292 \frac{\text{atm}\cdot\text{cm}^3}{\text{gmol}}} = 3.42 \times 10^{-5} \frac{\text{mol}}{\text{cm}^2\cdot\text{s}\cdot\text{atm}} \\ \frac{A}{G} &= \frac{N_g}{k_g} = \frac{6.9}{3.42 \times 10^{-5} \frac{\text{mol}}{\text{cm}^2\cdot\text{s}\cdot\text{atm}}} = 2.01 \times 10^5 \frac{\text{atm}\cdot\text{cm}^2\cdot\text{s}}{\text{gmol}} \end{aligned}$$

$$[S(\text{IV})]_i = 100 \text{ mM} = 0.1 \text{ M}$$

$$\text{pH}_i = 6$$

$$P_{\text{NO}_2,i} = 0.0002 \text{ atm}$$

By using the FORTRAN program in F1,

$$[\text{SO}_3^=]_i = 0.03 \text{ M}$$

$$[\text{HSO}_3^-]_i = 0.07 \text{ M}$$

$$\begin{aligned} k_1 &= k_{2,\text{SO}_3^=} [\text{SO}_3^=]_i + k_{2,\text{HSO}_3^-} [\text{HSO}_3^-]_i + \frac{2k_2 \text{H}_2\text{O} P_{\text{NO}_2,i}}{3 \text{HNO}_2} \\ &= 11.2 \times 10^5 \frac{1}{\text{M}\cdot\text{s}} \times 0.03 \text{ M} + 2.8 \times 10^4 \frac{1}{\text{M}\cdot\text{s}} \times 0.07 \text{ M} \end{aligned}$$

$$\begin{aligned}
& + \frac{2 \times 1.6 \times 10^7 \frac{1}{\text{M-s}} \times 0.0002 \text{ atm}}{3 \times 4.76 \times 10^4 \frac{\text{cm}^3\text{-atm}}{\text{mol}}} \times \frac{1000 \text{ cm}^3}{1 \text{ l}} \\
& = 33600 \frac{1}{\text{s}} + 1960 \frac{1}{\text{s}} + 44.8 \frac{1}{\text{s}} \\
& = 35605 \frac{1}{\text{s}} \\
\frac{1}{N_G} & = \frac{1}{N_g} + \frac{G}{Am\Phi k_1^\circ} \\
& = \frac{1}{N_g} + \frac{G}{Am\sqrt{k_1 D_{\text{NO}_2}}} \\
& = \frac{1}{6.9} + \frac{4.76 \times 10^4 \frac{\text{cm}^3\text{-atm}}{\text{mol}}}{2.01 \times 10^5 \frac{\text{atm-cm}^2\text{-s}}{\text{gmol}} \times \sqrt{35605 \frac{1}{\text{s}} \times 3.28 \times 10^{-5} \frac{\text{cm}^2}{\text{s}}}} \\
& = 0.1449 + 0.2191 \\
& = 0.3641 \\
N_G & = \frac{1}{0.3641} = 2.75 \\
\text{Fraction NO}_2 \text{ removal} & \\
& = 1 - \frac{Y_{\text{NO}_2 \text{ out}}}{Y_{\text{NO}_2 \text{ in}}} \\
& = 1 - \frac{1}{e^{N_G}} \\
& = 1 - \frac{1}{e^{2.75}} \\
& = 1 - 0.064 \\
& = 0.936
\end{aligned}$$

Appendix J

Sample Calculation of Hold Tank Depth Reduction

The following is a sample calculation of hold tank liquid depth reduction by NO₂ injection. For a base line oxidation case, it was assumed that a liquid depth of 30 ft was required to reduce the O₂ concentration in the oxidizing air from 0.2 mole fraction at the bottom of the tank to 0.1 mole fraction at the top of the liquid. The NO₂ injection was assumed to take place at the bottom of the tank, and the NO₂ was mixed with the inlet air. This calculation contains three parts. Part one (J1) calculates the ratio of A/G from forced oxidation case without the addition of NO₂; Part two (J2) determines the concentration profile of NO₂ as a function of the liquid depth after the injection; and part three (J3) calculates the new liquid depth required to achieve the same level of oxidation with the injection of NO₂. The difference between the original liquid depth of 30 ft and the new depth calculated in I3 represents the reduction in hold tank size.

J1 CALCULATION OF A/G

A material balance on O₂ yields:

$$\int_{Y_{O_2, in}}^{Y_{O_2, out}} G dY_{O_2} = \int_0^{30 \text{ ft}} N_{ox, phy} dA \quad (J.1)$$

$$\begin{aligned} N_{ox, phy} &= k_l^{\circ} O_2 ([O_2]_i - [O_2]_b) \\ &= k_l^{\circ} O_2 \frac{P_T (Y_{O_2} - 0)}{H_{O_2}} \end{aligned}$$

At a liquid depth ($\rho = 2.5 \times \rho_{H_2O}$) of x cm, the total pressure,

$$P_T = 1 \text{ atm} + \frac{2.5 * x \text{ cm of water}}{1033.3 \frac{\text{cm of water}}{\text{atm}}} = (1 + 2.419e-3x) \text{ atm}$$

$$k_l^{\circ} \text{O}_2 = 0.02 \frac{\text{cm}}{\text{s}}$$

$$H_{\text{O}_2} = 6.085 \times 10^4 \text{ atm/mol frac at } 55^\circ \text{C}$$

Let $dA = adx$, where a is the gas-liquid contact area per unit depth, equation J.1 becomes:

$$\begin{aligned} \int_{Y_{\text{O}_2, \text{in}}}^{Y_{\text{O}_2, \text{out}}} \frac{G}{Y_{\text{O}_2}} dY_{\text{O}_2} &= \int_0^{914.4 \text{ cm}} \frac{0.02 \frac{\text{cm}}{\text{s}} (1 + 2.419e-3x) \text{ atm}}{6.085e4 \frac{\text{atm}}{\text{mol - frac}}} * 55.6 \frac{\text{mol}}{\text{l}} * \frac{11}{1000 \text{ cm}^3} adx \\ &= \int_0^{914.4 \text{ cm}} (1.8274e-8 + 4.4206e-11x) \frac{\text{mol}}{\text{cm}^2 \cdot \text{s}} adx \end{aligned}$$

Integrate both sides:

$$\begin{aligned} \ln \frac{Y_{\text{O}_2, \text{out}}}{Y_{\text{O}_2, \text{in}}} &= -(1.8274e-8 \times 914.4 + 4.4206e-11 \times \frac{914.4^2}{2}) \frac{a}{G} \\ -0.6931 &= -3.5191e-5 \frac{a}{G} \frac{\text{mol}}{\text{cm} \cdot \text{s}} \\ a/G &= 19695 \frac{\text{cm} \cdot \text{s}}{\text{mol}} \end{aligned}$$

J2 CONCENTRATION PROFILE OF INJECTED NO₂

A mass balance on injected NO₂ yields:

$$\int_{Y_{\text{NO}_2, \text{in}}}^{Y_{\text{NO}_2, \text{out}}} G dY_{\text{NO}_2} = \int N_{\text{NO}_2} adx \quad (\text{J.2})$$

$$N_{\text{NO}_2} = \frac{Y_{\text{NO}_2} P_T}{H_{\text{NO}_2}} \sqrt{D_{\text{NO}_2} k_2 [\text{SO}_3^=]_i} \quad (\text{J.3})$$

For the case of $[\text{SO}_3^=]_i = 0.005 \text{ M}$,

$$N_{\text{NO}_2} = \frac{Y_{\text{NO}_2} (1 + 2.419e-3x) \text{ atm}}{4.76e4 \frac{\text{cm}^3 \cdot \text{atm}}{\text{mol}}} \sqrt{3.28e-5 \frac{\text{cm}^2}{\text{s}} * 11.2e5 \frac{1}{\text{M} \cdot \text{s}} * 0.005 \text{ M}}$$

Therefore, equation J.2 can be written as:

$$\int_{Y_{\text{NO}_2, \text{in}}}^{Y_{\text{NO}_2, \text{out}}} \frac{1}{Y_{\text{NO}_2}} dY_{\text{NO}_2} = \int - \frac{(1 + 2.419e-3x) \text{ atm}}{4.76e4 \frac{\text{cm}^3 \cdot \text{atm}}{\text{mol}}} * 0.4286 \frac{\text{cm}}{\text{s}} * 19695 \frac{\text{cm} \cdot \text{s}}{\text{mol}} dx$$

Integrate both sides:

$$\ln \frac{Y_{NO2 \text{ out}}}{Y_{NO2 \text{ in}}} = -0.1773x - 2.1444e-3x^2$$

At any liquid depth x, the concentration of NO₂

$$Y_{NO2} = \exp(\ln Y_{NO2, \text{in}} - 0.1773x - 2.1444e-3x^2) \quad (J.4)$$

J3 CALCULATION OF HOLD TANK LIQUID DEPTH REDUCTION

With NO₂ injection, a material balance on O₂ yields:

$$\int_{Y_{O2, \text{in}}}^{Y_{O2, \text{out}}} G dY_{O2} = \int_0^{D_{\text{ft}}} \dot{N}_{Ox} dx \quad (J.5)$$

$$N_{Ox} = C_1 \sqrt{N_{NO2}} [O_2]_i + C_2 \sqrt{N_{NO2}} [SO_3^{=}]_i + k_l^{\circ} O_2 [O_2]_i \quad (J.6)$$

For the case of [SO₃⁼]_i = 0.005 M,

$$N_{NO2} = \frac{Y_{NO2}(1+2.419e-3x) \text{ atm}}{4.76e4 \frac{\text{cm}^3\text{-atm}}{\text{mol}}} * 0.4286 \frac{\text{cm}}{\text{s}}$$

Therefore, equation J.5 can be reorganized as:

$$\begin{aligned} \int_{0.2}^{0.1} dY_{O2} &= \int_0^{30.48 \text{ Dcm}} 6900 \sqrt{\frac{Y_{NO2}(1+2.419e-3x)}{4.76e4}} * 0.4286 \\ &* \frac{Y_{O2}(1+2.419e-3x)}{6.085e4} * 0.00556 \\ &+ 210 \sqrt{\frac{Y_{NO2}(1+2.419e-3x)}{4.76e4}} * 0.4286 * \frac{0.005}{1000} \\ &+ \frac{0.02 * (1+2.419e-3x) * Y_{O2} * 0.0556}{6.085e4} * 19695 dx \end{aligned} \quad (J.7)$$

For the case of Y_{NO2, in} = 1000 ppm, from equation J.4:

$$Y_{NO2} = -6.908 - 0.1773x - 2.1444e-4x^2$$

Substituting Y_{NO2} in equation J.7 with the above expression, we have:

$$\int_{0.2}^{0.1} dY_{O_2} = \int_0^{30.48 D_{cm}} \left[6900 \sqrt{\frac{e^{(-6.908-0.1773x-2.144e-4x^2)}(1+2.419e-3x)}{4.76e4}} * 0.4286 \right. \\ \left. * \frac{Y_{O_2}(1+2.419e-3x)}{6.085e4} * 0.00556 \right. \\ \left. + 210 \sqrt{\frac{e^{(-6.908-0.1773x-2.144e-4x^2)}(1+2.419e-3x)}{4.76e4}} * 0.4286 * \frac{0.005}{1000} \right. \\ \left. + \frac{0.02 * (1+2.419e-3x) * Y_{O_2} * 0.0556}{6.085e4} \right] * 19695 dx$$

This expression can be rewritten into the form of a first order ordinary differential equation as:

$$\frac{dY_{O_2}}{dx} = \left[6900 \sqrt{\frac{e^{(-6.908-0.1773x-2.144e-4x^2)}(1+2.419e-3x)}{4.76e4}} * 0.4286 \right. \\ \left. * \frac{Y_{O_2}(1+2.419e-3x)}{6.085e4} * 0.00556 \right. \\ \left. + 210 \sqrt{\frac{e^{(-6.908-0.1773x-2.144e-4x^2)}(1+2.419e-3x)}{4.76e4}} * 0.4286 * \frac{0.005}{1000} \right. \\ \left. + \frac{0.02 * (1+2.419e-3x) * Y_{O_2} * 0.0556}{6.085e4} \right] * 19695$$

This first order ODE was solved by the function `lsode` in octave. The following is the `lsode` code for the ODE. $\dot{x}(1)$ represents $\frac{dY_{O_2}}{dx}$, and $x(1)$ is Y_{O_2} .

```
1;
function xdot=f(x,t)
xdot(1)=-(1000*6.9*sqrt(exp(-6.908-0.1773*t
(2.144e4)*t**2.)*(1+0.002419*t)
/(4.76e4)*0.4286)*x(1)*(1+0.002419*t)/(6.085e4)*0.0556+0.21*1.7*1000*
sqrt(exp(-6.908-0.1773*t-(2.144e-
4)*t**2.)*(1+0.002419*t)/(4.76e4)*0.4286)*0.005/1000.+0.02*x(1)/(6.085e4)*(1
+0.002419*t)*0.0556)*19695;
endfunction
```

The command for executing `lsode` calculation is:


```
x=lode("f",[0.2],(t=linspace(0,914.4,40')));
```

In the above command, 0.2 is the mole fraction of O_2 at the point $x=0$ (i.e., bottom of tank). zero and 914.4 cm are the lower and upper limits of x , and 40 is the number of the steps taken.

The output of lode is the mole fraction of O_2 at each liquid depth, starting with 0.2 mole fraction at $x=0$. The depth at which $Y_{O_2} = 0.1$ was taken to be the new tank depth required.

Glossary

- A = gas-liquid contact area, cm^2
 A' = gas-liquid contact area per unit liquid depth, cm^2/ft
 C_1, C_2, C_3 = regressed constants in oxidation model
 C = concentration of absorbed gas, M
 C_{ave} = average concentration of absorbed gas, M
 D_{NO_2} = diffusion coefficient of NO_2 , cm^2/s
 D_{O_2} = diffusion coefficient of O_2 , cm^2/s
 E = enhancement factor
 E_{act} = activation energy, kJ/mol
 G = gas flow rate, L/min
 Ha = Hatta's number
 H_{NO_2} = Henry's constant of NO_2 , $\text{cm}^3\text{-atm/mol}$
 H_{O_2} = Henry's constant of O_2 , atm/mol-frac
 $[HS^-]_b, [HS^-]_i$ = bulk and interfacial concentration of HS^- , M
 $[HSO_3^-]_b, [HSO_3^-]_i$ = bulk and interfacial concentration of HSO_3^- , M
 k_{2,H_2O} = reaction rate constant for NO_2 and water, $M^{-1}s^{-1}$
 k_{2,HS^-} = reaction rate constant for NO_2 and bisulfide, $M^{-1}s^{-1}$
 k_{2,HSO_3^-} = reaction rate constant for NO_2 and bisulfite, $M^{-1}s^{-1}$
 $k_{2,S_2O_3^{2-}}$ = reaction rate constant for NO_2 and thiosulfate, $M^{-1}s^{-1}$
 $k_{2,S_4^{2-}}$ = reaction rate constant for NO_2 and tetrasulfide, $M^{-1}s^{-1}$
 $k_{2,SO_3^{2-}}, k_{ini}$ = reaction rate constant for NO_2 and sulfite, $M^{-1}s^{-1}$
 k_g = gas phase mass transfer coefficient, $\text{mol/cm}^2\text{-s-atm}$

k_l° = liquid phase mass transfer coefficient, cm/s

k_{ox} = reaction rate constant for oxidation reaction, $M^{-1}s^{-1}$

k_t = reaction rate constant for termination step, $M^{-1}s^{-1}$

K_1, K_2, K_3 = equilibrium constants for polysulfides

K_g = overall gas phase mass transfer coefficient, $mol/cm^2-s-atm$

m = Henry's constant

N_g = number of gas film transfer units

N_G = number of overall mass transfer units

N_{NO_2} = flux of NO_2 , mol/cm^2-s

$N_{NO_2,exp}$ = rate of NO_2 absorption experimentally measured, mol/cm^2-s

$N_{NO_2,mod}$ = rate of NO_2 absorption predicted from model, mol/cm^2-s

N_{ox} = rate of sulfite or sulfide oxidation, mol/cm^2-s

$N_{ox,exp}$ = rate of oxidation experimentally measured, mol/cm^2-s

$N_{ox,mod}$ = rate of oxidation predicted from model, mol/cm^2-s

$N_{ox,phy}$ = rate of oxidation expected for physical absorption of O_2 , mol/cm^2-s

$[NO_2]_i$ = interfacial concentration of NO_2 , M

$[N_2O_4]$ = concentration of N_2O_4 , M

N_{SO_2} = rate of SO_2 absorption, mol/cm^2-s

$N_{S_2O_3}$ = rate of $S_2O_3^{2-}$ depletion, mol/cm^2-s

$[O_2]_i$ = interfacial O_2 concentration, M

$P_{NO_2,b}, P_{NO_2,i}$ = bulk and interfacial partial pressure of NO_2 , atm

P_T = total pressure, atm

r = rate of reaction, $mol/l-s$

R = gas constant, J/mol-K

R_g = normalized rate of absorption, mol/cm²-s-atm

$R_{g,exp}$ = normalized rate of absorption experimentally measured, mol/cm²-s-atm

$R_{g,mod}$ = normalized rate of absorption predicted by model, mol/cm²-s-atm

$[S_4^{=}]_b$ = bulk concentration of $S_4^{=}$, M

s = rate of surface renewal, s⁻¹

$[SO_3^{=}]_b, [SO_3^{=}]_i$ = bulk and interfacial concentration of $SO_3^{=}$, M

$[SO_5^{\cdot-}]$ = concentration of $SO_5^{\cdot-}$ radical, M

$[S(-II)]_o, [S(-II)]_f$ = initial and final concentration of S(-II), M

$[S(-II)]_{lit}$ = concentration of S(-II) in solution added to contactor, M

$[S(IV)]_o, [S(IV)]_f$ = initial and final concentration of S(IV), M

$[S(IV)]_{lit}$ = concentration of S(IV) in solution added to contactor, M

t_s = exposure time of fluid element, s

Δt = time interval, s

T = temperature, °C

V = solution volume, l

V_{lit} = volume of solution added to contactor, ml

Y_{NO_2} = NO₂ mole fraction

$Y_{NO_2,b}, Y_{NO_2,i}$ = bulk and interfacial concentration of NO₂, ppm

Y_{O_2} = bulk concentration of O₂, %

δ = film thickness, cm

Φ = enhancement factor for NO₂ absorption

References

- Andrew, S. P. S., and D. Hanson. "The Dynamics of Nitrous Gas Absorption." *AIChE J.*, 11, 105-113 (1965).
- Baveja, K. K., D. Subba Rao, and M. K. Sarkar. "Kinetics of Absorption of Nitric Oxide in Hydrogen Peroxide Solutions.: *J. Chem. Eng. of Japan*, 12, 322-325 (1979).
- Borders, R. A., and J. W. Birks. "High-Precision Measurements of Activation Energies over small Temperature Intervals: Curvature in the Arrhenius Plot for the Reaction $\text{NO} + \text{O}_3 \rightarrow \text{NO}_2 + \text{O}_2$." *J. Phy. Chem*, 86, 3295-3302 (1982).
- Clarke, A. G. and M. Radojevic. "Chloride Ion Effects on the Aqueous Oxidation of SO_2 ." *Atmospheric Environment*, 17(3), 617-624, (1983)
- Chang, C. S., and G. T. Rochelle. " SO_2 Absorption into Aqueous Solutions." *AIChE Journal*, 27, 385-393 (1981).
- Chen, K. Y. and J. C. Morris. *Envir. Sci. Technol.*, 6, 529 (1972).
- Danckwerts, P. V. "Absorption into Agitated Liquids." *Gas-Liquid Reactions*. McGraw-Hill Book Company, 1970.
- Daniel and Wood. *Fitting Equations to Data*, 2nd ed. John Wiley and Sons, Inc., 1980.
- Duvale, A. "Acid Rain Scrubber Retrofits May Cost Less Than Anticipated." *Power Engineering*, 95, 35-37 (1991).
- Ellison, T. K., and C. A. Eckert. "The Oxidation of Aqueous SO_2 . 4. The Influence of Nitrogen Dioxide at Low pH." *J. Phys. Chem.*, 88, 2335-2339, (1984)
- Epstein, M. "EPA Alkali Scrubbing Test Facility: Summary of Testing Through October 1974." EPA-650/2-75-047, NTIS No. PB-244 901 (1975).
- Giggenbach, W. F. "Equilibria Involving Polysulfide Ions in Aqueous Sulfide Solutions up to 240° ." *Inorg. Chem.*, 13(7), 1724-33 (1974).
- Glasscock, D. A., and G. T. Rochelle. "Approximate Simulation of CO_2 and H_2S Absorption into Aqueous Alkanolamines." *AIChE J.*, 39, 1389-1397 (1993).

- Higbie, R. "The Rate of Absorption of a Pure Gas into a Still Liquid During Short Periods of Exposure." *Trans. AICHE*, 31, 365 (1935).
- Hori, M., Matsunaga, N., Malte, P. C., and N. M. Marinov. "The Effect of Low-Concentration Fuels on the Conversion of Nitric Oxide to Nitrogen Dioxide," presented at the 24th International Symposium on Combustion/The Combustion Institute, Sydney, Australia (1992).
- Huasheng, L., and F. Wench. "Kinetics of Absorption of Nitric Oxide in Aqueous Fe(II)-EDTA Solution." *Ind. Eng. Chem. Res.*, 27, 855-864 (1988).
- Huie, R. E., and P. Neta. "Chemical Behavior of SO_3^- and SO_5^- Radicals in Aqueous Solutions." *J. Phys. Chem.*, 88, 5665-5669, (1984).
- Huie, R. E. and P. Neta. "Rate Constants For Some Oxidations of S(IV) by Radicals in Aqueous Solutions." *Atmospheric Environment*, 21(8), 1743-1747, (1987).
- Izumi, J., and N. Murakami. "Process for Controlling Nitrogen Oxides in Exhaust Gases." U.S. Patent 4,350,669. September 21, 1982.
- Jarvis, J. B., P. A. Nassos, and D. A. Stewart. "A Study of Sulfur-Nitrogen Compounds in Wet Lime/Limestone FGD Systems." Presented at EPA/EPRI Symposium on Flue Gas Desulfurization, Cincinnati, Ohio, June 4-7, 1985.
- Kameoka, Y., and R. L. Pigford. "Absorption of Nitrogen Dioxide into Water, Sulfuric Acid, Sodium Hydroxide, and Alkaline Sodium Sulfite Aqueous Solutions." *Ind. Eng. Chem., Fundam.*, 16(1), 163-9, (1977).
- Kobayashi, H., N. Takezawa, and T. Niki. "Removal of Nitrogen Oxides with Aqueous Solutions of Inorganic and Organic Reagents." *Environmental Science and Technology*, 11(2), 190-192, (1977).
- Kuehn, S. E. "Utility Plans Take Shape for Title IV Compliance." *Power Engineering*, 19-26 (1993).
- Kuhn, A. T., Kelsall, G. H., and Chana, M. S. "A Review of the Air Oxidation of Aqueous Sulphide Solutions." *J. Chem. Tech. Biotechnol.*, 33A, 406-414 (1983).
- Kuropka J., and M. A. Gostomczyk. "Reduction of Nitrogen Oxides by Alkaline Solutions of Sulfides and Sulfites." *Ochrona Powietrza*, Vol. 15, No. 1, 6-8 (1981).

- Lefers, J. B., Koetsier, W. T., and W. P. M. Van Swaaij. Chem. Eng. J., 15, 11 (1978).
- Lyon, R. K., J. A. Cole, J. C. Kramlich, and S. L. Chen. "The Selective Reduction of SO_3 to SO_2 and the Oxidation of NO to NO_2 by Methanol." Combustion and Flame, 81, 30-39 (1990).
- McGuire, L. M. "Sulfur Dioxide Absorption Experiments in Calcium Hydroxide Slurries." M.S. Thesis, Department of Chemical Engineering, University of Texas at Austin, 1990.
- Nash, T. "The Effect of Nitrogen Dioxide and of Some Transition Metals on the Oxidation of Dilute Bisulfite Solutions." Atm. Envir., 13, 1149-1154 (1979).
- Nelli, C. H. "Nitrogen Dioxide Removal by Calcium Silicate Solids." Ph.D. dissertation, Department of Chemical Engineering, University of Texas at Austin, 1996.
- Oblath, S. B., S. S. Markowitz, T. Novakov, and S. G. Chang. "Kinetics of the Formation of Hydroxylamine Disulfonate by the Reaction of Nitrite with Sulfites." J. Phy. Chem., 85, 1017-1021 (1981).
- Oblath, S. B., S. S. Markowitz, T. Novakov, and S. G. Chang. "Kinetics of the Initial Reaction of Nitrite Ion in Bisulfite Solutions." J. Phys. Chem., 86, 4853-4857 (1982).
- Owens, D. R. "Sulfite Oxidation Inhibited by Thiosulfate." Master Thesis, Department of Chemical Engineering, University of Texas at Austin, Dec. 1984.
- Perry, R. H., and D. W. Green. Perry's Chemical Engineers' Handbook, 6th edition. McGraw-Hill Book Company, 1984.
- Peters, M. S., Ross, C. P., and J. E. Klein. "Controlling Mechanism in the Aqueous Absorption of Nitrogen Oxides." A.I.Ch.E. Journal, 1(1), 105-111, (1955).
- Pont, J. N., Evans, A. B., Lyon, R. K., England, G. C., Moyeda, D. K., and W. R. Seeker. "Results from a Modeling and Experimental Evaluation of the Combi NO_x Process," presented at the 1993 American Chemical Society Meeting, Dencer, CO (April, 1993).
- Rochelle, G. T. "Flue Gas Desulfurization." Coal Processing and Pollution Control, 337-72.

- Rosenberg, H. S. and H. M. Grotta. "NO_x Influence on Sulfite Oxidation and Scaling in Lime/Limestone Flue Gas Desulfurization (FGD) Systems." *Environmental Science and Technology*, 470-472, (1980).
- Rosenberg, H. S., L. M. Curran, A. V. Slack, J. Ando and J. H. Oxley. "Post Combustion Methods for Control of NO_x Emissions." *Energy Combust. Sci.*, Vol. 6, 287-302 (1980).
- Sada, E. "Kinetics of Absorptions of Lean Sulfur Dioxide into Aqueous Slurries of Calcium Carbonate and Magnesium Hydroxide." *Chem. Eng. Sci.*, 36, 149-155 (1981).
- Seel, F., M. Wagner. "Reaction of Sulfides with Nitrogen Monoxide in Aqueous Solution". *Z. Anorg. Allg. Chem.*, 558, 189-92 (1988).
- Shen, C. H., and G. T. Rochelle. "NO₂ Absorption in Limestone Slurry for Flue Gas Desulfurization." 1995 SO₂ Control Symposium, March 28-31, 1995, Miami, Florida.
- Shen, S. H. "Waste Gas Pollution Control with Whirlwind Plate Tower." *Huan Ching Pao Hu*, No. 10, 16-7 (1990).
- Smith, D. J. "Low-NO_x Burners Lead Technologies to Meet CAA's Title IV." *Power Engineering*, 40-42 (1993).
- Stahl, J. W., and J. Jordan. "Thermometric Titration of Polysulfides." *Anal. Chem.*, 59, 1222-25 (1987).
- Takeuchi, H., M. Ando, and N. Kizawa. "Absorption of Nitrogen Oxides in Aqueous Sodium Sulfite and Bisulfite Solutions." *Ind. Eng. Chem., Process Des. Dev.*, 16, 303-308 (1977).
- Takeuchi, H., K. Takahashi, and N. Kizawa. "Absorption of Nitrogen Dioxide in Sodium Sulfite Solution from Air as a Diluent." *Ind. Eng. Chem., Process Des. Dev.*, 16, 486-490 (1977).
- Takeuchi, H., and Y. Yamanaka. "Simultaneous Absorption of SO₂ and NO₂ in Aqueous Solutions of NaOH and Na₂SO₃." *Ind. Eng. Chem., Process Des. Dev.*, 17, 389-393 (1978).
- Thermo Environmental Instruments Inc. "Instruction Manual-Model 43A, Pulsed Fluorescent Ambient SO₂ Analyzer," 1975.
- Thermo Environmental Instruments Inc. "Instruction Manual-Model 10AR, Chemiluminescent NO/NO_x Analyzer," 1975.

- Thorn, P. R. Jr. "Diethlenetriamine Solutions for Stack Gas Desulfurization by Absorption/Stripping." M.S. Thesis, Department of Chemical Engineering, University of Texas at Austin, 1981.
- Tseng, C. H. P. "Calcium Sulfite Hemihydrate Dissolution and Crystallization." Ph.D. dissertation, Department of Chemical Engineering, University of Texas at Austin, 1984.
- Uchida, S., H. Moriguchi, H. Maejima, K. Koide, and S. Kagetama. "Absorption of Sulfur Dioxide into Limestone Slurry in a Stirred Tank Reactor." *Can J. of Chem. Eng.*, 56, 696-697 (1978).
- Ulrich, R. K. "Sulfite Oxidation Under Flue Gas Desulfurization Conditions: Enhanced Oxygen Absorption Catalyzed by Transition Metals." Ph.D. dissertation, Department of Chemical Engineering, University of Texas at Austin, 1983.
- Versteeg, G. F., P. M. M. Blauwhoff, and W. P. M. Van Swaaij. "The Effect of Diffusivity on Gas-Liquid Mass Transfer in Stirred Vessels. Experiments at Atmospheric and Elevated Pressures." *Chem. Eng. Sci.*, 42, 1103-1119 (1987).
- Waterland, L. R. et al. Environmental Assessment of Stationary Source NO_x Control Technologies: First Annual Report, EPA 600/7-78/046, March, 1978.
- Wendel, M. M., and R. L. Pigford. *A.I.Ch.E. J.*, 4, 259 (1958).
- Wilke, C. R., and P. Chang. "Correlation of Diffusion Coefficients in Dilute Solutions." *AIChE J.*, 1, 261-270 (1955).
- Whitman, W. G. "The Two-Film Theory of Gas Absorption." *Chem. and Met. Eng.*, 29, 147 (1923).
- Wood, S. C. "Select the Right NO_x Control Technology." *Chemical Engineering Progress*, 32-38 (1994).
- Yano T. and Ito, K., *Bull. JSME*, 26, 94 (1983).
- Zamansky, V. M., Ho, L., Maly, R. M., and W. R. Seeker. "Hydrogen Peroxide Injection-A Novel Technology for Multiple Air Pollutant Emissions Removal," presented at the third International Conference on Combustion Technologies for a Clean Environment, Lisbon, Portugal (July, 1995).
- Zhao, L. B. "Mercury absorption in aqueous solutions." Ph.D. dissertation, Department of Chemical Engineering, University of Texas at Austin, 1997.

Vita

Chen Hua Shen was born in Shanghai, the People's Republic of China, on July 4, 1969, the only child of Mou Zhuang Shen and Betty Chou-Rong Zhu. In September 1985, after completing one year of study at Shi-Xi High School, he immigrated to the US, accompanied by his parents. He attended and graduated from Robert E. Lee High School in Baton Rouge, LA. In 1987, he was admitted to Louisiana State University, majoring in Chemical Engineering. During the period of 1990-1991, he has worked part-time for the Research and Development section of Ethyl Corporation in Baton Rouge as an intern engineer. In 1991, he graduated at the top of his class, receiving a BS in Chemical Engineering. In fall 1991, he joined the graduate program at University of Texas at Austin, under the supervision of Professor Gary T. Rochelle. He received a Ph.D. in Chemical Engineering in May, 1997. He has accepted employment at Covington Research Center of Westvaco Corporation in Covington, VA.

Permanent address: 12166 Metric Blvd., Apt. 172
Austin, TX 78758

This dissertation was typed by the author.